Homochiral vs. heterochiral crystal packing dilemma. Interplay between intrinsic chirality and supramolecular chirality

Marine Hoquante

Normandie Université

THÈSE

Pour obtenir le diplôme de doctorat

Spécialité PHYSIQUE

Préparée au sein de l'Université de Rouen Normandie

Homochiral vs. heterochiral crystal packing dilemna. Interplay between intrinsic chirality and supramolecular chirality.

Présentée et soutenue par
Marine HOQUANTE

Thèse soutenue le 25/11/2021 devant le jury composé de		
Mme JEANNE CRASSOUS	DIRECTEUR DE RECHERCHE, UNIVERSITE RENNES 1	Rapporteur du jury
M. RICHARD KELLOGG	DIRECTEUR DE RECHERCHE, University of Groningen	Rapporteur du jury
Mme ISABELLE CHATAIGNER	PROFESSEUR DES UNIVERSITES, Université de Rouen Normandie	Membre du jury
M. JASON HEIN	MAITRE DE CONFERENCES, University of British Columbia	Membre du jury
M. IVO RIETVELD	MAITRE DE CONFERENCES, UNIVERSITE PARIS 5 UNIVERSITE PARIS DESC	Directeur de thèse
M. GÉRARD COQUEREL	PROFESSEUR DES UNIVERSITES, Université de Rouen Normandie	Co-directeur de thèse

Thèse dirigée par IVO RIETVELD et GÉRARD COQUEREL, SCIENCES ET METHODES SEPARATIVES

UNIVERSITÉ DE ROUEN NORMANDIE

ED 591 PSIME

SMS Sciences et Méthodes Séparatives

Contents

Abbreviations

API	Active Pharmaceutical Ingredient
AS3PC	Auto-Seeded Polythermic Programmed Preferential Crystallization
S3PC	Seeded Polythermic Programmed Preferential Crystallization
ASPreCISE	Auto-Seeded Preferential Crystallization Induced by Solvent Evaporation
CSD	Cambridge Structural Database
CSD	Crystal Size Distribution
DCM	Dichloromethane
DIAD	Diisopropyl azodicarboxylate
DIFECS	Deracemization Induced by a Flux of Energy Crossing the Suspension
DKR	Dynamic Kinetic Resolution
DSC	Differential Scanning Calorimetry
e.e.	Enantiomeric Excess
EtOAc	Ethyl acetate
GRD	Growth Rate Dispersion
HPLC	High-Performance Liquid Chromatography
IPA	Isopropyl alcohol
IR	InfraRed
KR	Kinetic Resolution
MSZW	MetaStable Zone Width
NMR	Nuclear Magnetic Resonance
PBC	Periodic Bond Chain
PE	Preferential Enrichment
PC	Preferential Crystallization
PXRD	Powder X-ray diffraction
SHG	Second Harmonic Generation
SC-XRD	Single Crystal X-ray diffraction
SOAT	Second-Order Asymmetric Transformation
TCID	Temperature Cycle-Induced Deracemization
THF	Tetrahydrofuran

General Introduction and outline of the manuscript

Chirality has been known for more than two centuries. Nevertheless, the pharmaceutical industry has only been concerned about the chirality of active pharmaceutical ingredients when new pharmaceutical restrictions resulted in a stricter control over the difference in activity and side effects between two enantiomers. Presently, chirality has become a major scientific and economic issue. However, two enantiomers share many molecular properties making their separation difficult. Now more than ever, access to a single chirality is a challenge that needs to be addressed.

Among the possible methods to obtain pure enantiomers, one can either directly synthesize the desired enantiomer or one can choose to synthesize the racemic mixture followed by resolution depending on economic and feasibility limitations. Crystallization offers various robust and effective processes to resolve racemic mixtures such as Pasteurian resolution or preferential crystallization.

The aim of this work is to study resolution processes using crystallization, in particular Preferential Crystallization and to rationalize its applications via heterogeneous equilibria. Indeed, this process is based on both thermodynamics and kinetics. Thermodynamics provide information on the driving force of crystallization, whereas kinetics give the limit of the stereoselective crystallization.

The first chapter of this manuscript describes the state of the art in crystallization-based resolution methods, essential to understand the studies in the next two chapters.

The second chapter is devoted to an atropisomer, the benzyl ether of binol, presenting axial chirality. This compound exhibits a stable racemic compound despite having been reported as a conglomerate. The heterochiral phase appears to be more stable than the conglomerate irrespective of the temperature. Its melting point exceeds by 20 °C that of the racemic eutectic. In conjunction with the construction of the revised phase diagram, the crystal structures of the racemic compound and of the pure enantiomer have been compared. In the structure of the racemic compound ($Z' = 3$), hydrogen bonds are present, whereas in the structure of the pure enantiomer ($Z' = 1$) only $\pi-\pi$ and van der Waals interactions are observed. The threat of a more stable racemic compound appearing during preferential crystallization is discussed.

The third chapter is devoted to a chiral aryl sulfoxide and its corresponding sulfone. The former compound meets the crystallographic requirements for a resolution by preferential crystallization, but it also forms a complete solid solution with its sulfone. The thermodynamic and kinetic parameters required to design the preferential crystallization process have been determined. Since preferential crystallization is a robust and well-known resolution process, the innovative part of this study resides in the chirality transfer from supramolecular chirality to intrinsic chirality to induce the stereoselective crystallization of the sulfoxide. The benefit from such a chirality transfer is discussed and some perspectives are showcased to continue this work.

1. State of the art

1.1 Chirality

1.1.1 Foreword

Chirality is an asymmetry property of 3D objects which are not superimposable to their mirror images. The term chiral is derived from the Greek "χειρ" meaning "hand", the most ubiquitous example of chirality (Figure 1.1).

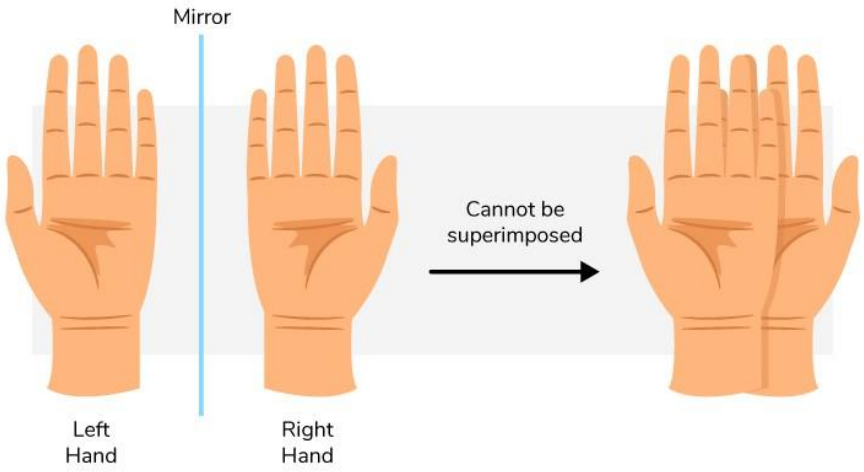

Figure 1.1: The best-known example of chirality, i.e., the hands

In chemistry, many molecules are chiral. Most of the time, this feature is due to the presence of an asymmetric atom (carbon, sulfur,…) as in Figure 1.2, but various other types of chirality exist.

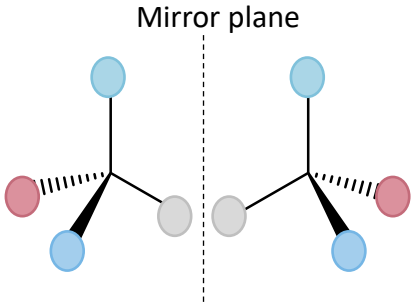

Figure 1.2: Example of a chiral molecule due to an asymmetric atom

The two mirror images of a chiral molecule are called enantiomers. They share the same physical properties; this includes their melting points, solubility, etc. However, because of the asymmetry, they do not have the same reactivity with other chiral elements (for instance other chiral molecules or polarized light). Accordingly, chiral molecules play an important role

in biology. Indeed, among the twenty eukaryotic amino acids, which are the building blocks of proteins, nineteen of them are chiral and exist in the L (levorotary) form in most organisms. As a consequence, two enantiomers can have distinct activities on cells. As an example, one can cite the molecule of limonene (Figure 1.3) because both enantiomers interact differently with biological receptors in the human nose giving the R-enantiomer an orange smell whereas the S-enantiomer smells like lemons; this highlights a clear effect that is purely caused by chirality.

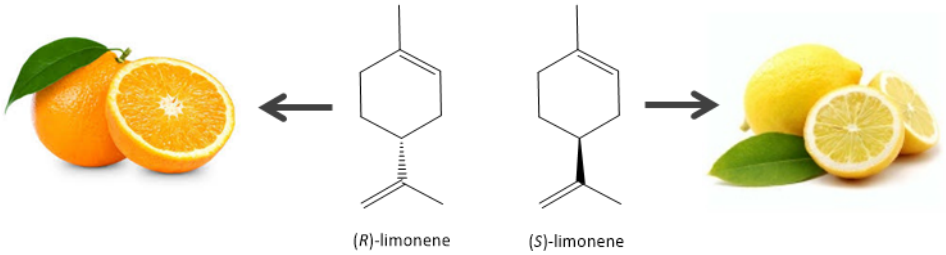

Figure 1.3: Chemical formulae of limonene enantiomers

The quantification of both enantiomers in a system is commonly described by the enantiomeric excess (e.e.) (Eq. 1):

$$\text{Enantiomeric excess (e.e.)}(\%) = \frac{[\text{R}] - [\text{S}]}{[\text{R}] + [\text{S}]} \times 100 \qquad \text{Eq. 1}$$

With [R] and [S] being the amount of enantiomer R and S respectively.

A mixture of equal amounts of both enantiomers (e.e. = 0) is referred to as a racemic mixture (sometimes also racemate even if there is no salt formation). A mixture with a ratio other than 1:1 (0 < e.e. < 1) is called a scalemic mixture.

The interaction with polarized light is a property of chiral materials.[1] Hence, an enantiomer is labelled (+) when it rotates the plan of the polarized light to the right, and (-) when it rotates the plane of the polarized light to the left. The classifications (+) and (-) are also termed d- and l-, respectively for dextrorotatory and levorotatory. The terms R (rectus) and S (sinister), were introduced by Cahn, Ingold and Prelog to describe the configuration of the asymmetric carbon,[2] which is independent of the designation (+) and (-).

1.1.2 History

The word “chiral” was first introduced by Lord Kelvin, Professor of Natural Philosophy at the University of Glasgow, in 1884: “I call any geometrical figure, or group of points, chiral, and say that it has chirality, if its image in a plane mirror, ideally realized, cannot be brought to coincide with itself.”[3] The discovery of chirality was closely related to crystallography. In the early eighteenth century, René-Just Haüy, a French mineralogist, observed that quartz crystals could exhibit two different hemihedries, called “plagièdre droit” and “plagièdre gauche”.[4] This was the discovery of enantiomorphism (Figure 1.4).[1]

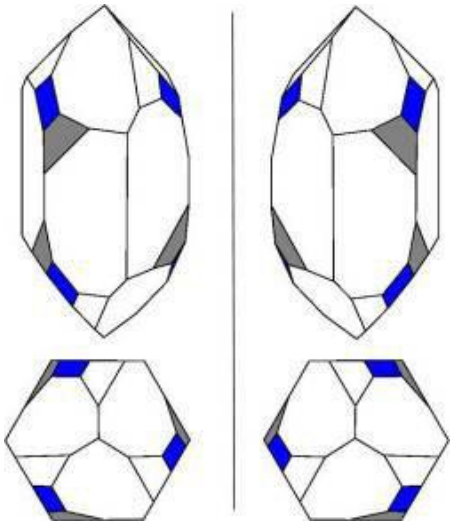

Figure 1.4: Morphology of enantiomorphous crystals of quartz

In 1815, Jean-Baptiste Biot observed that molecules such as sucrose, tartaric acid and camphor could rotate the polarized light clockwise or counter-clockwise in the solid and the liquid state and in solution. He assumed that this ability was directly correlated to their molecular properties.

In 1848 Louis Pasteur was the first who linked these two phenomena, by studying a racemic mixture (i.e. a mixture composed of both enantiomers in equal proportion) of sodium ammonium tartrate tetrahydrate. By looking closely to the crystals he noticed that the sample was not composed of one but of two kinds of crystals with a symmetrical shape.[5] Indeed, the mixture was composed of 50 % of crystals that exhibited right hemihedrism and 50 % of crystals that exhibited left hemihedrism. He was also able to separate manually the two populations of crystals using a pair of tweezers.[6] In 1866, Pasteur’s student Desiré Gernez, crystallized a pure enantiomer of sodium ammonium tartrate tetrahydrate by seeding a

racemic supersaturated solution with enantiopure crystals. Therefore, he discovered the principle of preferential crystallization.[7]

The next step in establishing the bases of stereochemistry are attributed to Jacobus Henricus van't Hoff and Joseph Achille Le Bel who proposed in 1874 that chirality was due to the spatial arrangement of tetrahedral carbon (i.e. asymmetric carbon).[8,9]

Nowadays, chirality is a concept of great importance for chemists and especially for the pharmaceutical industry (see below).[10] A more fundamental question "remains" unanswered but is highly debated: how did high homochirality assemblies (e.g. life) came or spontaneously developed on Earth?[11–13]

1.1.3 Chirality in pharmaceutical applications

All biopolymers in living organisms consist of chiral segments, (e.g. amino acids, sugars, nucleic acids...) and their functions are specifically related to their supramolecular interactions. The DNA and RNA molecules themselves exhibit chirality (both intrinsic and supramolecular); they are right-handed (Figure 1.5).

Figure 1.5: 3D model of DNA

Since 1992, the United States Food and Drug Administration requires the absolute stereochemistry to be known for registered drug molecules with chiral centers.[14] Accordingly, in the past decades, the demand for pure enantiomers has been constantly increasing due to pressure from the regulatory authorities for chiral drugs to be administered in an enantiomerically pure form. That is why the pharmaceutical industry tends to market chiral solids in their pure enantiomeric form.[15] In the pharmaceutical industry, 56% of the drugs currently in use are chiral and 88% of these molecules are marketed as racemic compounds (consisting of an equimolar mixture of two enantiomers).[16,17] The advantages of enantiopure

drugs range from an improved efficacity, to more easily measured pharmacokinetics and to reduced toxicity.[18] The desired enantiomer is called a eutomer, the undesired one distomer. Also, many agrochemicals (insecticides, herbicides…), fragrances and flavors are chiral molecules.[19]

Examples can be found in the literature supporting this approach. For instance, the S enantiomer of ibuprofen –a widely used analgesic– is three time more effective than its R enantiomer. [20] The L enantiomer of penicillamine –an α-amino acid– is highly toxic, whereas the D enantiomer is a valuable pharmaceutical used against rheumatoid arthritis.[21] That is why, chirality is now of general importance for both the academic and the industrial scientists.

1.1.4 Access to a single enantiomer: General overview

As previously discussed, obtaining pure enantiomers is a major issue for the pharmaceutical and agrochemical industries, first to understand and study the biological activities of each enantiopure forms and secondly to determine which of the two enantiomers is the most suitable for the purpose at hand. Between the numerous techniques used to obtain enantiopure compounds, two groups can be distinguished.

a. Stereoselective synthesis

In this case, the synthesis consists either of the conversion of a prochiral building block by asymmetric synthesis or of the use of a compound coming from the chiral pool. It can carried out using prochiral substances and achiral reagents either through organocatalysis,[22] the use of coordination complexes,[23] autocatalysis,[24] or enzymes.[25,26] Asymmetric synthesis can also be carried out through the temporary incorporation of an auxiliary chiral agent. Another possibility is to use reagents that already contain the desired stereochemistry (Chiral pool). The main issue is to keep a good enantiomeric excess (e.e.) through all the steps of the synthesis, as stereoselective syntheses often produce stereoisomeric products in unequal amounts. Stereoselective synthesis can be an approach of choice as it is straightforward and more environmentally friendly than the synthesis of the racemic mixture, where 50% of the product is being wasted. However, due to the complexity to implement asymmetric synthesis, the synthesis of the racemic mixture is often economically favored.

b. Resolution of a racemic mixture

If the synthesis is not stereoselective, it is possible to resolve the racemic mixture afterwards to access the pure enantiomers, meaning that the eutomer and the distomer will be separated through a purification step. Consequently, half of the product (i.e. the distomer) is considered waste; unless it can be racemized, because in that case it can be recycled to produce more eutomer. Hence, we can differentiate the racemate resolution with and without racemization.

Without racemization:

- Kinetic Resolution (KR) is based on the different reaction rates between a chiral substance and two enantiomers of a racemic mixture: one enantiomer will react faster allowing easy separation of the formed chiral substance from the unreacted remaining enantiomer.[27]

- Pasteurian resolution or diastereomeric resolution is probably the most popular method due to its simplicity and is widely used in the production of APIs.[28] Typically, this method consists in forming diastereomeric entities because diastereomers have different physical and chemical properties and can be often easily separated. A resolving agent which is enantiomerically pure is added to the racemic mixture, generating a salt or cocrystal with two (or more) fixed stereogenic centers leading to differences in the properties of the two enantiomer entities.

- Preparative chiral chromatography is a straightforward method for the separation of enantiomers once optimized.[29] Even though the range of stationary phases is increasing making the technique more versatile, it has high economic costs in terms of stationary phase and equipment and environmental cost because of the use of large quantities of solvent.

- Preferential Crystallization (PC)[30] is a crystallization based-technique presenting the interest of being an efficient separation and purification process. After fine tuning of the crystallization parameters, it has many advantages such as low cost and easy upscaling for the production of pure commercial products.

- Preferential Enrichment (PE)[31] is an unusual, out of equilibrium, spontaneous symmetry breaking by means of a crystallization process developed by Prof. Tamura's group. Starting with a slightly enriched supersaturated solution in one enantiomer, this process permits the system to deviate from standard crystallization, in stagnant conditions, in order to obtain a highly enriched mother liquor and deposited crystals slightly enriched in the opposite enantiomer. It could be described has the reverse case of preferential crystallization.

With racemization:

- Dynamic Kinetic Resolution (DKR) is an evolution of the KR technique which introduces the racemization to recycle the distomer.[32]

- Deracemization is a broad term including several chiral symmetry breaking processes by means of crystallization including Viedma ripening,[33] Temperature Cycle-Induced Deracemization (TCID)[34] and Second-Order Asymmetric Transformation (SOAT).[35]. Their benefit lies in the combination of a chemical and highly effective optical purification and the direct obtention of a powder.

Details of the techniques are discussed in the corresponding references and some crystallization-based techniques will be discussed afterwards.

1.1.5 Types of Chirality

Various types of chirality exist depending on the nature of the origin of the asymmetry. A distinction needs to be made between intrinsic chirality and supramolecular chirality.

1.1.5.1 Intrinsic Chirality

a. Point Chirality

In point chirality, the asymmetry arises from a stereogenic center. Generally, this center is an asymmetric atom such as carbon, phosphorus, or sulfur. For instance, L-lysine represented in Figure 1.6 is asymmetrical due to the four different substituents on the carbon marked with an asterisk (*), an amine group, a carboxylic acid group, an alkyl group and a hydrogen atom.

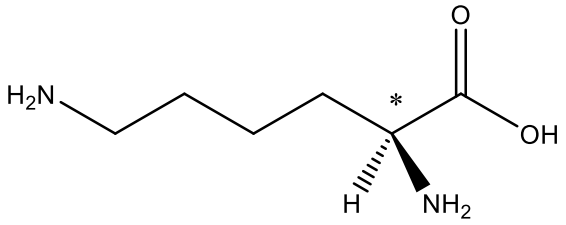

Figure 1.6: Cram's representation of the amino acid L-Lysine

b. Inherent Chirality

In contrast to point chirality, inherent chirality doesn't emerge from a chiral center, but from the shape, e.g. twisting, of a molecule in space.[36] This can be due to a blocked rotation around an axis or a plane.

In axial chirality, non-equivalent substituents are held in a spatial arrangement that is not superposable on its mirror image because rotation around the axis is limited due to steric hindrance. Such enantiomers are called atropisomers.[37] Some are easily isolated because the energy barrier for rotation is high, others, however, are hardly discernable as atropisomers if the steric strain is limited. The best-known examples of axial chirality are probably the binaphthyls wherein the rotation around the naphthyl-naphthyl bond is hindered (Figure 1.7).

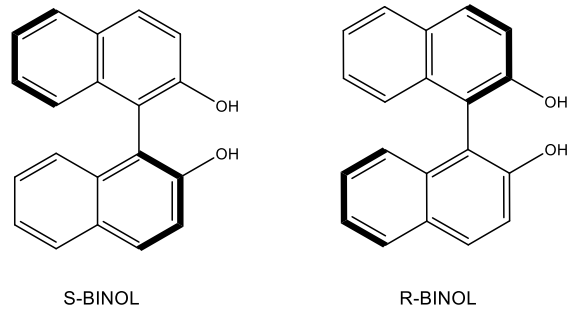

Figure 1.7: Cram's representation of the atropoisomers 1,1'-Bi-2-naphtol

In planar Chirality, a molecule possesses two non-coplanar dissymmetric rings which cannot easily rotate around the chemical bond connecting them. For instance, the metallo-organic compound in Figure 1.8 exhibits planar chirality around the iron atom.

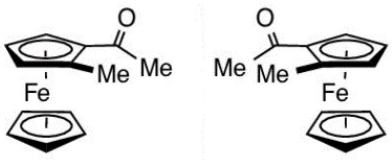

Figure 1.8: Cram's representation of a ferrocene metallocene derivative

1.1.5.2 Supramolecular chirality

In supramolecular chirality, components assemble themselves in a non-covalent way to create a dissymmetric assembly that is not superposable to its mirror image.[38] For instance, sodium chlorate, an achiral molecule crystallizes in a chiral space group (see part 1.2.3) giving rise to supramolecular crystals with right- and left-handedness (see Figure 1.9). However, to distinguish each supramolecular enantiomer it is necessary to perform the analyses in the solid state, as chirality doesn't exist in the liquid or solution state. Different methods are

available such as X-ray single crystal analysis, careful observation of the morphology of the crystals (two macroscopic single crystals of the two enantiomers are mirror image related, as in Figure 1.10) or circular dichroism.[39]

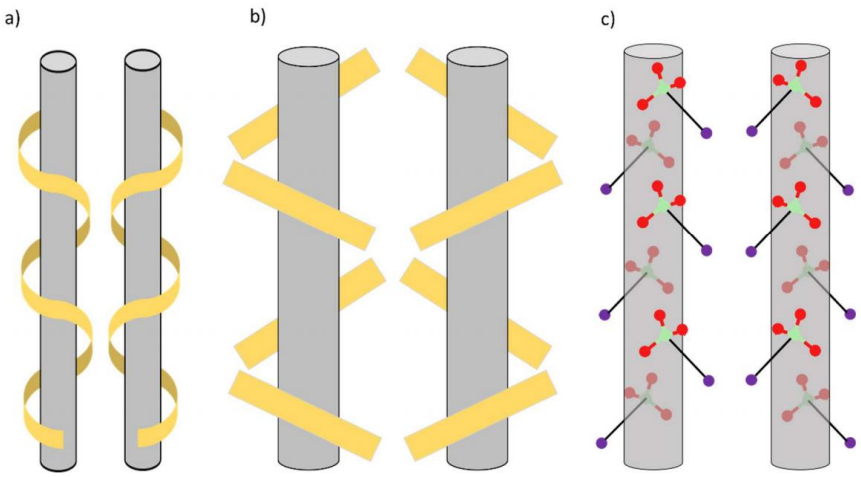

Figure 1.9: Schematic representation of chirality generation via supramolecular assemblies of a) helix, b) bars and c) sodium chlorate crystal structure.[40]

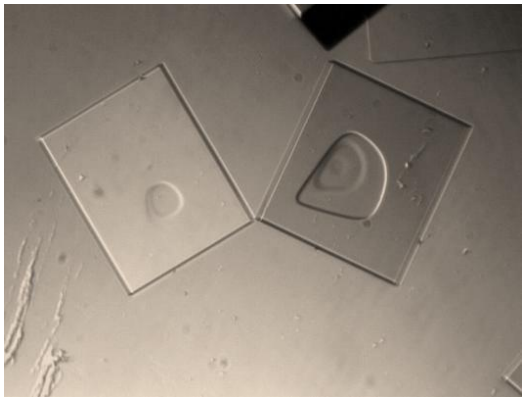

Figure 1.10: Crystals of sodium chlorate under polarized light

1.2 Fundamentals of crystallization

1.2.1 Introduction

A system is part of the universe delimited by real or fictive boundaries. A phase is part of a thermodynamic system that can be considered homogeneous in its properties (e.g composition, density, temperature, …) and constant for a certain period of time.[41] Thermodynamics provide information on the driving force of the crystallization.

Crystalline phases exhibit a periodic, three-dimensional arrangement of chemical entities. These so-called crystals present long range order. In contrast, in the (ideal) vapor phase, molecules do not interact with each other. In the liquid phase, molecules interact with other molecules at close range leading to the presence of short range order.

1.2.2 Thermodynamic aspects

A system is in equilibrium when it is in thermal, chemical, and mechanical equilibrium. Thus, for a system of n components, the intensive parameters, i.e. the temperature T (thermal equilibrium), the pressure P (mechanical equilibrium) and the chemical potentials μ_i (chemical equilibrium for the component i), are equal in all phases. In a system of n independent components, with φ phases in equilibrium, there are $n + 2$ intensive parameters which are related to φ equations. The variance v defined by the Gibbs rule (Eq. 2) corresponds to the number of intensive variables which can be varied independently without changing the equilibrium between all phases involved:

$$v = n + 2 - \varphi \qquad Eq. 2$$

In the case of a pair of enantiomers, the components of the system are linked together. The chemical potentials of both enantiomers in an achiral (i.e. racemic) phase (α) are identical. Furthermore, when a phase is chiral (i.e. contains an excess of one enantiomer), there is a symmetrical phase (i.e. the phase that contains an excess of the other enantiomer). In this instance, it is the Gibbs-Scott phase rule (Eq. 3) that must be applied in which $\frac{n'}{2}$ is the independent variable for each enantiomer pair and n the independent variable for optically inactive substance.[42]

$$v = n + \frac{n'}{2} + 2 - \varphi - \frac{\varphi}{2} \qquad Eq. 3$$

1.2.3 Chirality in crystals

A crystalline solid is a material whose constituents (such as atoms, molecules, or ions) are arranged in a highly ordered microscopic structure, forming a crystal lattice that extends in all directions.[43,44] The space group defines the symmetry operations in the crystal structure. Space groups can be gathered in sets called point groups.[45] Introducing chirality in crystals necessarily forbid some symmetry elements implying a limited number of available point groups in which pure enantiomers can crystallize. Three types of point groups exists:[46]

- Centrosymmetric Achiral point groups (CA): $\bar{1}, 2/\mathrm{m}$, mmm, $4/\mathrm{m}$, $4/\mathrm{mmm}$, $\bar{3}$, $\bar{3}\mathrm{m}$, $6/\mathrm{m}$, $6/\mathrm{mmm}$, $\mathrm{m3}$, and $\mathrm{m3m}$.
- Non-centrosymmetric Achiral point groups (NA): m, $\mathrm{mm2}$, $\bar{4}$, $4\mathrm{mm}$, $\bar{4}\,2\mathrm{m}$, $3\mathrm{m}$, $\bar{6}$, $6\,\mathrm{mm}$, $\bar{6}\mathrm{m2}$, and $\bar{4}3\mathrm{m}$.
- Non-centrosymmetric Chiral point groups (NC): 1, 2, 222, 4, 422, 3, 32, 6, 622, 23 and 432.

Only the last type of point groups (NC) is compatible with pure enantiomers. To completely characterize a crystalline structure, point groups are coupled to a Bravais lattice leading to space groups. Although there are 230 space groups, only 65, known as the Sohncke groups (combination of Bravais lattice and NC point groups), are compatible with chiral crystal structures.[47]

For a racemic mixture of enantiomers, the three above-mentioned types of point groups are permitted, resulting different crystalline phases with different degrees of chiral discrimination in the solid state.[48] In the first case, there is an important heterochiral recognition corresponding to the formation of a stable <1-1> stoichiometric intermediate solid phase, called the “racemic compound” (Figure 1.11.A). This is by far the most common case: it accounts for 90–95% of the enantiomer pairs. Crystallographic surveys show that most of these racemic compounds crystallize in a centrosymmetric space group ($P2_1/c$, P-1, Pbca, C2/c have the highest prevalence), despite all space groups being permitted. Secondly, the top chiral discrimination occurs when every single crystal contains a single enantiomer, which is called conglomerate. This is often defined as “spontaneous resolution” represented in Figure 1.11.B and the system will necessarily crystallize in one of the Sohncke groups. The third case represents the possibility of a complete solid solution where any enantiomer can be substituted by the other (Figure 1.11.C), once again all space groups are permitted.

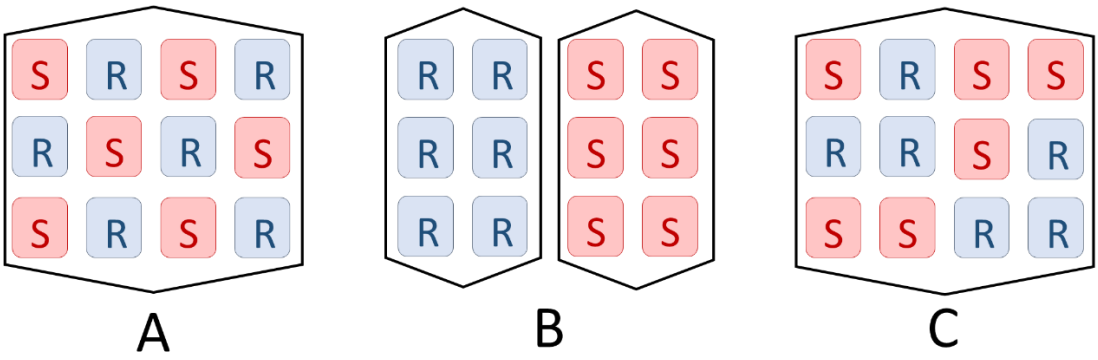

Figure 1.11: Schematic representation of a) a racemic compound, b) a conglomerate and c) a solid solution between a pair of enantiomers

1.2.3.1 Phase diagrams

To understand and rationalize crystallization behavior, a good strategy is to rely on heterogenous equilibria and to establish the corresponding phase diagram. A phase diagram is a graphical representation of the physical states of a substance in equilibrium.[49] Due to the mirror properties of enantiomers, heterogeneous equilibria involving a pair of enantiomers are symmetrical and the axis of symmetry is centered at the racemic composition.

Two behaviors of the R–S system regarding racemization need to be distinguished. In the first case, the two enantiomers do not interconvert under the operating conditions or in the time scale of the experiment. Therefore, the system is a symmetrical binary system where the two components have exactly the same thermodynamic properties (temperature, enthalpy and entropy of fusion, density, Cp versus T, etc.). This behavior is represented in Figure 1.12. In the second case, the two enantiomers racemize rapidly in the liquid state. There is a relationship of interdependence between the two components, so the system is a degenerate binary system, as depicted in Figure 1.14.

a. Binary phase diagrams of a pair of enantiomers

A) A racemic compound is a solid phase with the two enantiomers present in equal amounts in the unit cell of the crystal lattice with particular symmetrical requirements in the packing.

B) A conglomerate is a physical mixture of enantiopure crystals.

C) A complete solid solution forms a single phase over the full composition range where both enantiomers are randomly distributed over the crystallographic sites. In Figure 1.12 a complete solid solution with a maximum in the melting curve is depicted but the same type of system can also occur with a minimum. In the case of a solid solution, if there is no miscibility gap in the solid state, chiral discrimination will be very poor.

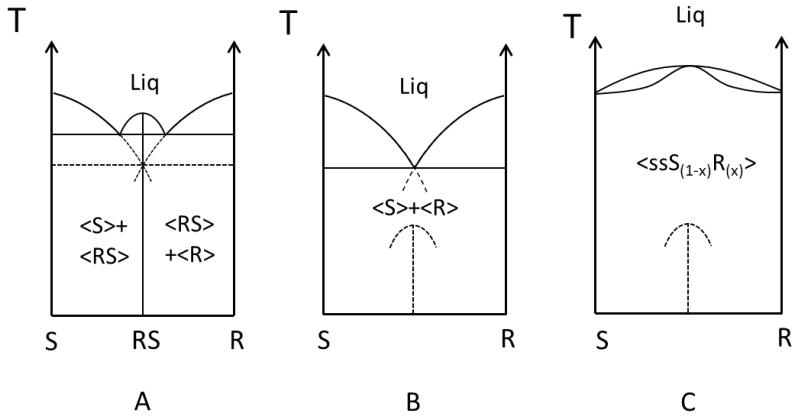

Figure 1.12: Binary phase diagrams of a pair of enantiomers (in the absence of racemization in the liquid), a) a racemic compound forming system, b) a conglomerate forming system c) a solid solution forming system. (The dashed lines represent metastable equilibria)

The three cases (Figure 1.12 A, B and C) depicted here are extreme examples. Of course, there is a continuity between them. A complete solid solution at high temperature does not rule out the existence of a miscibility gap in the solid state at low temperature.[50] In this case, chiral discrimination in the solid state increases continuously with the separation of the two symmetrical solvus curves towards lower temperatures.[50,51] Partial solid solutions between enantiomers are also well known.[52] Such cases represent intermediates between ideal conglomerates (Figure 1.12.B) and complete solid solutions (Figure 1.12.C). In some systems, crystallization into a crystal can lead to peculiar microstructures named lamellar conglomerate due to epitaxies, which is structurally different form a racemic compound.[53]

A change in temperature can slightly or completely alter the chiral discrimination. A conglomerate is a useful system since an optimized recrystallization can “virtually” be carried out to resolve a racemic mixture without any loss of enantiomeric excess.[54] Moreover, when coupled to racemization, a single, almost pure enantiomer can be obtained by attrition from the racemic mixture.[55] Accordingly, studies are carried out to find approaches to push the system towards conglomerate formation. For instance, in certain cases, from a racemic compound at low temperature, a stable conglomerate can be obtained at higher temperature through a three-phase peritectoid invariant (Figure 1.13).[48]

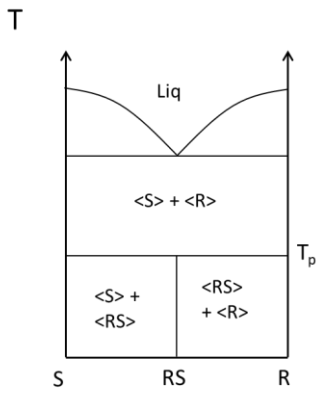

Figure 1.13: Binary phase diagram of a pair of enantiomer forming a racemic compound a low temperature and a conglomerate at high temperature

The opposite situation is also well known. The three-phase invariant is then a eutectoid.[56] The switch from a racemic compound to a conglomerate-forming system can also occur with the addition of a particular solvent or co-crystal former or both.[57] The addition of crystal co-formers (isolated or in a mixture of solvents, counter-ions, co-crystal former, etc.) greatly increases the number of possibilities to explore in order to spot at least one conglomerate.[58,59] It increases the order of the system, which will no longer be binary, but ternary, quaternary, quinary, or even of higher order.[60] High-throughput techniques which rapidly spot conglomerate forming systems and alleviate the amount of work due to the overwhelming number of tests, will be discussed in the next part of this chapter.

Figure 1.14, represents the first two cases (a racemic compound and a conglomerate forming system) depicted in Figure 1.12 in the case of racemization in the liquid state (or in the case of no chirality at all, e.g. sodium chlorate). If the racemization is instantaneous, the liquid must remain racemic.

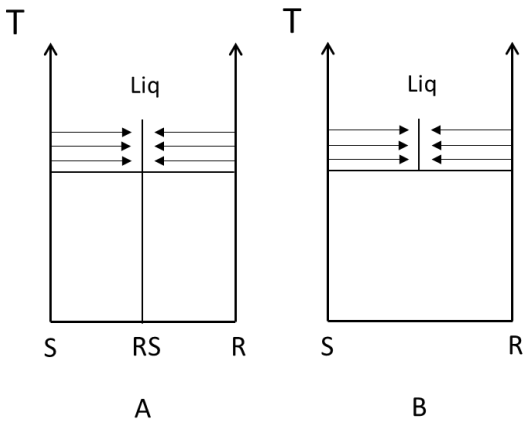

Figure 1.14: Binary phase diagrams of a pair of racemizable enantiomers, a) a racemic compound forming system, b) a conglomerate forming system.

b. Ternary phase diagrams of a pair of enantiomers and a solvent

Most crystallizations of organic materials are carried out in solution to avoid degradation, which may occur on melting due to elevated temperatures. As an achiral solvent is added to the system it is necessary to expand the binary phase diagram and to introduce the role of the solvent (V, hereafter). In analogy with Figure 1.12, isothermal ternary phase diagrams between a pair of enantiomers and a solvent showing different types of chiral discrimination in the solid state are depicted in Figure 1.15.

Figure 1.16 shows the equilibrium in the case of racemization in solution. If the racemization is instantaneous, the solution e.e. remains 0 and the undersaturated solution domain with a e.e. > 0 is prohibited. If the system crystallizes as a conglomerate at equilibrium and if a spontaneous break of symmetry occurs, the system can tend towards a single enantiomer in the solid state and the saturated solution remains racemic (Figure 1.16.B).[61]

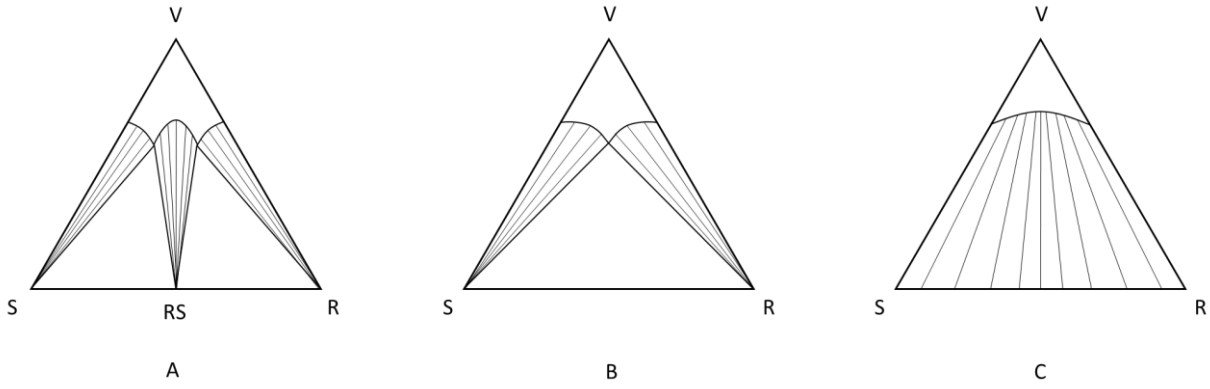

Figure 1.15: Ternary phase diagrams of a pair of enantiomers and a solvent (in the absence of racemization), a) a racemic compound forming system, b) a conglomerate forming system, c) a solid solution forming system

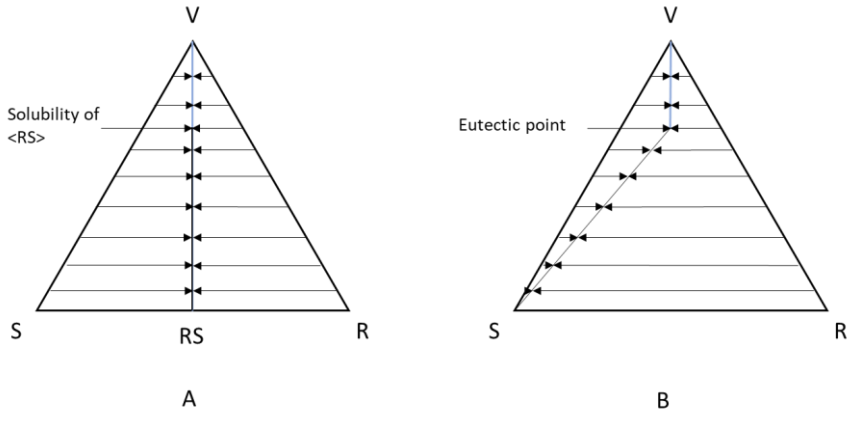

Figure 1.16: Degenerated ternary system of a couple of enantiomers which racemize in solution, a) a racemic compound forming system, b) a conglomerate forming system (towards the S enantiomer in this case, the mirror situation equally exists)

1.2.3.2 How to detect a conglomerate forming system?

Regarding the strength of chiral discrimination in the solid state and its relevance towards the resolution of racemic mixtures, detection of conglomerate forming systems is of major importance. Therefore, fast methods to detect conglomerates is of great value. Three main methods can be distinguished.

a. Second Harmonic Generation

A new use of SHG (Second Harmonic Generation) was developed in the SMS laboratory especially for screening of conglomerate forming systems.[62,63] It is a nonlinear optical technique, in which photons in interaction with a non-centrosymmetric material merge to form new photons of twice the initial energy. A schematic representation of the set-up can be found in Figure 1.17. A powder sample is irradiated by a laser with a known wavelength and the signal generated by the sample is recorded. If the material is non-centrosymmetric, part of the signal generated by the sample will possess half the wavelength of the incident beam,[64] whereas the signal generated by a material presenting a center of symmetry will not change in wavelength.[62]

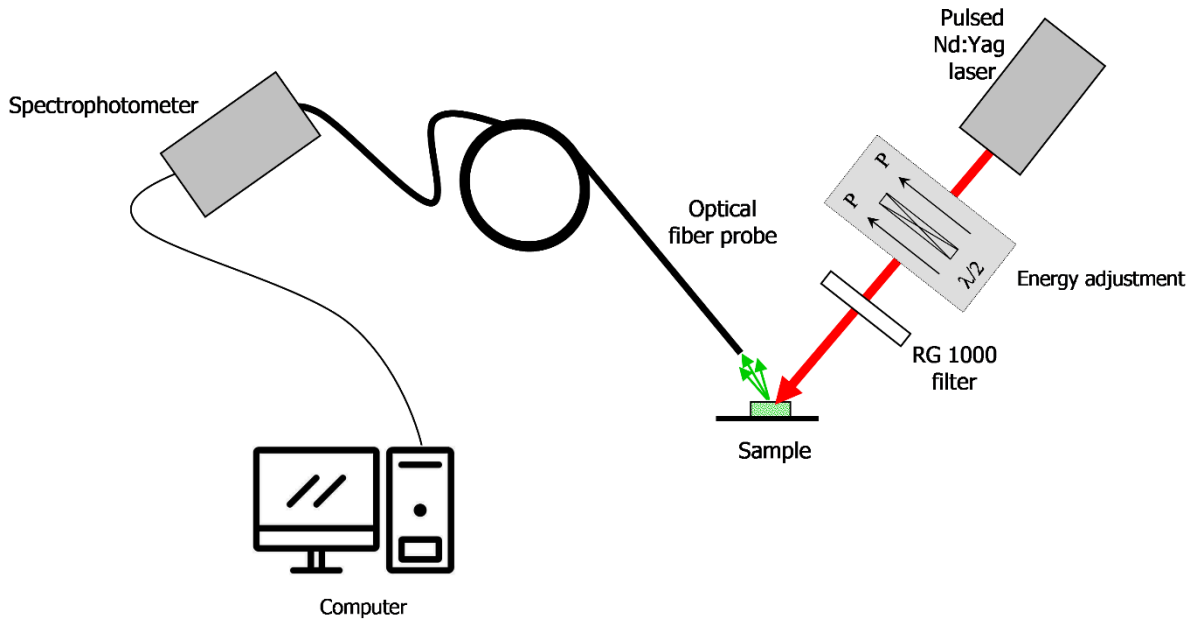

Figure 1.17: Second harmonic generation setup from Galland et al.[62]

Conglomerate forming systems crystallize in a non-centrosymmetric space group because the presence of an inversion center in the crystal is incompatible with the asymmetry of the

molecule or the supramolecular assembly. Conversely, a centrosymmetric space group requires the presence of both enantiomers in the asymmetric unit. Nonetheless, a positive SHG signal indicating a non-centrosymmetric space group does not prove that the sample is a conglomerate, as there are no restrictions for the racemic compound to crystallize in a non-centrosymmetric achiral (i.e. NA) space group (the most frequent being Pca2, Pna2, Pc and Cc) representing ca. 6% of the racemic compounds.[65] Moreover, some racemic compounds even crystallize in a non-centrosymmetric chiral space group (i.e. NC or Sohncke space group like $P2_12_12_1$ and $P2_1$) with Z'=2 (i.e. both enantiomers are present in the asymmetric unit). Such kryptoracemic compounds are unusual and represent only about 1% of the reported structures of enantiomer pairs in the Cambridge Structural Database (CSD).[65,66] Regarding the small proportion of false positives, SHG remains a fast and relatively accurate method to screen for conglomerate forming systems, even if additional data is needed to confirm the presence of a conglomerate.

b. Spectroscopic methods

In the part 1.2.3, we saw that a conglomerate forming system is a physical mixture of pure enantiomers, every crystal being homochiral. Consequently, a conglomerate-forming racemic mixture shares the spectroscopic data of the enantiomers (X-Ray diffraction, infrared, solid state NMR, or Raman), while in the case of a racemic compound, these data will be different. Therefore, a simple comparison of spectroscopic data will demonstrate the presence of a conglomerate. However, the case of a complete solid solution can be mistaken for a conglomerate, as all concentrations in the phase diagram will share a single phase. Even though solid solutions are rare, one should pay attention to possible small changes in the spectra due to the substitution of one enantiomer by the other.[67] In order not to confuse a solid solution with a conglomerate, other methods should be used in tandem for confirmation.

The drawback of spectroscopic methods is the need of the pure enantiomer for the comparison. When pure enantiomers are not available, other methods will need to be applied.

c. Crystal Structure resolution

The most accurate method to properly characterize a crystalline system is the resolution of its structure by X-ray crystallography. This is also valid for mixtures of enantiomers. Structural resolution provides all crystallographic data (i.e. the space group and the asymmetric unit), which will prove the presence or absence of a conglomerate without any uncertainty. However, it is the most time-consuming method among the three mentioned here. In cases

of a presumption of a conglomerate –either by comparison of spectroscopic data or because a signal could be observed in SHG– it becomes relevant to run the structural resolution to confirm the character of the system.

1.2.4 Kinetic aspects

The driving force of the crystallization (Eq. 4) from a solution is the supersaturation β (C and S stand for the concentration of the solution and the solubility respectively).

$$\beta = \frac{C}{S} \qquad Eq.4$$

The crystallization kinetic of a chiral compound does not differ from achiral crystallization unless a single enantiomer is crystallized from a nearly racemic mixture. In this case, half of the dissolved molecules can be considered as impurities. The crystallization kinetics comparison between an enantiomer and a racemic compound has been carried out by Fabrice Dufour et al.[68] They conclude that the crystallization kinetic of the racemic compound is favored if both phases (i.e. the conglomerate and the racemic compound) exhibit a similar crystal packing. Furthermore, other parameters such as diffusion also give a clear advantage to the crystallization of the racemic compound.

Crystallization is usually described by a two-step mechanism: nucleation and crystal growth.

1.2.4.1 Nucleation

a. Primary Nucleation

In a supersaturated solution, the system cannot tends towards a heterogeneous equilibrium and the dissolved molecules start to aggregate to form nuclei. Classical Nucleation Theory (CNT) is an attempt to conceptualize homogeneous nucleation from an energetic point of view.[69] Assuming that a nucleus adopts a spherical shape of radius r, the free enthalpy variation $\Delta G_{nucleation}$ related to the nucleus is given by eq.5 :

$$\Delta G_{nucleation} = \frac{4}{3}\pi r^3 \Delta g_v + 4\pi r^2 \gamma \qquad Eq.5$$

With Δg_v, the variation in Gibbs free energy per unit of volume and γ the surface tension.

One can distinguish two terms in the equation, the first one is related to the volume of the nucleus; it contributes to stabilize the system representing the cohesive energy between the molecules. The second one is related to the surface of the nucleus representing the interaction between the molecules crystallized at the surface of the nucleus and the solution, which causes a positive contribution to the overall energy and destabilizes the system.

A critical radius $r*$ is associated to a maximum of free enthalpy $\Delta G_{nucleation}*$. When the nucleus has a radius smaller than $r*$, its redissolution is favored (the sum of the two contributions $\Delta G_{surface}$ + ΔG_{volume} results in $\Delta G_{nucleation}$ in Figure 1.18). For a size larger than $r*$, the nucleus will grow.

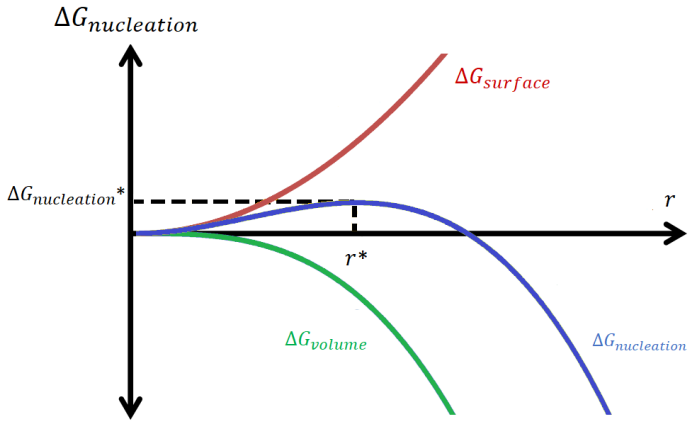

Figure 1.18: Evolution of the free enthalpy of a nucleus depending on its radius

Nucleation can be homogeneous if nuclei appear freely inside the solution, or heterogeneous when nuclei appear on a solid interface (dust, reactor wall, stirrer, etc). The latter is much more frequently observed because it minimizes the surface energy of the nuclei and lowers the energy barrier of the nucleation.

In the case of nucleation of a conglomerate forming compound, both enantiomers would ideally nucleate simultaneously, since they share the same activation energy and critical radius due to their mirror symmetry relationship; in practice this is rarely observed.

b. Secondary Nucleation

During the crystallization process, crystals are often subjected to intense mechanical stresses like shear stress or collisions with other crystals or reactor walls. In such conditions, small crystallites can break off the mother crystals, and generate new daughter crystals.[70]

If the crystals are chiral, the secondary nucleation will generate daughter crystals of the same handedness as the mother crystal.[71]

c. Metastable zone

In practice, solutions can be concentrated up to conditions where the solution is significantly less stable than the crystal, but no crystals will form for minutes, hours, weeks or even longer. This is due to the activation energy required to generate the first nuclei; a supersaturated solution spontaneously crystallizes only if the supersaturation exceeds a threshold capable to overcome the nucleation energy barrier to produce nuclei that reach the critical size, i.e. the Ostwald limit (Figure 1.19). Ostwald defined the concept of this metastable zone in 1897.[72]

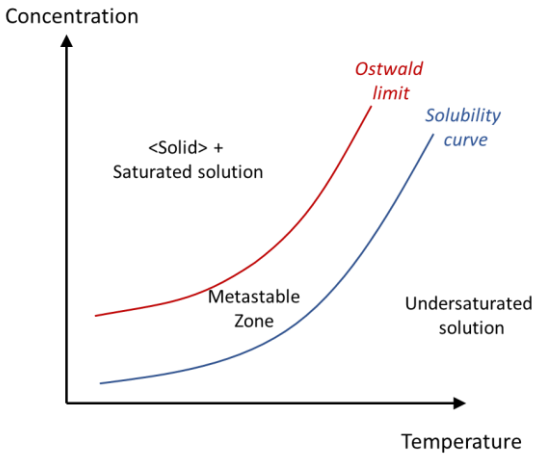

Figure 1.19: Ostwald limit representation

The width of the metastable zone depends on many factors including kinetic factors: the rate of increase in supersaturation (the cooling rate in cooling crystallization or the evaporation rate in solvent evaporation crystallization), stirring rate and mode, the nature of the reactor, impurities, etc.

1.2.4.2 Crystal Growth

When a nucleus is larger than the critical radius, the crystal can grow by successive adsorptions of molecules at the interface. Solvated molecules dock to the surfaces and will be incorporated into the crystal until the system reaches its equilibrium, i.e. a saturated solution. The mechanism of incorporation depends of the roughness of the surface, which can be divided into three modes:[73]

- In the first case, the crystal grows continuously on screw dislocations which provide large preferential sites where chemical motifs can dock on the crystal. Spiral growth is observed at low supersaturation and produces a more regular development.[74]
- In the second case, the crystal grows layer by layer on flat surfaces since molecules cannot find any preferential sites; this is called the two dimensional nucleation and this way of incorporation is favored at higher supersaturation.[75]
- Finally, at very high supersaturation, the crystal grows uncontrolled. This unbridled development that favors defects in the final crystals is past the roughening transition.[76]

The final morphology of a crystal depends on the growth rates of its faces. The faces, which appear in final crystal morphologies, are the slow growing faces.

1.3 Chiral Symmetry breaking by means of crystallization

The content of this section is mainly based on the review by Coquerel, G. and Hoquante, M.: Spontaneous and Controlled Macroscopic Chiral Symmetry Breaking by Means of Crystallization published in Chemical Symmetry Breaking in 2020.[77,78]

Macroscopic chiral symmetry breaking refers to the process in which a mixture of enantiomers departs from 50–50 symmetry to favor one chirality, resulting in either a scalemic mixture or a pure enantiomer. In this domain, crystallization offers various possibilities, from the classical Viedma ripening or Temperature Cycle-Induced Deracemization to the famous Kondepudi experiment and then to the so-called Preferential Enrichment. Given that not every technique is relevant to this manuscript nor was studied, the complex case of preferential enrichment will not be addressed here. For more information see the work of Tamura et al. and a study by the group of Coquerel. [31,79–81]

1.3.1 Types of chiral symmetry breaking

1.3.1.1 Deracemization Induced by a Flux of Energy Crossing the Suspension (DIFECS)

When fast racemization takes place in solution under the same conditions as the crystallization of a conglomerate, it is possible to observe a spontaneous macroscopic break in symmetry. The corresponding phase diagrams are no longer those displayed in Figure 1.15, as detailed by the group of Coquerel.[82,83] Indeed, the phase diagrams will have become degenerate, because the liquid phase can only contain an equimolar number of enantiomers (i.e., a racemic composition, see Figure 1.16). Under those circumstances, any energy flux passing through the suspension for a long enough time will lead to the disappearance of one population of homochiral crystals as illustrated by Figure 1.20. A constant mechanical stress such as grinding (known as Viedma ripening),[33] numerous temperature cycles,[34] long exposure to ultrasound,[84] pressure stress,[85] microwaves[86] or a combination of grinding and photo irradiation for light sensitive racemizable compounds[58] are general methods enabling the evolution of the initial dual population of particles to a single population of crystals containing a single enantiomer only, i.e., deracemization. These methods operate close to thermodynamic equilibrium.

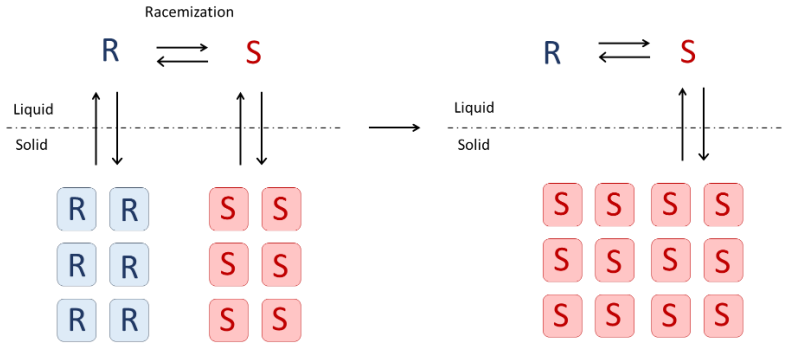

Figure 1.20: Schematic representation of the deracemization process

a. Viedma Ripening

In Figure 1.21, the isotherm shows the main feature of the process. V stands for the solvent, while S and R are the two enantiomorphic chemical entities. Due to the fast racemization in solution or simply the absence of chirality in solution, the attainable states of the system are inside the triangle S-R- L_{SAT} and along the racemic line V- L_{SAT}. L_{SAT} is the point representative of the saturated racemic solution at that temperature. Under strong enough continuous attrition, the initial doubly saturated suspension (composed of a solution LSAT and an equimolar mixture of pure chiral solids) represented by point I evolves towards F_R or F_S (Figure 1.21 A or B respectively). Simultaneously, the racemic mixture of solids represented by point M evolves towards S or R, i.e., the pure enantiomers. The tie lines connecting the constant saturated liquid L_{SAT}, the point representative of the overall synthetic mixture and the point representative of the solid composition move from L_{SAT}–I–M to L_{SAT}–F_S–R or L_{SAT}–F_R–S.

If the system does not contain any chiral impurity and the initial two populations of crystals are symmetrical in terms of Crystal Size Distribution (CSD) and Growth Rate Dispersion (GRD), the outcome of the evolution, that is, crystals of pure S or else pure R in equilibrium with L_{SAT}, is purely stochastic. Usually, the kinetics of this spontaneous evolution are of the first order. In other words, the logarithm of enantiomeric excess (e.e.) versus time is linear. The more the overall composition departs from 50–50 composition, the faster the evolution towards homochirality is. It is an auto-catalytic process. However, if the system contains chiral impurities, the growth and dissolution rates of the two enantiomers may become different, promoting one enantiomer over the other. The final evolution of Viedma ripening can be directed using a chiral impurity.[87]

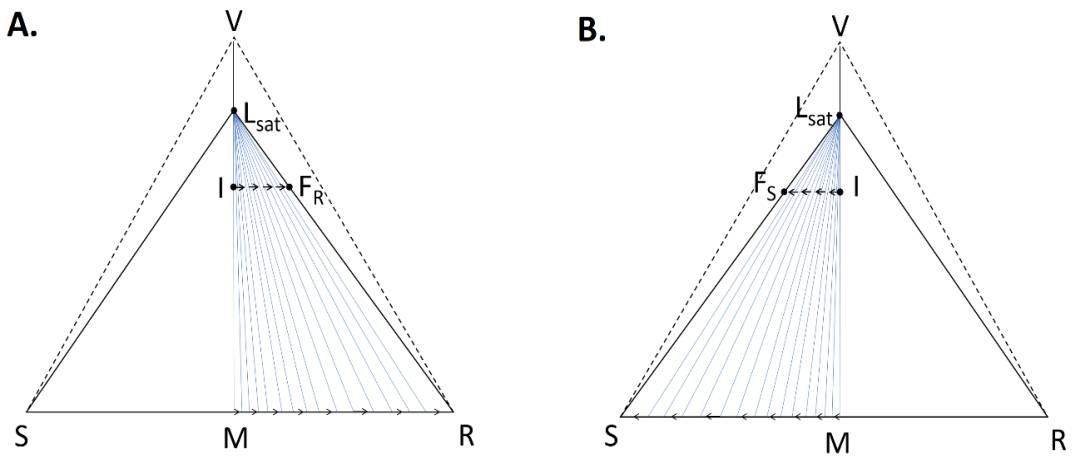

Figure 1.21: Spontaneous deracemization by Viedma ripening, ultrasound, microwaves towards the R enantiomer in A and towards the S enantiomer in B.

Viedma ripening can be implemented directly during synthesis; this method is called asymmetric synthesis, involving dynamic enantioselective crystallization.[88] For example, isoindolinones, a class of compounds used as core structures for pharmaceutical applications, were resolved successfully using Viedma ripening by the group of Vlieg.[89] Indeed, isoindolinones 1–3 (Figure 1.22) crystallize in a conglomerate-forming system and racemize quickly in solution without a catalyst.

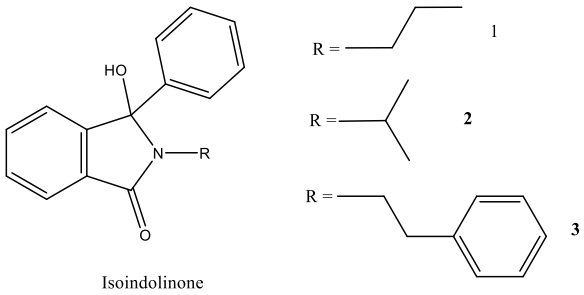

Figure 1.22: Isoindolinones that have been deracemized by Viedma ripening by Vlieg et al.[89]

b. Temperature Cycle-Induced Deracemization (TCID)

Repetitive temperature oscillations may also be used to induce deracemization towards pure enantiomers. This spontaneous process is known as Temperature Cycle-Induced Deracemization (TCID).[34] The temperature gradient could be in space[90] or in time, [91] or even both.[92] Figure 1.23 schematizes the principle of deracemization by TCID through the corresponding phase diagram, which illustrates the evolution of the system when the temperature of the whole system fluctuates between T_L and T_H, the low and high

temperatures, respectively. The inset of Figure 1.23 shows the racemic vertical section versus temperature M–V–T, starting from a suspension of composition I, composed of a racemic mixture M of pure enantiomers in equilibrium with their saturated solution at T_L. When the initial suspension I withstands repetitive thermal oscillations of the suspension from T_L to T_H back and forth, it undergoes partial dissolution and recrystallization cycles leading to complete deracemization (i.e., chiral symmetry breaking). The overall synthetic mixture evolves towards $F_{R/H}$ at T_H and $F_{R/L}$ at T_L. Simultaneously, the composition of the solid phase evolves towards the pure enantiomer R (or S; the latter case is the mirror image of the one represented in Figure 1.23). Here, only the evolution to R is represented, but, in the absence of any chiral bias, the system can evolve to S as well.

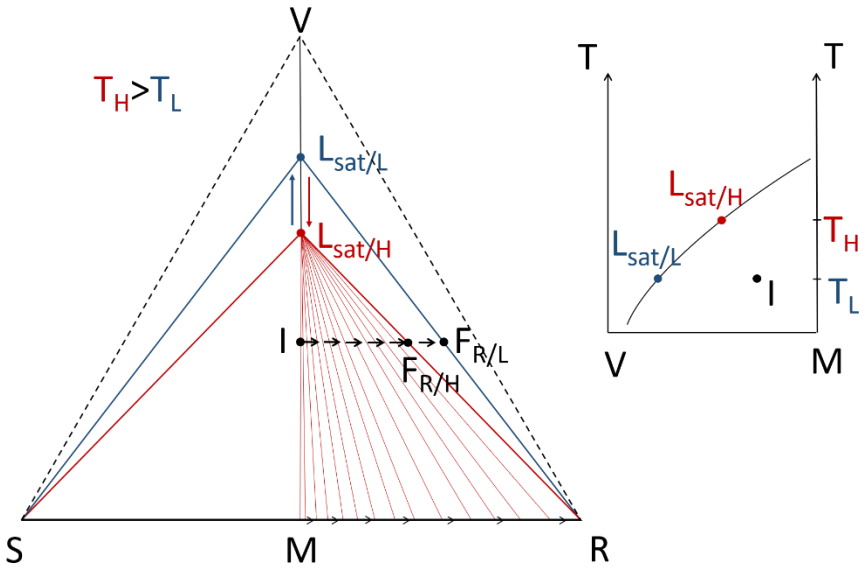

Figure 1.23: The TCID experiment

The temperature-time profile must be precisely tuned to achieve efficient deracemization and to maximize productivity, while chemical degradation, if present, should be minimized. The variation in solubility versus temperature is, of course, an important factor, but the cooling rate is also important for the generation of small nuclei via secondary nucleation. These dissolution and growth cycles contribute to the turnover of the conglomerate into one of the two populations of crystals.[93] Once the e.e. of the solid phase strongly departs from zero, it is beneficial to decrease the amplitude of the temperature oscillation. The damped temperature oscillation avoids wasting time and energy by preventing significant dissolution of the enantiomer in excess.[94]

TCID was used to produce pure enantiomers of a precursor of paclobutrazol, a molecule of interest because of its role as a plant growth inhibitor (Figure 1.24).[91] In this case, the temperature fluctuations range between 20 °C and 25 °C or 30 °C and racemization is induced by a basic medium (e.g. sodium hydroxide).

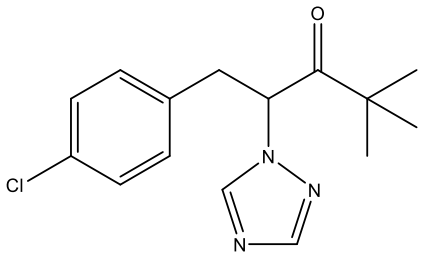

Figure 1.24 : 1-(4-chlorophenyl)-4,4-dimethyl-2-(1H-1,2,4-triazol-1-yl)pentan-3-one, a precursor of paclobutrazol, which served as a model compound for TCID.

c. DIFECS overview

In addition to mechanical or thermal energy fluxes (see above), other energetic fluxes passing through the suspension lead to complete deracemization (Deracemization Induced by a Flux of Energy Crossing the Suspension (DIFECS)). For instance, periodic variations in pressure[85] or pressure and temperature,[95] microwaves,[86] and photons for light-sensitive molecules[58] have proved to induce complete chiral symmetry breaking. This is not an exhaustive list. In addition, the mentioned stimuli have agonist effects and can be combined to speed-up macroscopic chiral symmetry breaking.[96] The common features of these processes are that they are operated close to thermodynamic equilibrium with a stochastic character regarding the final outcome, obtaining either R or S crystals. This does not mean that the predominant mechanisms are all the same. For instance, the application of ultrasound could be faster than attrition to induce complete deracemization, and produces bigger final crystals.[84] The agonist effects observed when various fluxes of energy are applied, seem more consistent with several –concomitant– possible mechanisms of deracemization.

Usually, the kinetics of all DIFECS methods are of the first order and several mathematical models have been proposed that fit reasonably well with the sigmoid shape of e.e. variation in the solid versus time.[97–101] It is worth noting that there is an initial period without a noticeable evolution in the e.e. of the solid phase. However, the CSD (Crystal Size Distribution) and GRD (Growth Rate Dispersion) and probably other solid-phase attributes change during that period. This first step ends with what is called the “take-off”. Kinetics plays a substantial role here, e.g., the system can remain sitting on the “racemic fence” for several days before the take-off. This phenomenon illustrates the stochastic aspect of spontaneous symmetry breaking.

DIFECS has been proven to be suitable for general application, provided that the two following conditions are fulfilled: a conglomerate is in equilibrium with a doubly saturated solution and the chemical entities undergo rapid racemization in solution.

Lamellar epitaxies between crystals of opposite handedness could be a serious problem for Preferential Crystallization (see part 1.3.3).[53] The remedy is to rely on DIFECS, which has been proven to achieved 100% e.e. even when the crystals of the two enantiomers can produce repeated epitaxies showing the strength of this technique.[102]

1.3.1.2 Kondepudi's experiment

Kondepudi's experiment[103] is another illustration of spontaneous chiral macroscopic symmetry breaking applying crystallization in a conglomerate-forming system with racemization in the molten or solution state. Figure 1.25 illustrates this experiment. Typically, a racemic solution is cooled down with an appropriate cooling rate in a stirred medium. If the system is able to generate a single nucleus (the "Eve" crystal) for a sufficient period of time and if the stirring rate and stirring mode[104] are adequately tuned, numerous offspring crystals will be created by its collision with the stirrer or the reactor wall leading to fast secondary nucleation, which results in a drop of the supersaturation. In the inset of Figure 1.25, the temperature versus composition pathway of the mother liquor is represented. This is the racemic section as the liquid phase cannot deviate from enantiomeric excess (e.e.) = 0 because of the racemization. The points K_1, K_2 and K_M represent different nucleation points at different cooling rates. In this experiment, I-K_1-LSAT and I-K_2-LSAT pathways lead to homochirality of the solid phase. At the end of the process, a homochiral population of crystals will have been generated that are all descendants of the "Eve" crystal. Ideally, by repeating numerous experiments, the results should be a random series of pure (−) and (+) crystals populations of which the distribution is statistically close to 50–50%. By contrast, K_M corresponds to an excessive undercooling which leads to several quasi-simultaneous primary nucleation events and thus a heterochiral final population of crystals.

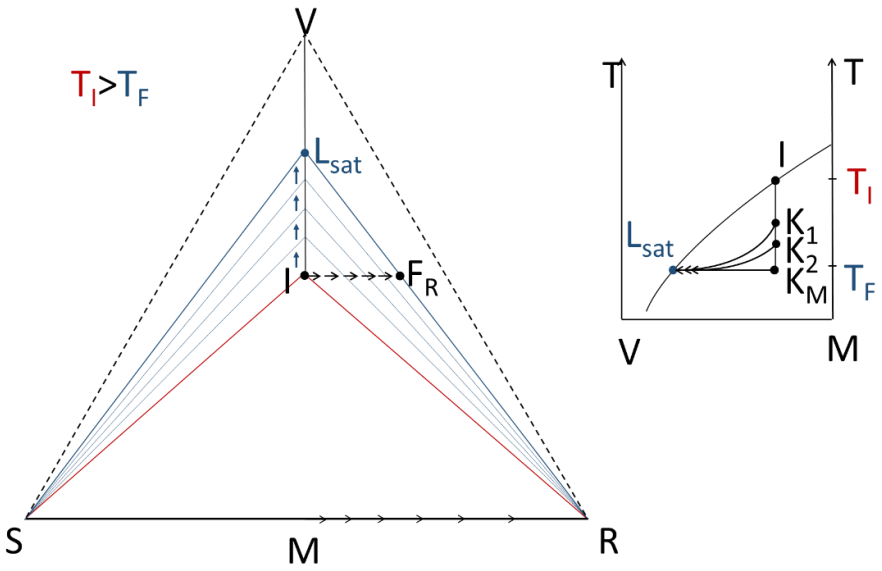

Figure 1.25: Kondepudi's experiment

This process was first described by Kondepudi, who found that spontaneous symmetry breaking occurs upon crystallization of sodium chlorate in stirred solutions, whereas static conditions give an equal amount of L and D crystals.[105] Kondepudi's experiment is also applicable to the molten state, as a supercooled melt of 1,1'-binaphthyl has been shown to crystallize with a large enantiomeric excess when vigorously stirred.[106]

1.3.2 Control of macroscopic chiral symmetry breaking by means of crystallization

It is possible to direct symmetry breaking towards a desired enantiomer through several, robust methods. The general approach involves breaking the symmetry of the system purposely prior to the onset of crystallization. For instance, Deracemization Induced by a Flux of Energy Crossing the Suspension (DIFECS) will provide the eutomer (the desired enantiomer) by implementing a small bias, through an investment in the eutomer beforehand.[107] For example, only a small percentage of e.e. (S) in the solid state is sufficient to conduct the complete deracemization by using Viedma ripening, TCID, ultrasound, microwaves, etc., towards the S enantiomer as illustrated by Figure 1.26.

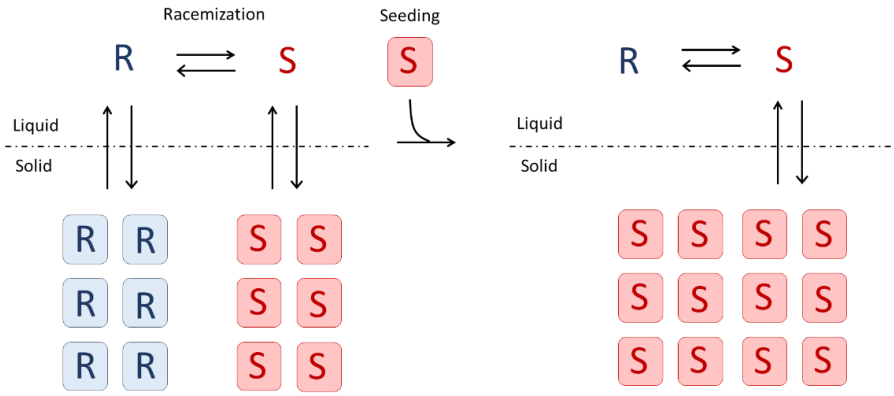

Figure 1.26: Schematic representation of controlled deracemization by enantiopure seeding

However, the presence of a chiral impurity in the system could compensate the initial purposely introduced bias.[108] This is illustrated by Viedma ripening of sodium chlorate (used as received; see Figure 1.27). The evolution is systematically towards the same chirality even if an initial investment in the counter enantiomer is performed. One experiment shows an evolution of up to 70% e.e. before reversing. A simple recrystallization of the initial racemic mixture in water is enough to remove the effect. It is likely that a small (maybe minute) amount of chiral impurity "pushes" the system towards the same chirality. This phenomenon has been observed with organic compounds too.[109] Dissymmetry in crystal size distributions is also able to systematically direct the symmetry breaking towards the population of bigger crystals. A study has shown that there is actually a relation between the initial e.e. and the dissymmetry of crystal size distributions.[110] Bigger crystals of (+) can, for instance, compensate a slight initial excess in small (−) crystals.[111]

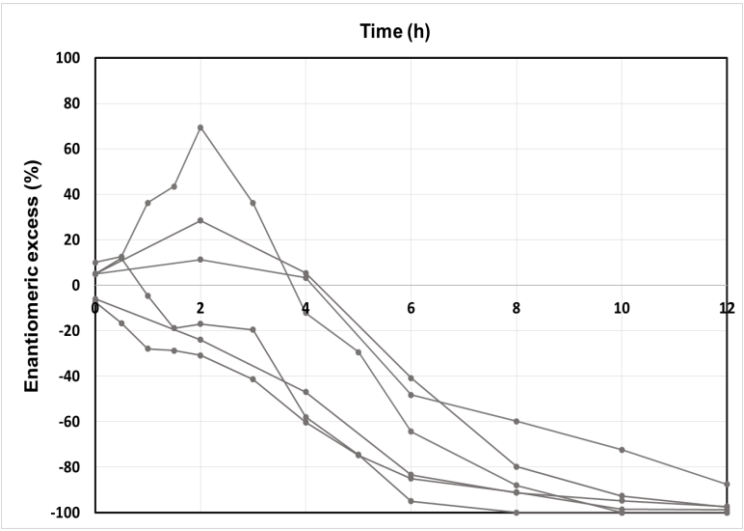

Figure 1.27: Impurity effect on the handedness of the attrition-enhanced deracemization in a non-recrystallized batch of sodium chlorate leading to the same pure enantiomer at every run.[40]

Kondepudi's experiments can also be controlled by the addition of specific chiral impurities, if a small amount of right-handed additive (called R* hereafter) is added to a racemic supersaturated solution of a conglomerate-forming system. If R* is sufficiently similar to R (R enantiomer of the compound to resolve), nucleation and growth of R and S will become significantly different, and precipitation leads to an excess of S in the solid. This effect is known as the rule of reversal.[112] Kondepudi's experiment, seeded with very pure enantiomer prior to any primary nucleation of either enantiomer, is equivalent to preferential crystallization. A detailed analysis of the process with different protocols for the inoculation of seeds and temperature profiles will be discussed in the next part of this chapter.

It is also possible to induce stereoselective nucleation by using a polarized laser beam in a supersaturated solution. This process, known as Non-Photochemical Laser Induced Nucleation (NPLIN), has received some attention.[113]

1.3.3 Preferential Crystallization

In contrast to the various deracemization techniques, the only requirement for preferential crystallization is a conglomerate forming system; no coupled racemization is needed. This stereoselective crystallization method allows crystallization of a single enantiomer from a racemic solution where both enantiomers are expected to crystallize simultaneously. In a slightly enriched mother liquor, a careful tuning of crystallization parameters leads to the transfer of one of the enantiomers from the mother liquor to the solid state, whereas the other enantiomer remains in the liquid. This process has been discovered by Gernez in 1866 when he seeded a racemic supersaturated solution of sodium ammonium tartrate tetrahydrate with enantiopure crystals, and noticed the crystallization of the single enantiomer identical to that inoculated.[7]

1.3.3.1 Preferential Crystallization principle

The principle of preferential crystallization is relatively simple, although the management of the parameters can be complex. Various modes exist but, in this work, only the Auto Seeded Polythermic Programmed Preferential Crystallization (AS3PC) mode has been studied. Its schematic representation is provided in Figure 1.28. Starting from the racemic solution, a bias is induced by introducing fine seeds of a single enantiomer (e.g. the R enantiomer, step 1 in Figure 1.28) and supersaturation (by cooling in this case) is induced to start the process. The enantiopure crystal seeds lead to stereoselective growth and secondary nucleation; during this period, the counter enantiomer remains in the supersaturated solution (step 2).

Subsequently, the solid is collected by filtration during the third step (the mass of solid recovered is generally about twice the mass of the initial excess).

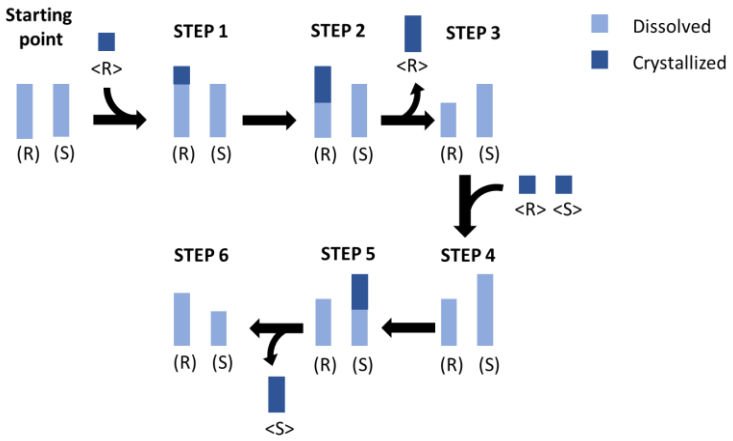

Figure 1.28: Schematic representation of preferential crystallization

To compensate the loss of R enantiomer, racemic mixture is added to the mother liquor (step 4), the quantity is precisely measured in order to return to the same supersaturation level as the initial point and the temperature is increased back to its initial point. Thus, the system is a mirror image of the initial situation (e.g. a mixture slightly enriched in S enantiomer). Temperature and supersaturation is precisely adjusted so that the system remains slightly supersaturated in the S-enantiomer, thus it is auto-seeded with S crystals. During the second cooling, the reverse phenomenon takes place: selective crystallization of the S enantiomer (step 5). Filtration will provide approximatively the same mass of solid as obtained in the first operation. Finally, the initial situation (i.e. a mixture enriched in R enantiomer) is obtained by once again the addition of racemic mixture (step 6).

In the case of PC, the symmetry of the system is purposely broken by the seeding, i.e. if the solid is the (+) enantiomer, the mother liquor evolves towards an excess of (−) in the absence of racemization. This occurrence is called the “entrainment” effect.[30] The induced symmetry breaking lasts for some minutes to some hours. If the system is left for too long, the second enantiomer starts to spontaneously crystallize so that the ultimate evolution of the system is a mixture of crystallized enantiomers in equilibrium with a doubly saturated racemic solution. Preferential crystallization is based both on thermodynamics providing the driving force of the crystallization and on kinetics giving the limit of the stereoselective crystallization (i.e. if the system exceeds the Ostwald limit, spontaneous nucleation of the counter enantiomer spoils the stereoselectivity of the crystallization).

Preferential crystallization has been successfully applied at the industrial scale to separate enantiomers of familiar compounds such as Esomeprazol[114] (which is a proton pump inhibitor sold under the name Nexium representing a billion dollar market),[115] or amino acids like threonine.[116]

1.3.3.2 The various modes of Preferential Crystallization

a. Seeded Isothermal Preferential Crystallization (SIPC)

Historically, PC was achieved in a single experimental step and the notion of recycling the mother liquor did not exist. A solution of racemic or purposely slightly enriched mixture is cooled down to obtain supersaturation. Seeds of one enantiomer (the eutomer) are then added at this metastable homogeneous doubly saturated solution to skip the primary nucleation and induce selective crystallization. Filtration is performed before the nucleation of the counter enantiomer to collect the pure desired enantiomer.

b. Seeded Polythermic Programmed Preferential Crystallization (S3PC)

Seeded Polythermic Programmed Preferential Crystallization (S3PC) evolved from SIPC. In order to increase the crystallizing enantiomer quantity, the temperature is cooled down once the solution is seeded. The same approach is used for the Auto Seeded Polythermal Programmed Preferential Crystallization (AS3PC) except that the mother liquor is recycled. Indeed, at the end of the first run, the mother liquor is slightly enriched in the mirror enantiomer, this enrichment can be used as “seeds” to induce the stereoselective crystallization of the mirror enantiomer in a second run. By addition of a precise mass of racemic mixture in order to compensate the loss, the second run can be carried out to crystallize the mirror enantiomer. Again, a third run would produce the same chirality as the first run. AS3PC was developed by Coquerel et al. in 1995.[117] The AS3PC allows a more precise tuning of the supersaturation than in SPIC or S3PC: one enantiomer crystallizes during cooling and the system is, thus, supersaturated in only one of the enantiomers. Crystal growth and secondary nucleation are favored. This method will be used in chapter 3, thus, it is important to note that it requires fine adjustments for which the following elements are of importance:

- The solvent: a medium solubility, a variation of solubility with temperature and a good chiral discrimination (e.g. no undesirable solvate leading to a racemic compound)

- The cooling and stirring rate: the cooling rate must be high. Faster cooling rates enlarge the width of the Ostwald metastable zone promoting crystal growth and secondary nucleation

over primary nucleation, the counter enantiomers primary nucleation is avoided. However, high cooling rates provide less control over the stereoselective crystallization and a shorter filtration window before the nucleation of the counter enantiomer which can be challenging. Regarding the stirring, it is important to homogenize the temperature and concentration of the system, however a high stirring rate with strong shearing forces can promote heteronucleation of the counter-enantiomer.

- The initial and final temperature: The temperatures must be adjusted to have a good variation of solubility to increase the yield. The higher the initial temperature, the better will be the yield. The final temperature is set by the stereoselective crystallization limit, below this temperature, the probability for the counter enantiomer to nucleate becomes too high.

- Finally, the crystal size distribution of the seeds has limited influence during the AS3PC process, but they must be fine enough and numerous.

c. Auto-Seeded Preferential Crystallization Induced by Solvent Evaporation (ASPreCISE)

In 2011, a new variation of PC was developed by Coquerel et al.: the Auto-Seeded Preferential Crystallization Induced by Solvent Evaporation (ASPreCISE).[118] The principle is similar except that supersaturation is induced by solvent evaporation.

1.3.3.3 Second-Order Asymmetric Transformation (SOAT)

Second-Order Asymmetric Transformation (SOAT, Figure 1.29) is a chiral symmetry breaking process by means of crystallization that could be regarded as an improved preferential crystallization (see above) for racemizable conglomerates.[19] If fast racemization takes place in the system (or in the absence of chirality in solution), the mother liquor cannot deviate from 0% e.e, as illustrated in Figure 1.16.

During a SOAT process, a supersaturated solution is seeded with enantiopure crystals (point I in Figure 1.29) to trigger stereoselective crystallization via crystal growth and secondary nucleation of the seed crystals. The inset of Figure 1.29 shows the temperature versus composition pathway of the mother liquor that remains racemic due to racemization reactions. Thus, the system is never more supersaturated in the distomer than in the eutomer. Point I does not belong to the isopleth section represented in the inset, as the seed crystals are enantiopure. The overall composition of the system evolves towards F_R at T_L while the composition of the solid phase evolves towards the pure enantiomer R upon cooling.

Supersaturation has to be kept within reasonable limits so that crystal growth and secondary nucleation remain stereoselective. Here, only the evolution to R is represented, but, the system can be directed towards S too. Since the mixture is initially far from the equilibrium in the final state, the SOAT process is generally a fast and productive process and could be two orders of magnitude more productive than any variant of DIFECS.[35]

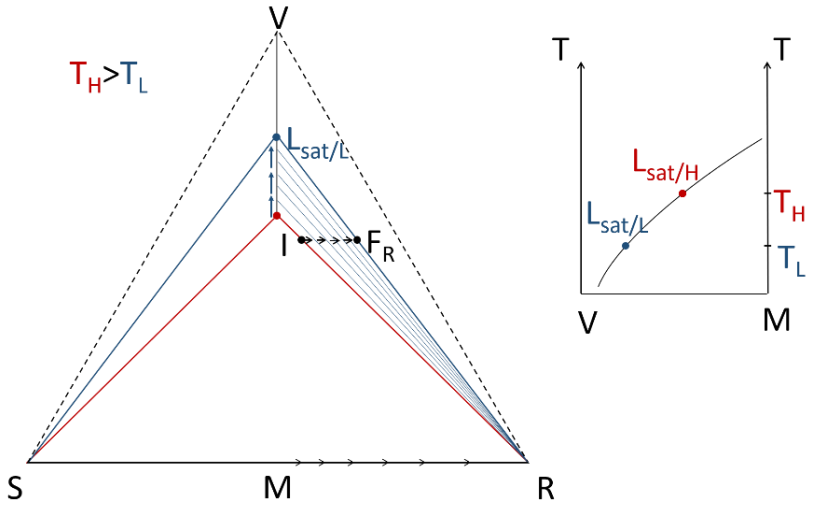

Figure 1.29: Second-Order Asymmetric Transformation (SOAT) experiment

In 1979, SOAT was used to resolve (DL)-α-amino-ε-caprolactam, a lysine precursor, with the racemization being induced by potassium hydroxide in ethanol at 80 °C (Figure 1.30).[119] Likewise, the enantiomers of the precursors of paclobutrazol, which served as an example for TCID, were also obtained in high enantiomeric purity with SOAT by Black et al. in 1989.[120]

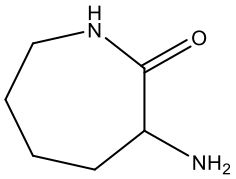

Figure 1.30: (DL)-α-amino-ε-caprolactam can be resolved by SOAT to produce enantiopure lysine after hydrolysis.

1.4 Conclusion

The need for pure enantiomers has accelerated since the nineties, when new pharmaceutical restrictions imposed by medicinal agencies resulted in a strict control over the activities and side effects related to enantiomers. Among the possibilities to produce pure enantiomers, one can directly synthesize the desirable enantiomer. If this is not possible or not economically viable, the resolution of the racemic mixture will need to be carried out after its synthesis.

Crystallization offers a variety of methods for the resolution of the racemic mixture (Viedma ripening, TCID, Preferential Crystallization...). Some of them coupled with racemization, offer a promising yield of almost 100%. Although the techniques -except preferential enrichment which has other requirements- are usually limited to conglomerate forming systems, it is possible to manage metastable equilibrium and resolve a metastable conglomerate when the system forms a stable racemic compound.[57,121] Moreover, a convenient technique for rapid screening of derivatives for conglomerate formation, using second harmonic generation has been developed, increasing the scope of applicability of crystallization-based resolution methods.

2. A disappearing conglomerate: BINOL-OBn

The content of this chapter has been published in Crystal Growth & Design, a peer-reviewed journal, by Hoquante, M.; Sanselme, M.; Rietveld, I. B. and Coquerel, G. in 2019.[122]

2.1 Introduction

1-1'-Binaphtyls[123] and particularly 1-1'-Bi-2-naphtol (BINOL) and some of its derivatives are known to photoracemize in solution.[124,125] In 2016 Maria et al[126] reported the crystal structure of 2'-benzyloxy-1-1'-binaphtalene-2-ol (BINOL-OBn, Figure 2.1) and investigated the phase diagram of binary enantiomer mixtures. The system crystallizes in a $P2_12_12_1$ space group (reference code UBULUB, CCDC 1443741) meeting the crystallographic requirement to reach homochirality in a deracemization process. Previously, Takahashi et al. reported the melting points of the pure enantiomer and of the racemic mixture, respectively 122°C and 103°C implying the presence of a eutectic transition at the racemic composition.[127] Because of its conglomerate, which makes the system amenable for resolution by crystallization, BINOL-OBn seemed to be a good candidate for any variant of Deracemization Induced by a Flux of Energy Crossing the Suspension (DIFECS) see part 1.3.1.1 for more information.

BINOL-OBn is an atropisomer, which means that it exhibits axial chirality. The rotation of the bond connecting the two naphthyl groups is inhibited because of the steric hindrance caused by the two oxygen groups so that two conformers can be isolated.

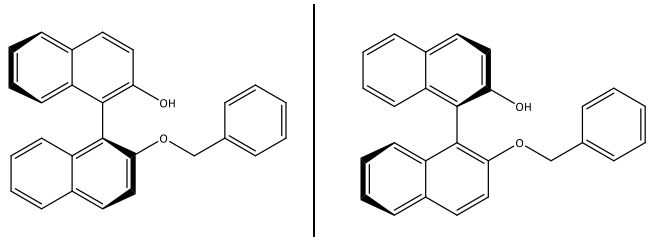

Figure 2.1: Cram's representation of the two enantiomers of 2'-benzyloxy-1-1'-binaphtalene-2-ol

2.2 Synthesis and characterization

Pure R enantiomer, S enantiomer and racemic BINOL-OBn were synthesized according to a previously reported procedure.[128] Pure enantiomers of BINOL and its racemic mixture were subjected to a Mitsunobu coupling reaction to convert one of the hydroxy group into an ether using triphenylphosphine (PPh_3) and an oxidizing azo reagent in the form of an azodicarboxylate like diisopropyl azodicarboxylate (DIAD).

The typical protocol of a Mitsunobu reaction is to add the phosphine and azodicarboxylate together until the formation of the ylide. Then solutions containing the nucleophile on one side and the alcohol on the other side are added together and the reaction medium is usually heated to reflux. The alcohol reacts with the phosphine to create a good leaving group and then undergoes an inversion of stereochemistry in classic SN_2 fashion as the nucleophile displaces the leaving group. Besides the desired coupled product, a hydrazide such as diisopropyl hydrazinedicarboxylate (DIAD-H2) from DIAD and a phosphine oxide such as triphenylphosphine oxide from PPh_3 are also formed as by-products.[129]

Herein, we use an expedient method for the monoetherification of BINOL in agreement with some modifications of the Mitsunobu procedure previously reported (Figure 2.2).[128] Interestingly, no inversion of the stereogenic center was observed on the derivatives of Binol atropisomers and the stereochemical profile of the reaction was only dependent on the stereochemistry of BINOL used as the starting material.[127]

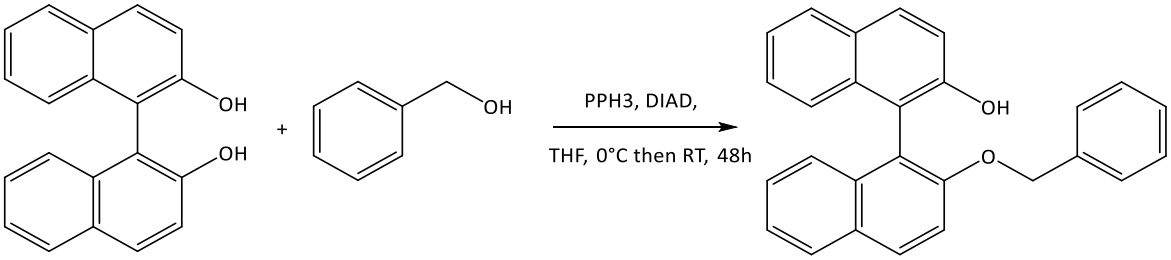

Figure 2.2: Synthesis of racemic BINOL-OBn

As the reaction is sensitive to water (R)-BINOL (5.0 g, 17 mmol) was dried azeotropically with toluene. It was dissolved in 100 ml of distillated tetrahydrofuran (THF), triphenylphosphine (PPh_3) (4.5 g, 17 mmol) and benzyl alcohol (2.1 ml, 20 mmol) were added to the stirred solution. Diisopropyl azodicarboxylate (DIAD) (3.35 ml, 17 mmol diluted in THF 5 ml) was slowly added dropwise, at 0 °C and then the mixture was stirred at room temperature for 48h. The reaction's progress can be followed by TLC (CH_2Cl_2/n-hexane 2:1). After near completion, the reaction was quenched by addition of a few drops of distilled water. The solvent was

evaporated under reduced pressure and the crude mixture was dissolved in dichloromethane (50 ml). The organic layer was washed with water and brine (3×50 ml). The organic layer was then dried over anhydrous $MgSO_4$. After solvent removal under reduced pressure, the product BINOL-OBn was isolated by column chromatography on silica gel, using a gradient mixture of CH_2Cl_2/n-hexane as eluent, and further purified by crystallization from CH_2Cl_2/n-hexane. (Colorless crystals, 5.696 g, 89% yield).

The Mitsunobu coupling on enantiopure BINOL gave satisfying results, however, the synthesis of racemic BINOL-OBn first gave rise to a viscous oil and crystallization was not straightforward despite the absence of an apparent purity problem. However, after a month at room temperature, a stable racemic compound appeared. This new racemic compound was characterized by means of Differential Scanning Calorimetry (DSC), InfraRed spectroscopy (IR), Powder X-Ray diffraction (PXRD), Second Harmonic Generation (SHG) and Single Crystal X-Ray Diffraction (SC-XRD).

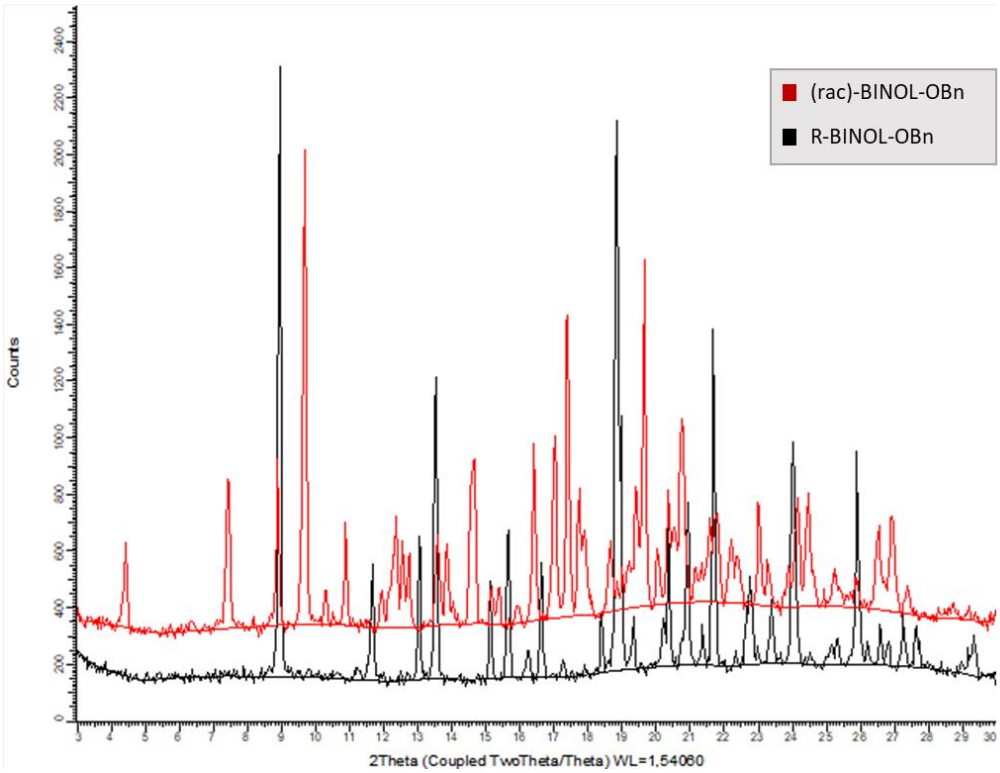

Figure 2.3: X-Ray powder diffraction patterns of racemic and enantiopure BINOL-OBn

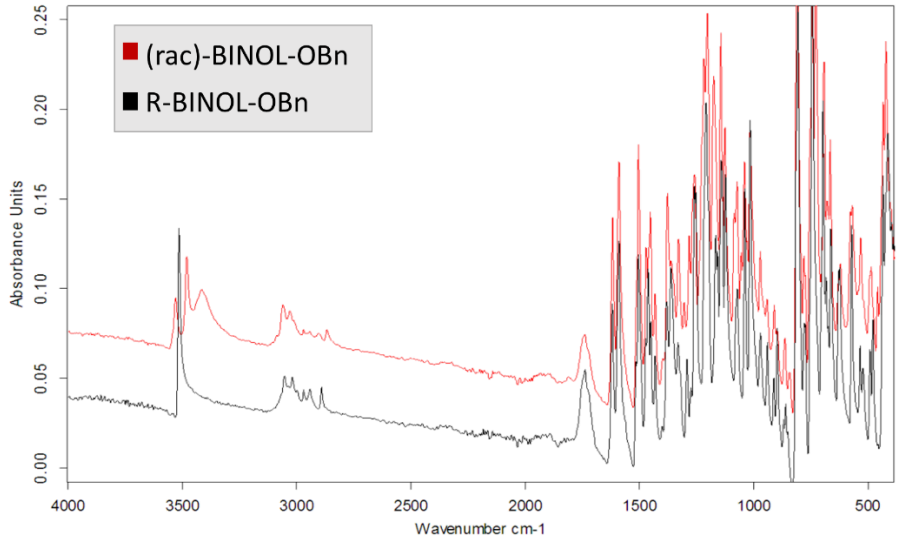

Figure 2.4: Infrared spectra of racemic and enantiopure BINOL-OBn

Clearly, the PXRD patterns of the enantiopure and of the racemic crystals do not overlap (Figure 2.3). Moreover, the infrared spectrum of the racemic compound (Figure 2.4) shows three bands for the OH stretching vibrations at vOH = 3413 cm^{-1}, vOH = 3482 cm^{-1} and vOH = 3529 cm^{-1} implying that there are three hydroxyl groups with different interactions in the structure, whereas for the enantiopure structure a single OH stretching band exists at vOH = 3515 cm^{-1}. The differences between the spectra and diffraction patterns prove the existence of two different phases of which the (rac)-BINOL-OBn has never been observed before. The centrosymmetry of the crystals was investigated by SHG. While irradiating at 900 nm, no SHG signal at 450 nm was observed confirming the heterochiral packing of this new phase.

2.3 Phase diagram

Considering the appearance of the racemic compound, the previously reported phase diagram needed to be revised. Pure enantiomer, racemic compound and their mixtures were analyzed by DSC (heating rate = 5 K/min), the resulting curves can be found in the appendices. Mixtures with different enantiomeric compositions were prepared by manual grinding assisted by a small amount of solvent either between the pure R enantiomer and the racemic compound or between the pure enantiomers together. Similarly, an artificial conglomerate was prepared by mixing rigorously weighted 200 mg of (R)-BINOL-OBn crystals and 200 mg of (S)-BINOL-OBn crystals and the physical mixture was gently grinded. The results are summarized in Table 2.1 and Table 2.2. Only one side of the phase diagram was investigated due to the mirror relationship between the two atropisomers.

Table 2.1: Temperature of solidus and liquidus for binary mixtures between the pure enantiomer and the racemic compound of BINOL-OBn

$x_{(R)\text{-BINOL-OBn}}$	$T_{solidus}$ /K	$T_{liquidus}$ /K	Enthaply of fusion /J.g^{-1}
1		393.8[a]	76.9 ± 5[a]
0.919	380.2	391.2	
0.872	381.4	388.1	
0.791	381.6	386.0	
0.752	382.1	382.4	
0.656	382.1	386.9	
0.57	383.1	388.4	
0.5		388.8[a]	79 ± 5[a]

[a] Results are the mean of n = 4 experiments. Temperatures are given with an uncertainty of ± 0.5K.

Table 2.2: Temperature of solidus and liquidus for metastable binary mixtures between the pure enantiomers R and S-BINOL-OBn

$x_{(R)\text{-BINOL-OBn}}$	$T_{solidus}$ /K	$T_{liquidus}$ /K	Enthaply of fusion /J.g^{-1}
1		393.8[a]	76.9 ± 5[a]
0.817	364.6	385.7	
0.62	366.2	376.6	
0.5	365.1		72.7 ± 5

[a] Results are the mean of n = 4 experiments. Temperatures are given with an uncertainty of ± 0.5K.

The liquidus of the racemic compound was calculated using its melting point (388.7 ± 0.5 K) and enthalpy (79 ± 5 $J.g^{-1}$) assuming an ideal behavior (Prigogine-Defay).[130] The metastable eutectic liquid between the pure enantiomers corresponds to the racemic composition ($x_{metastable\ eutectic}$ = 0.5) with a melting temperature experimentally found at 365.1 ± 0.5 K, equal within error to the temperature obtained by the intersection of the Schröder equation ($T_{calculated\ eutectic}$ = 366 ± 1 K) for the liquidus lines of the R and S enantiomers. The eutectic transition between the enantiomer and the racemic compound is obtained through the intersection of the two equations (Prigogine-Defay for the racemic compound liquidus and Schröder for the liquidi of the pure enantiomers) at 382 ± 1 K and it was experimentally found at 381.7 ± 0.5 K indicating no significant deviation from ideality. The phase diagram for the BINOL-OBn system based on these equations and confirmed by experimental points, is shown in Figure 2.5.

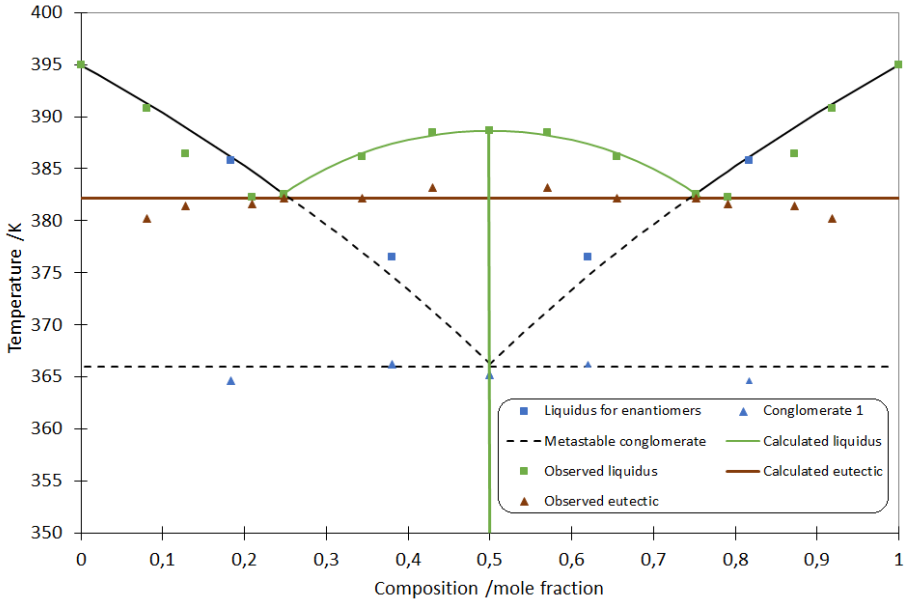

Figure 2.5: Binary phase diagram of BINOL-OBn based on the experimental data in Tables 1 and 2. The liquidus lines of the enantiomers are obtained by the Schröder equation and the liquidus line of the racemic compound has been calculated with the Prigogine-Defay equation. They have not been fitted to the liquidus points.

To test the stability of the conglomerate versus the racemic compound, 'artificial' conglomerate was prepared mixing powdered crystals of R and S enantiomers rigorously respecting the <1-1> composition. A cross-seeding experiment was conducted at -10°C in diethyl ether. After 48 hours, the diffractogram showed that the suspension was exclusively composed of the racemic compound indicating that it is the stable phase at -10°C (Figure 2.6). Therefore, BINOL-OBn is not amenable to resolution by preferential crystallization.

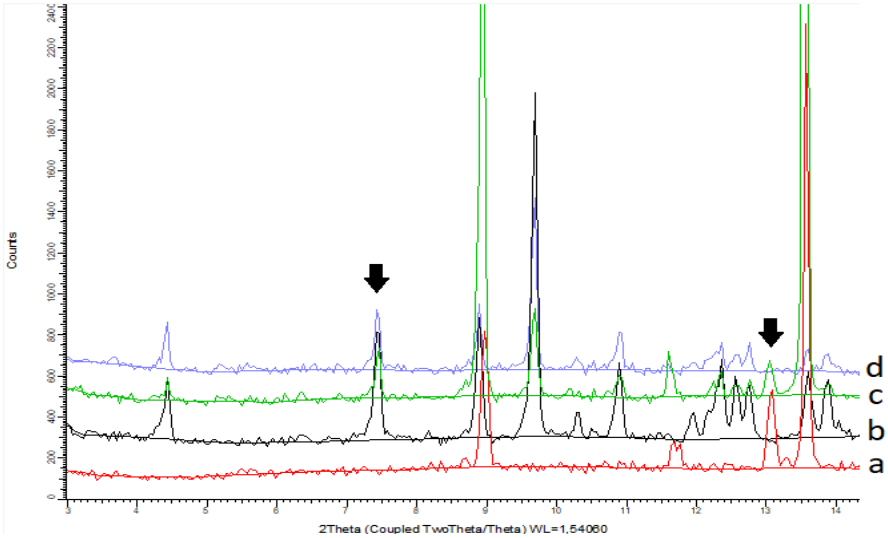

Figure 2.6. Diffractograms of a) (R)-BINOL-OBn, b) (rac)-BINOL-OBn, c) cross-seeding experiment after 6 hours, d) cross-seeding experiment after 48 hours.

Taking into consideration the cross-seeding experiment and the fact that the racemic compound has a melting point of 115.6 ± 0.5°C with a melting enthalpy of 79 ± 5 J/g, whereas the eutectic temperature of the conglomerate is found at 92°C with a melting enthalpy of 73 ± 5 J/g, the racemic compound is clearly the more stable phase at room temperature. It is even likely that this stability is 'monotropic' in nature (i.e. the phase is stable over entire temperature range), considering that the melting enthalpy of the racemic compound appears to be 6 J/g higher than that of the conglomerate –however, strictly speaking this is not polymorphism since the following irreversible transformation (ΔG < 0): <S> + <R> → <RS> involves three solid phases, nevertheless, by analogy with a genuine monotropy we use that term. Nonetheless, the enthalpies have overlapping experimental errors, so a stable temperature domain for the conglomerate below – 10°C cannot entirely be excluded (through a eutectoid invariant).

It is surprising however, that the conglomerate has been observed in the first place and even by two groups independently,[126,127] because the newly identified racemic compound melts more than 20 degrees higher than the racemic conglomerate and is the more stable form at room temperature. The complexity of the structure of the racemic compound with three molecules possessing different conformations in the asymmetric unit (Z' = 3) might justify this behavior.

2.4 Structural aspects

Single crystals of (rac)-BINOL-OBn were obtained by evaporation crystallization from chloroform/n-hexane and the crystalline structure was resolved by single crystal X-ray diffraction.

Table 2.3 Crystal data for (rac)-BINOL-OBn compared to the pure enantiomer

	(rac)-BINOL-OBn	(S)-BINOL-OBn[126]
CCDC Ref code	1949382	1443741
Molecular Weight / g.mol^{-1}	376.4	376.4
Crystal System	Monoclinic	Orthorhombic
Space Group	$P2_1/n$	$P2_12_12_1$
Z, Z'	12, 3	4, 1
a / Å	10.2821(7)	8.4850(3)
b / Å	40.035(3)	11.3174(3)
c / Å	14.808(1)	20.5379(7)
β / °	92.216(2)	
V / Å^3	6091.0(7)	1972.22(12)
d_{calc} / g.cm^{-3}	1.231	1.264
F(000) / e$^-$	2376	788
Absorption coefficient μ (MoKα_1) / mm^{-1}	0.076	0.079
Temperature / K	293	293 ± 2

As shown in the crystallographic data collected in Table 2.3, in the crystal lattice of the racemic compound, three independent molecules with different conformations are present in the asymmetric unit (see Figure 2.7) as inferred from the infrared spectrum (Figure 2.4). When considering the energies of isolated molecules in vacuum, one of the conformations displays a higher energy than the others (about 1.3 times higher for so-called MolA represented in yellow in Figure 2.7). The other two conformations (MolO and MolB) form dimers together through hydrogen bonds (Figure 2.8). These dimers exhibit π - π interactions with adjacent dimers along the c axis giving rise to periodic bond chains (PBCs) in this direction (Figure 2.9). The interaction between adjacent PBCs along the *b* and *a* axes is ensured by MolA through π - π interactions. The packing diagram is shown in Figure 2.10.

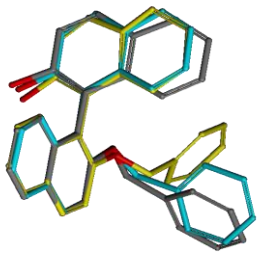

Figure 2.7: The three independent molecules in (rac)-BINOL-OBn asymmetric unit (MolA in yellow, MolO in blue and MolB in grey)

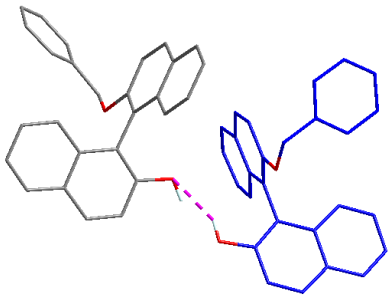

Figure 2.8: One dimer formed by the hydrogen-bond interaction (dashed pink line) between MolO (blue) and MolB (grey)

Whereas the pure enantiomer structure contains only π - π and Van der Waals interactions, the racemic compound exhibits hydrogen bonding too. The cost in energy required to put one third of the molecules in the conformation A and the global lower density seems balanced by the gain in stability created by hydrogen bonds. However, kinetically this new phase is not favored because of the lower probability for the molecules to occur in three different conformations during crystallization, which may in particular be difficult for conformation A. This could explain why a metastable conglomerate has been observed before the racemic compound. The belated crystallization of the racemic BINOL-OBn is reminiscent of the molecules discussed in the papers by Bernstein on disappearing polymorphs mostly involving molecules that can adopt different conformations (i.e. conformational freedom).[131–133] This case shows that the lack of hydrogen bonds in the conglomerate and the flexibility of the molecule are telltale signs of the possible crystallization of a racemic compound.

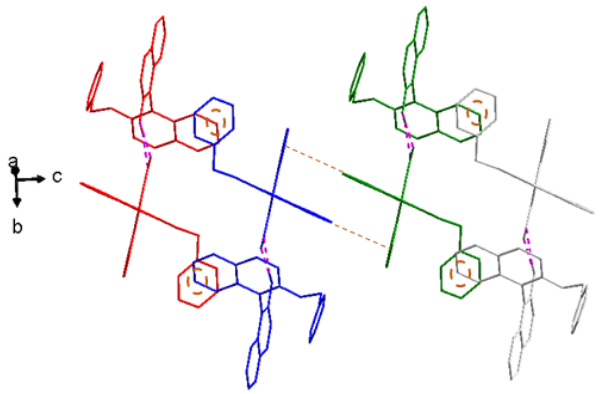

Figure 2.9. Consecutive dimers (red, blue, green and light grey) along *c*, establishing π interactions (dashed red lines) at multiple points forming a PBC

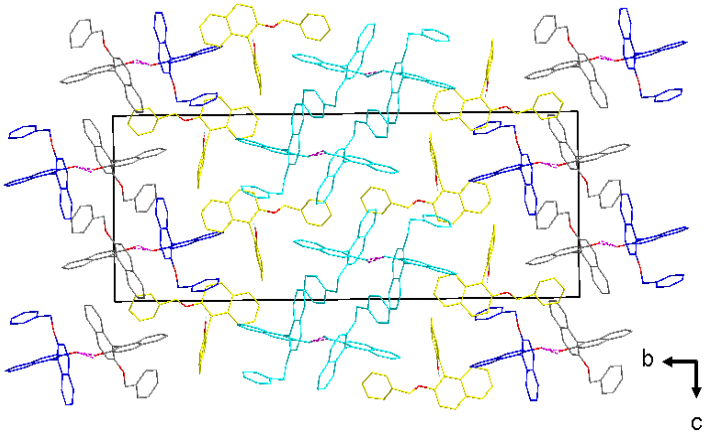

Figure 2.10. Projection along *a* of the cell packing diagram (one ribbon is displayed in light blue, in yellow MolA)

It is possible to anticipate this threat by challenging the stability of the conglomerate phase implementing the following procedure:

(i) Introduce as many variations of crystallization as possible with oscillatory physical stimuli (temperature cycling, spells of ultrasounds, rubbing effects on the inner wall of the container, different solvents and supersaturation, etc.).

(ii) Use different routes for the synthesis of the racemic mixture. Indeed, different impurity profiles could change the nucleation and crystal growth rates drastically.

(iii) Seed with racemic compounds of related chiral molecules.

(iv) Compute possible racemic compounds especially with common space groups (e.g. $P2_1/c$; P-1; C2/c) and with Z'>1 and different conformations and assess their energies versus the energy of the pure enantiomer.

(v) Above all, the time is essential here as a metastable form can be kinetically favored.[134]

So far, the 'reappearing' conglomerate has not been observed. Considering its relative stability, it will not be easy to obtain it again, even if it has been demonstrated that it is possible to obtain and to work on a metastable phase once a more stable one has been observed.[135] To do so, the right experimental conditions must be found (e.g. a solvent or an impurity that inhibits the formation of nuclei of the stable form).[57,136,137]

Before adding some concluding remarks, it should be noted that independently and simultaneously to the present study, Vlieg's group obtained the same results. In addition, they found a metastable conglomerate solvate which could be deracemized by Viedma ripening in an alkali medium.[58]

2.5 Conclusion

This work demonstrates that pure racemic BINOL-OBn, as is, does not constitute a suitable system for deracemization because, contrary to earlier reports, a racemic compound appears to be more stable than the conglomerate. The melting point of the racemic compound exceeds by 20°C the eutectic temperature of the conglomerate. However, an alternative conglomerate can be obtained with an appropriate solvent or coformer.[58] As with any crystallization process, it is difficult to predict such behavior and chemists should be aware of the possibility that a more stable form may appear. The risk may be more pronounced if the crystal structure mainly depends on Van der Waals interactions, whereas H-bond donors and acceptors are available in the molecule in particular when combined with molecular flexibility.

3. Continuum between supramolecular and intrinsic chirality: Transfer of chirality between a sulfoxide and its corresponding prochiral sulfone

3.1 Introduction

Sulfoxides are chemical compounds containing a sulfinyl functional group bonded to two carbon atoms (Figure 3.1). The sulfur atom possesses 16 electrons; its valence band configuration is $3s^2$, $3p^4$ so its valence could be expected to be 2 like oxygen just above it in the same column or group of the periodic table of elements. It is usually 4 to 6, so sulfur is hypervalent. As is the case for the sulfoxide, in which additionally a lone pair of electrons can be found in a molecular orbital on the sulfur atom, giving it a tetrahedral geometry and a trigonal pyramidal shape similar to an sp^3 hybridized carbon. If the R and R' groups (Figure 3.1) are inequivalent, the sulfur atom will be a stereocenter. The energy barrier required to invert this chiral center is sufficiently high so that sulfoxides are usually optically stable at room temperature.[138,139] The activation enthalpy of racemization is found between 35 to 42 kcal/mol, while for allylic and benzylic substituents, the activation barriers are lower.[140] The Cahn-Ingold-Prelog priority rule applies to decide the stereochemistry of chiral sulfoxide compounds with the lone pair of electrons assigned as the lowest priority group.[141]

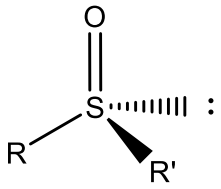

Figure 3.1: Sulfoxide group

Chiral sulfoxides are efficient chiral auxiliaries able to promote important asymmetric transformations. Since the 80's, they are frequently used in asymmetric synthesis, the chiral sulfinyl group being seen as one of the most efficient and versatile chiral controllers in C−C and C−X bond formations.[142] Therefore, the production of enantiopure sulfoxides became an area of considerable interest.[143–145]

Besides their application in asymmetric synthesis, chiral sulfoxides are also encountered as Active Pharmaceutical Ingredients (API) in their enantiopure form.[141] One can cite the examples of esomeprazole (medication which reduces stomach acidity),[146] armodafinil (a stimulant approved for treatment of sleep disorders),[147] aprikalim (an antihypertensive drug)[148] or whether oxisurane (an immunosuppressor).[149,150] Among them, enantiomers of armodafinil[151] and omeprazole[114] have been separated in industrial scale by preferential crystallization.

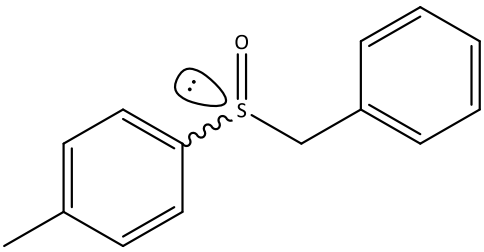

Figure 3.2: Cram's representation of 1-(benzylsulfinyl)-4-methylbenzene

In 2008, Fuller et al. investigated the structures of a range of sulfoxides containing aryl and alkyl substituents.[152] Among them, they found that benzyl phenyl sulfoxide (Figure 3.2) crystallizes in a $P2_12_12_1$ space group (i.e. a chiral space group) with Z'=1 (i.e. there is only one molecule in the asymmetric unit, excluding the possibility of a kryptoracemic compound) implying a chiral discrimination in the solid state. Moreover, this sulfoxide possesses two different substituents; thus, the sulfur atom is a stereocenter implying that it crystallizes in a conglomerate forming system. Accordingly, the system meets the crystallographic requirement for resolution by crystallization, which attracted our interest.

It is worth noting that the nature of the S=O bond is debated. Compared to other molecules with an equivalent C=O bond, it shows atypical behavior. Unlike carbon, sulfur does not form a typical π bond with oxygen[153] and its bond possesses significant ionic character as depicted in Figure 3.3.[154]

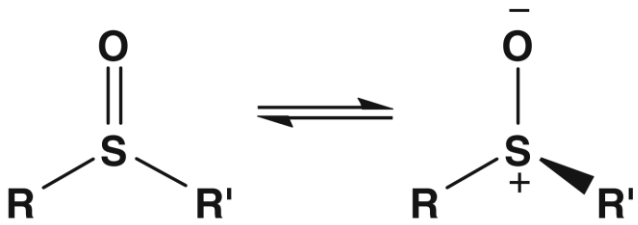

Figure 3.3: Two resonance structures of the sulfoxide bond

3.2 Synthesis

Benzyl 4-methylphenyl sulfoxide (hereafter called the sulfoxide) is obtained through a two-step synthesis (Figure 3.4): first alkylation of the thiol is carried out in a green medium to produce a sulfide, followed by the oxidation of the sulfide to sulfoxide in the presence of hydrogen peroxide.

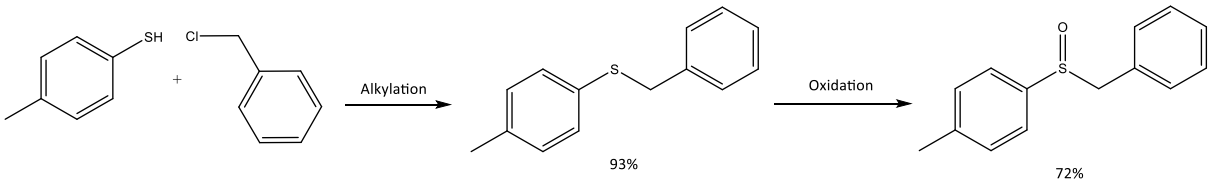

Figure 3.4: Synthetic route to benzyl 4-methylphenyl sulfoxide

The first part of the synthetic route, the alkylation represented in Figure 3.5, is conducted according to a procedure previously reported by Azizi et al.[155] The synthesis was first conducted at a small scale (3 mmol) with a yield of 96% and reproduced at a bigger scale afterwards (60 mmol) with a very acceptable yield of 93.9%.

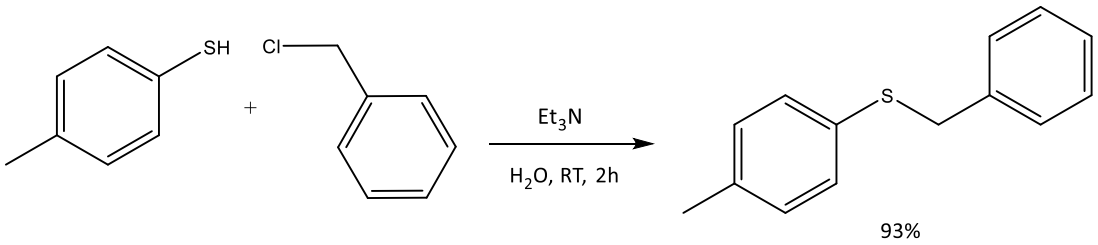

Figure 3.5: Alkylation of the thiol

To a mixture of benzyl chloride (7.595 g, 60 mmol) and *p*-thiocresol (7.452 g, 60 mmol), in water (40 ml), Et_3N (8.64 ml, 64 mmol) was added and stirred at room temperature for 2 hours. The progress of the reaction was monitored by TLC. The thioether was extracted by ethyl acetate (EtOAc) and dried over $MgSO_4$. Evaporation of the organic layers under reduced pressure afforded the desired product as a colorless oil that crystallizes upon standing (56.37 mmol, 12.984 g). Drying under reduced pressure needs to be carried out with care since this compound is prone to sublimation.

The second part of the synthetic route, i.e. the oxidation of the sulfide to the sulfoxide, has received some attention in the past decades because it can be challenging to stop the oxidation at the sulfoxide and not to overoxidize the sulfide into a sulfone.[156–160] Among the

oxidation methods, cyanuric chloride promoting oxidation in the presence of hydrogen peroxide suggested by Lakouraj et al.[159] gave the best results (Figure 3.6). Several batches of oxidation were necessary to produce sufficient sulfoxide for our investigations. This is due to difficulties with scaling-up of the reaction; a 10 mmol scale proved to be an acceptable balance between the amount of side products and yield of desired product.

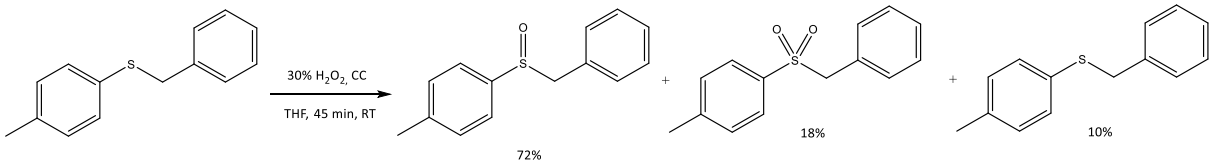

Figure 3.6: Oxidation of the sulfide

A solution of sulfide (2.15 g, 10 mmol) was prepared in THF (40 ml) and 30% w/w H_2O_2 in H_2O (1.03 ml, 1 equivalent) and cyanuric chloride (CC) (737 mg, 4 mmol) was added to start the reaction. The reaction medium was stirred magnetically at room temperature for 45 minutes. The progress of the reaction was monitored by TLC (solvent n-heptane/EtOAc 2:1). After completion of the reaction, solid cyanuric acid (CA), i.e. the oxidation byproduct, precipitated and was filtered and washed with a small amount of dichloromethane (DCM). The filtrate was neutralized by adding a 10% w/w solution of $NaHCO_3$ in water. The product was extracted with DCM (3 × 50 ml) and the combined extracts were dried over $MgSO_4$. The solvent was removed under reduced pressure to give the corresponding sulfoxide, the main impurity –the sulfone– and unreacted sulfide. Further purification was achieved by short-column chromatography on silica gel with a solvent gradient (n-heptane/EtOAc) as the eluent. Pure sulfoxide was obtained as white needles (1.658 g, 7.2 mmol) while sulfone was obtained as a white powder (432 mg, 1.76 mmol) and sulfide as a highly viscous oil (209 mg, 9.8 mmol). A purification by recrystallization was not an option as it does not remove the sulfone byproduct.

The three compounds were characterized by comparisons of their NMR spectra, melting points and Powder X-ray Diffraction (PXRD) patterns to those in the literature.

3.3 Structural aspects

The crystallographic data collected in Table 3.1, demonstrates that the crystal lattices of the sulfoxide and of the sulfone are extremely close. It is interesting to note that the crystal structure of the sulfone is chiral (i.e. the space group $P2_12_12_1$ is chiral), although the molecule itself has no chiral center. Likewise this sulfone, prochiral molecules that crystallize in a chiral space group could predict conglomerate forming systems of closely related chiral molecules.[82]

Table 3.1: Crystallographic data of the sulfoxide and its related sulfone

	Sulfoxide[152]	Sulfone[161]
CCDC Ref code	689270	282551
Molecular Weight / g.mol^{-1}	230.32	246.31
Crystal System	Orthorhombic	Orthorhombic
Space Group	$P2_12_12_1$	$P2_12_12_1$
Z, Z'	4, 1	4, 1
a / Å	5.7569 (6)	5.7135 (5)
b / Å	12.2139 (12)	12.6191 (10)
c / Å	17.5974 (18)	17.1549 (14)
V / Å^3	1237.35 (2)	1236.85 (18)
d_{calc} / g.cm^{-3}	1.236	1.323
Temperature / K	293 ± 1	298 ± 2

If sulfur is attached to an aryl group, the structure will be stabilized due to a weak conjugation of the double bonds with the aryl group and due to an intramolecular interaction between the sulfoxide oxygen and the *o*-hydrogen (H_{aryl}) on the neighboring aromatic ring.[162] The strength of the $O\cdots H_{aryl}$ interaction influences how the aromatic ring is oriented in the molecule. A stronger interaction will result in a shorter $O\cdots H_{aryl}$ distance and a smaller torsion angle.[152]

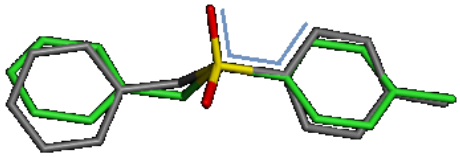

Figure 3.7: Comparison between the conformation of the sulfoxide (in green) and the sulfone (in grey); the torsion angle is represented in blue

In this study, the sulfoxide (represented in green in Figure 3.7) has a tight torsion angle (8.16°represented in blue in the Figure 3.7) meaning strong intramolecular interactions.[152] The S-O bond in the sulfoxide measures 1.5032(16) Å. The two aromatic rings are almost in the same plane with a small angle of 2.25°. In the sulfone (represented in grey in Figure 3.7), the S-O bond lengths are 1.4252 (16) Å and 1.4370 (17) Å, the torsion angle is 17.97° (represented in blue in the Figure 3.7) and the angle between the planes of the aromatic rings is 5.44°. Therefore, except a tilt of the aryl group, the sulfoxide conformation is highly similar to that of the sulfone, meaning that the double bond with the second oxygen in the sulfone can replace the lone pair of electrons, almost without change in molecular volume.

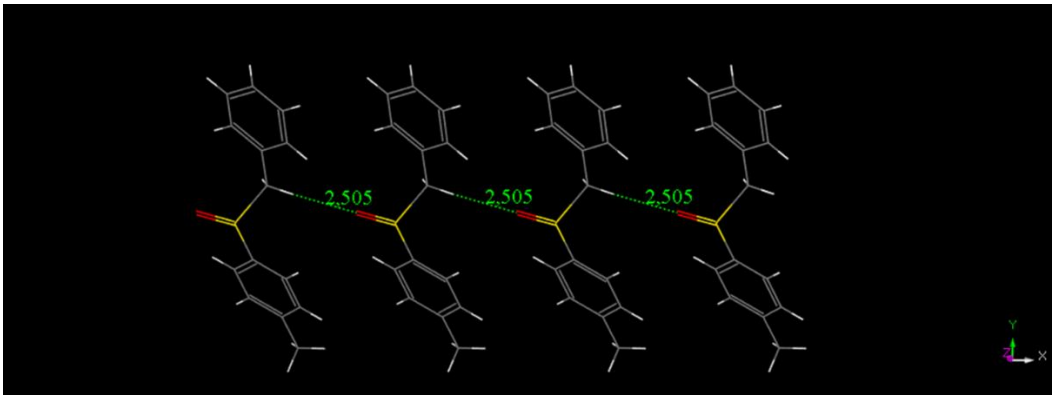

Figure 3.8: Hydrogen bonds in the sulfoxide structure forming a Periodic Bond Chain (PBC) along *a*

Moreover, intermolecular hydrogen bonds are present in the crystal structures of both the sulfoxide and the sulfone (Figure 3.8). The intermolecular C_{alkyl}-H···O hydrogen bond links the molecules to establish a Periodic Bond Chain (PBC) in the form of a zigzag chain along the *a* axis (see Figure 3.9 for the sulfoxide and Figure 3.10 for the sulfone). The structures of the sulfone and the sulfoxide are very similar even if the origins of the respective crystal lattices are displaced.

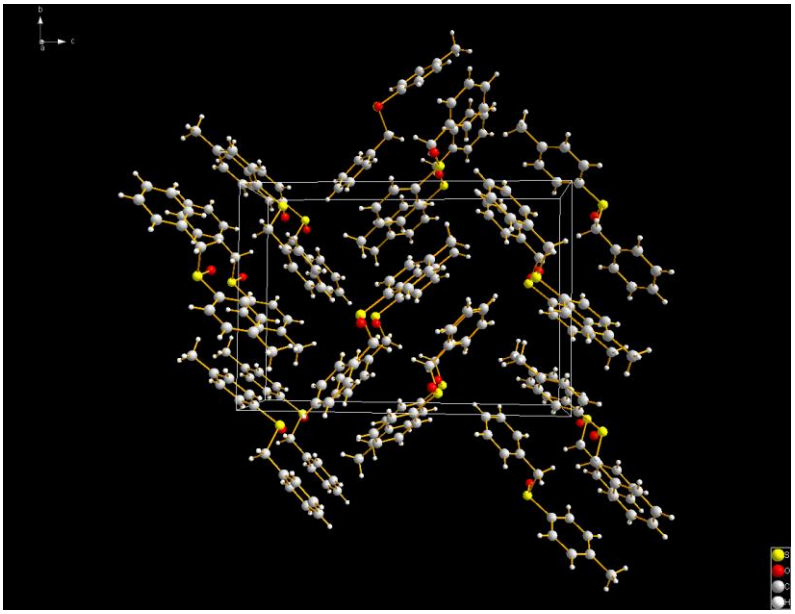

Figure 3.9: Projection along *a* of the cell packing diagram of the sulfoxide

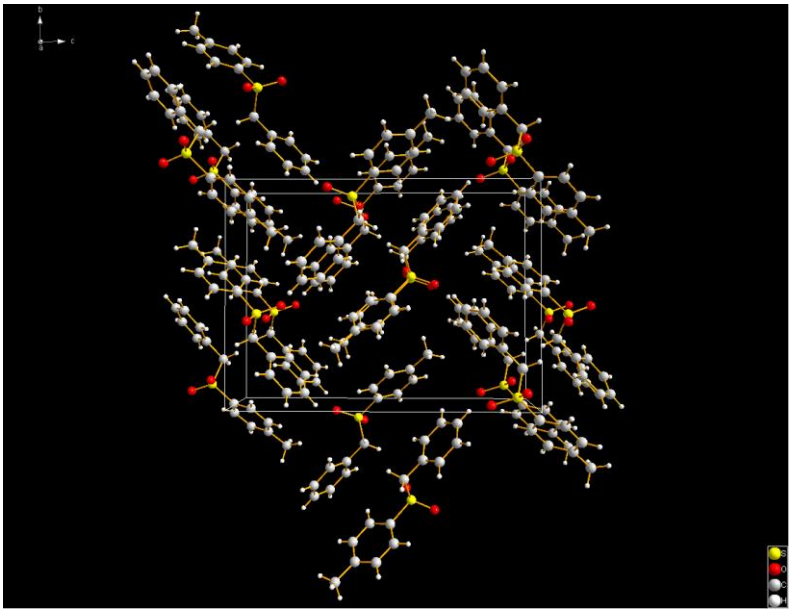

Figure 3.10: Projection along *a* of the cell packing diagram of the sulfone

3.4 Heterogeneous equilibria

3.4.1 Binary section between the two sulfoxide enantiomers

The racemic mixture of the sulfoxide crystallizes in a chiral space group, i.e. the crystals are homochiral. Since the sulfoxide presents a total chiral discrimination in the solid state, this system meets the crystallographic requirement for a resolution by crystallization. The phase diagram associated with this conglomerate forming system is presented in Figure 3.11. The melting temperatures have been found by Differential Scanning Calorimetry (DSC) and the Powder X-Ray Diffraction (PXRD) patterns of the racemic mixture and of the pure enantiomer indicate the conglomerate nature of this system (available in the appendices). The liquidus curves have not been fitted and are only placed as a guide for the eye.

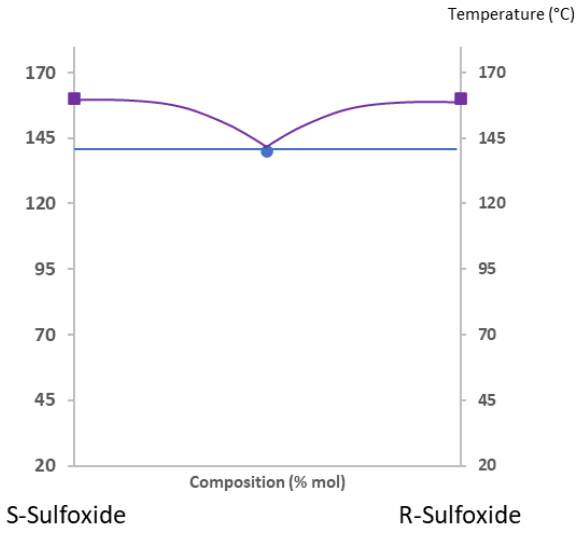

Figure 3.11: Binary section between the two sulfoxide enantiomers

3.4.2 Binary section between the related sulfone and racemic sulfoxide

The similarities in the crystallographic parameters of the sulfone and the sulfoxide resulted in purification issue during recrystallization (i.e. impurities of sulfone could not be removed from the sulfoxide by recrystallization) foreshadowed the presence of a solid solution between the two related compounds. The binary phase diagram between the racemic sulfoxide and its corresponding sulfone was investigated by means of PXRD and DSC analyses. The PXRD patterns of binary mixtures confirmed the presence of a solid solution over the entire composition range (Figure 3.12). There is a clear continuity between the pattern of the pure sulfoxide up to the pure sulfone. The peak at 8.85° representative of the sulfoxide moves to

8.70° representative of the sulfone as the mixture becomes richer in sulfone; the peak at 10° in the pure sulfoxide PXRD shifts towards 10.4°, if the percentage of sulfone in the mixture increases. The absence of the emergence of a new phase confirms that the solid solution is total at room temperature. The solidus and liquidus points could not be extracted from the DSC analyses due to chemical degradation upon heating. The melting transition in the phase diagram could not be established accurately.

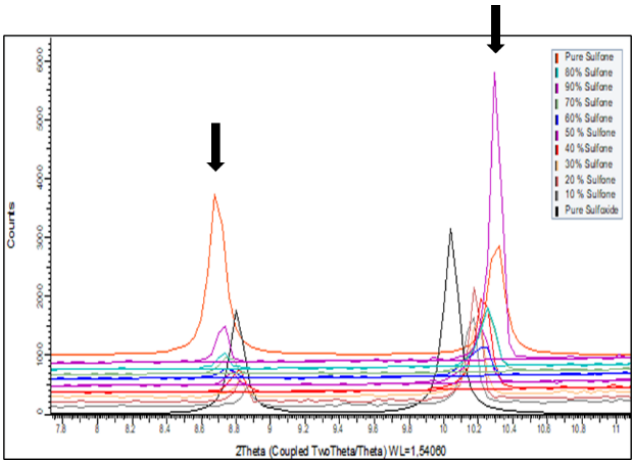

Figure 3.12: PXRD of binary mixtures of (rac)-sulfoxide and (rac)-sulfone obtained by solvent evaporation crystallization. The arrows indicate the shift in the peaks of interest.

Even though the heterogeneous equilibria at high temperature are not accessible, some useful information can be extracted. Sulfone molecules can replace sulfoxide molecules in the crystal lattice when the overall mixture is racemic.

If the supramolecular chirality of the sulfone is taken into account, the system becomes more complicated and the chiral compatibility must be considered. This compatibility issue is discussed and rationalized by phase diagrams in the next part of this chapter.

3.4.3 Phase diagrams of the system

Phase diagrams are a powerful tool to rationalize crystallization processes; in this case, even though the heterogeneous equilibria were not accessible, schematic phase diagrams are proposed in order to acquire a better understanding of the system. Several cases are depicted, from the simplest to the more elaborated one (i.e. taking into account both supramolecular chirality and racemization).

The enantiomers of the sulfoxide are represented as S and R. The sulfone is called A hereafter. A schematic phase diagram of the system in case of no solid solution between R and S but two complete solid solutions between A and S and between A and R, is suggested in Figure 3.13. In this first figure, the chirality of the sulfone in the solid state was not taken into account and it is assumed that R and S enantiomers do not racemize. Another possibility consistent with the structural and experimental observations (see part 3.3 and 3.4.1) would have been the presence of a solid solution between the enantiomers with a miscibility gap at room temperature similarly to the case presented by Gendron et al[50] or minute solid solutions between the enantiomers enlarging with the presence of sulfone.

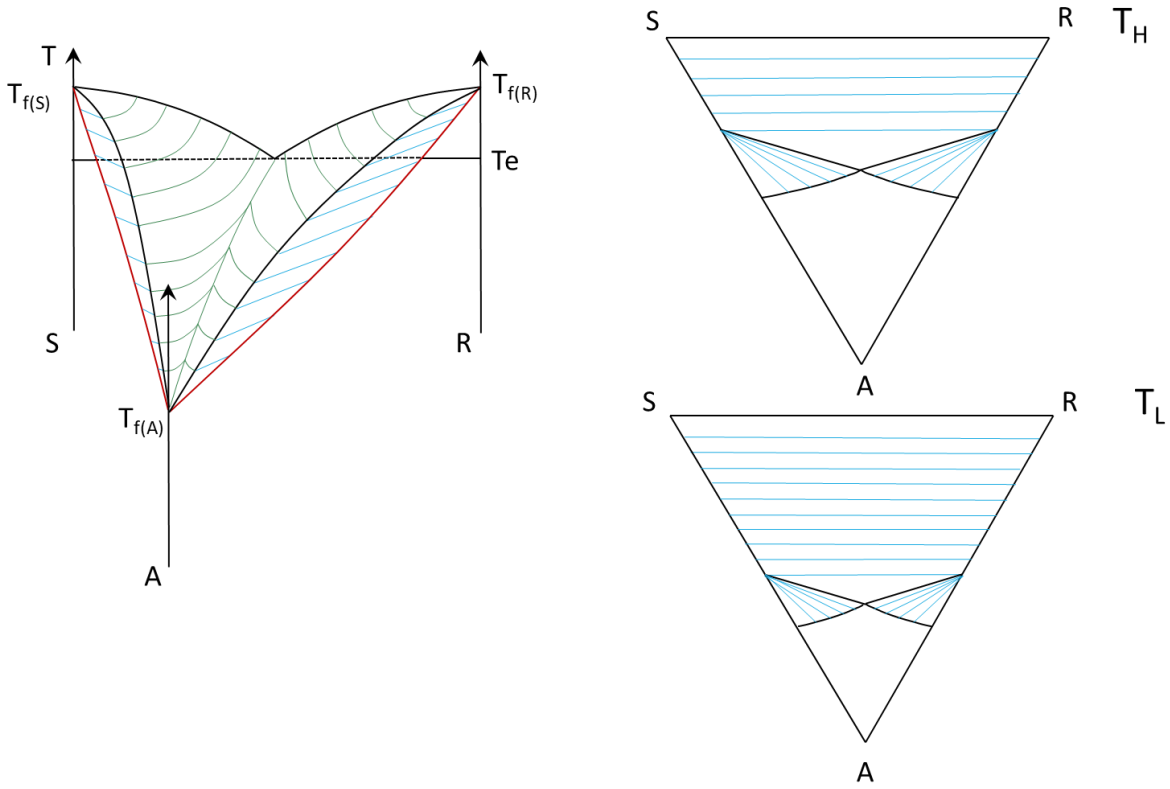

Figure 3.13: Schematic phase diagram of the system in case of a complete solid solution between A and S and also between A and R. R and S enantiomers form a conglomerate and do not racemize. The liquidi are represented in black and green, the solidi are represented in red. The tie-lines connecting the composition of two phases in equilibrium are represented as blue segments. Two isopleth sections at different temperatures are also presented.

Compounds exhibiting supramolecular chirality are, usually, represented as one and only one component in phase diagrams (Figure 3.13), although there are composed of two supramolecular chiral entities in the solid state (i.e. right-handed and left-handed crystals). Therefore, the sulfone can be decomposed in A\\ and //A (standing for left-handed and right handed respectively) and the phase diagram exploded as proposed in Figure 3.14.

The supramolecular chirality of component A\\ (in the solid state only) gives a complete solid solution with the enantiomer S and A// gives a complete solid solution with R. The sulfone can enter the crystal lattice of the sulfoxide whatever the handedness of the sulfoxide, it interconverts to fit the requirements of the sulfoxide chirality. The reverse (i.e the sulfoxide entering the crystal lattice of the sulfone) is not necessarily true, depending on the handedness of the crystals A and the chirality of the sulfoxide. The sulfoxide, with its intrinsic chiral center, is not capable to racemize and, therefore, controls the chirality of the system. S is able to interchange with the sulfone only in the left-handed crystal lattice A\\ to give a solid solution $SS_{S\text{ - }A\backslash\backslash}$, alike R can exclusively enter A// to form the solid solution $SS_{R\text{ - }//A}$. However, S will not be able to crystallize within the right-handed crystal of sulfone //A, similarly R and A\\ are incompatible in the solid state due to their antipodal chirality. The symmetry axes by which they repeat in the crystal lattice rotate in different directions, alike screws in which the screw thread would be opposite, they cannot enter the crystal lattice of each other. The schematic phase diagram proposed in Figure 3.14 seems the most relevant to the system studied compared to experimental observations.

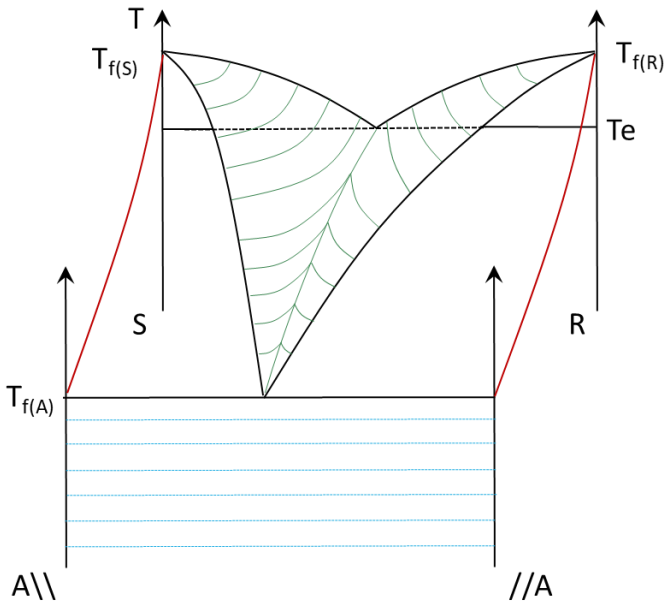

Figure 3.14: Schematic phase diagram of the system when taking into account the supramolecular chirality of component A in the solid state. A\\ and S, and A// and R form a complete solid solution. R and S enantiomers form a conglomerate and do not racemize. The liquidi (in black) and the solidi (in red) are not in the same plane. The liquid A is not chiral, thus, the composition of the liquid is lying in the triangle S-R-A. The doted blue segments connect the opposite supramolecular entities A\\ and //A.

The corresponding isothermal sections are represented in Figure 3.15. The areas delineated, even partially, by dashed lines are physically inaccessible due the absence of chirality in the molten state of the sulfone. The tie-lines (in purple) connect the opposite solid solutions $SS_{S\,-\,A\backslash\backslash}$ and $SS_{R\,-\,//A}$.

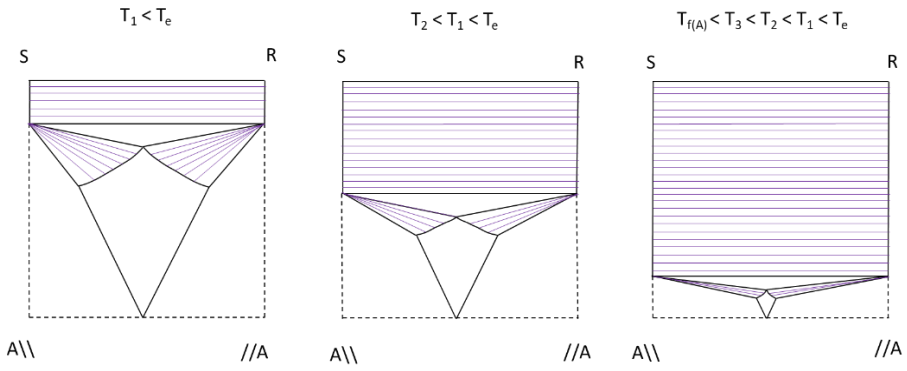

Figure 3.15: Isothermal sections between supramolecular Chirality (A is either A\\ or //A) and intrinsic chirality (R and S enantiomers).

To go further, one can envisage the effect of the racemization of the enantiomers in the molten state on the system proposed in Figure 3.14. In this case, the system would meet all the requirements for a complete chiral symmetry breaking and would tend towards the complete deracemization and the formation of either a solid solution $SS_{S\,-\,A\backslash\backslash}$ or $SS_{R\,-\,//A}$ (Figure 3.16 a and b respectively). This system would be a valuable candidate for Second-Order Asymmetric Transformation (SOAT).

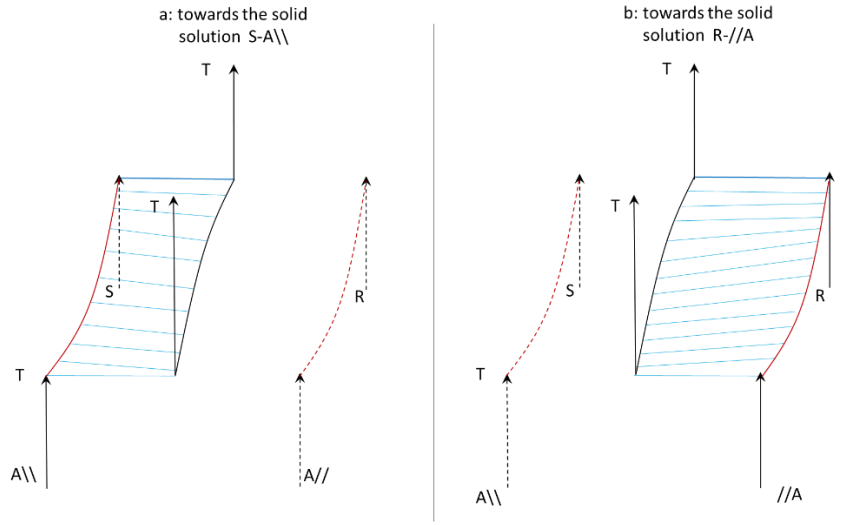

Figure 3.16: Schematic phase diagram of the system taking into account the chirality in the solid state of the component A and if R and S enantiomers rapidly racemize in the liquid state. The two cases depict the stochastic final evolution to the complete deracemization (in case a: towards the solid solution S-A\\; in case b: towards the solid solution R-//A). The liquidus (in black) and the solidi (in red) are not in the same plane. The liquid A is not chiral and R and S racemize rapidly in the molten state. Thus, the composition of any liquid is lying within the vertical plane rac-(RS) – A (±) – T.

3.5 Preferential Crystallization of the sulfoxide

Once the conglomerate of the sulfoxide confirmed, an assessment of the feasibility of resolution by preferential crystallization should be carried out.[163] The AS3PC mode of preferential crystallization has been chosen and the corresponding procedure for the validation runs is presented below. Then the crystallization parameters have been tuned to achieve an efficient entrainment effect.

3.5.1 Preferential Crystallization procedure

(i) A volume V (8 ml) of a doubly saturated solution of racemic sulfoxide is prepared at $T_{doubly\ sat}$. The solution is placed in a closed cylindric tube (25 mm in diameter and 80 mm in length) called the reactor hereafter with a cross-shaped magnetic stirring bar for agitation.

(ii) Between 10 to 25 mg (about 2 to 5% of the racemic mass) of enantiopure sulfoxide (obtained from a ground single crystal) is introduced in the reactor.

(iii) The suspension is slightly heated to $T_{initial} = T_{doubly\ sat} + 0.1°C$ for a short period of time to ensure a partial dissolution of the seeds (in this case 1 h). The system is now a light suspension of the enantiomer corresponding to the remaining seeds of R-sulfoxide and a S-sulfoxide undersaturated solution (saturated in R). The seeding of the first run is over and the stereoselective crystallization can start.

The step (i) to (iii) are relevant only for the first run of an experiment; in AS3PC, only the first run is manually seeded and the following runs are autoseeded.

(iv) The supersaturation is induced by cooling from $T_{initial}$ to T_{final} with a controlled cooling ramp $^{dT}/_{dt}$. R-sulfoxide starts to crystallize, whereas the nucleation of S-sulfoxide is delayed.

(v) The suspension is filtrated at T_{final}. The solid is dried and weighed (m_{crop}). At this stage the first PC run is completed.

(vi) The mother liquor is recycled in a clean reactor and the exact same mass of racemic sulfoxide as the mass of the crops (m_{crop}) is added to compensate the loss and solvent is refilled to V.

(vii) Temperature is set back to $T_{initial}$ for a time t to reach thermodynamic equilibrium. At this step the system is the mirror image of step (iii), i.e. a light suspension of S-sulfoxide and an undersaturated solution in R-sulfoxide.

(iix) The same temperature program as used in step (iv) is applied. S-sulfoxide crystallizes while R-sulfoxide remains in solution.

(ix) At T_{final}, the suspension is filtrated. Crops are dried and weighed. The second run has been completed.

(x) Yet again, the mother liquor is recycled by means of an addition of the same mass of racemic sulfoxide as the crops and the loss of solvent is compensated up to volume V.

(xi) After time t at temperature $T_{initial}$, the system is back to the same equilibrium as in step (iii) and the first cycle of PC is completed. Steps (iv) to (x) are repeated to produce successively R- and S-sulfoxide crystals.

3.5.2 Determination of suitable Preferential Crystallization parameters

Every crystallization process is thermodynamically driven, i.e. the system tends to reach a more stable state. Nevertheless, preferential crystallization is performed out of equilibrium, thus, kinetics play an important role during stereoselective crystallization. Various other parameters –such as the solvent, the cooling ramp, the initial and final temperatures– influence the PC and require a fine tuning. The determination of suitable crystallization parameters is discussed in the following subsections.

3.5.2.1 Solvent screening

The solvent used for preferential crystallization must fulfill several requirements (in descending order of importance):

(i) No chemical reaction must occur between the solvent and the solute to be resolved.

(ii) The solute must not form an undesired solvate with the solvent (unless the conglomerate is a solvate).[114,164]

(iii) As a rule of thumb, the higher the solubility, the higher the productivity. However, at high concentration, problems of viscosity and filtration can be encountered.

Typical solvents were screened for solubility and it was found that the racemic mixture of sulfoxide is poorly soluble in most solvents. Solubilities were determined by the dry extract method and the results presented in Table 3.2 are the mean values over 10 experiments. None of the tested solvents induced the appearance of a new phase nor caused chemical degradation.

Table 3.2: Solubilities of rac-sulfoxide in organic solvents at 20°C

Solvent	Solubility w/w%
Acetone	3.37
Acetonitrile	4.29
DCM	> 30
Diethyl ether	3.58
Ethyl acetate	2.42
THF	6.82
Toluene	2.16

Regarding the requirements mentioned above, the best solvent would be dichloromethane (DCM), however, the solutions in DCM resulted in a viscous oil, impossible to filter. The second-best solvents were acetonitrile and tetrahydrofuran (THF). Through observation by microscope of the growing crystals in both solvents (Figure 3.17), THF was chosen over acetonitrile. The morphology of the crystals extracted from a suspension of THF was nicer, with bigger crystals and less defects than those grown in acetonitrile. In addition, the solubility is somewhat higher in THF.

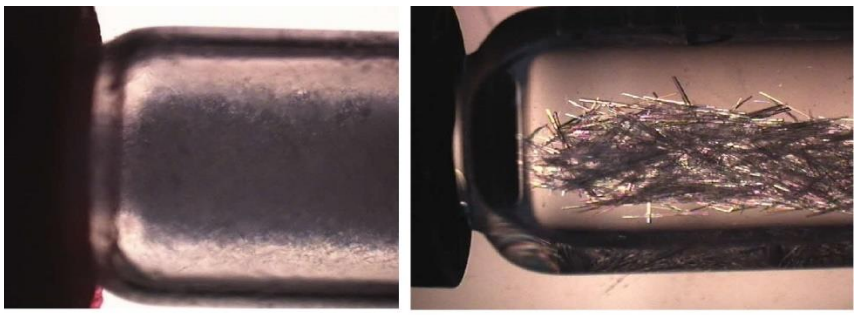

Figure 3.17: Crystals grown from a supersaturated solution at β = 1.1 in A. acetonitrile and B. THF

3.5.2.2 Kinetic aspects

In the AS3PC mode of preferential crystallization, the supersaturated solution is seeded the first time and auto seeded afterwards, hence, nucleation of the conglomerate does not impact the feasibility of stereoselective crystallization. However, it is very important to avoid nucleation of the opposite enantiomer during the process. Nucleation experiments were used to establish the metastable zone width (MSZW) and the Ostwald limit.

At first, experiments were conducted to determine if the sulfoxide could be subjected to high supersaturation to facilitate the entrainment effect during PC. A defined mass of racemic sulfoxide was dissolved in THF at 30 °C. Once complete dissolution was observed, the solution was cooled rapidly to 20 °C. As soon as crystallization was observed, the solid was collected by filtration and PXRD analysis was carried out to rule out crystallization of another phase (e.g. an undesired racemic solvate). The results are summarized in Table 3.3. The conglomerate phase crystallizes at all observed supersaturations, however, it is not possible to reach high supersaturation for this system, which may limit the efficiency of the application of preferential crystallization.

Table 3.3: Summary of the nucleation experiment as a function of supersaturation

β	Induction time
1.1	50 min
1.15	45 min
1.2	20 min
1.25	15 min
1.5	5 sec

Secondly, experiments were conducted in a Crystal16 parallel crystallizer to determine the Ostwald limit with a cooling rate of 0.1 °C per minute, which is lower than the standard cooling ramp for PC, however, higher cooling rates did not lead to consistent results in the Crystal16 (Figure 3.18). The MSZW seems sufficient to run preferential crystallization.

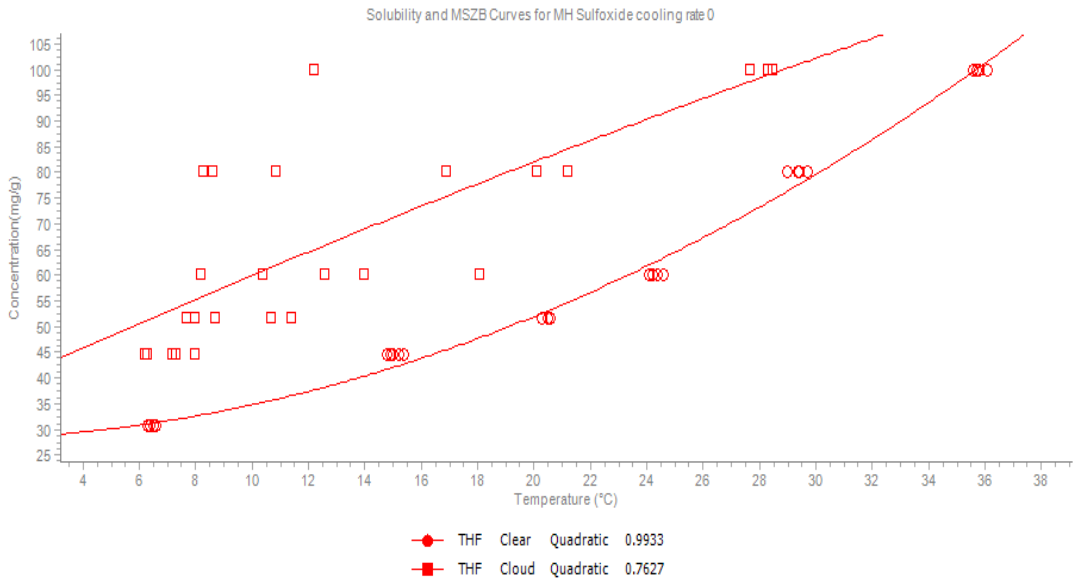

Figure 3.18: Solubility and Ostwald curves of the sulfoxide in THF (heating rate = 0.3 °C/min and cooling rate = 0.1 °C/min), the quadratic function was chosen to fit the curves because it gave the best coefficient of determination

3.5.2.3 Determination of the temperatures and filtration window

Because sulfoxide cannot be maintained at high supersaturation, the initial temperature, $T_{initial}$, was chosen close to room temperature. Therefore, 25 °C was selected to be $T_{doubly\ sat}$. The cooling ramp $^{dT}/_{dt}$ and T_{final} were determined by carrying out several crystallizations.

Figure 3.19 illustrates the influence of the theoretical final temperature on the outcome of the preferential crystallization and more particularly 'the filtration window'.

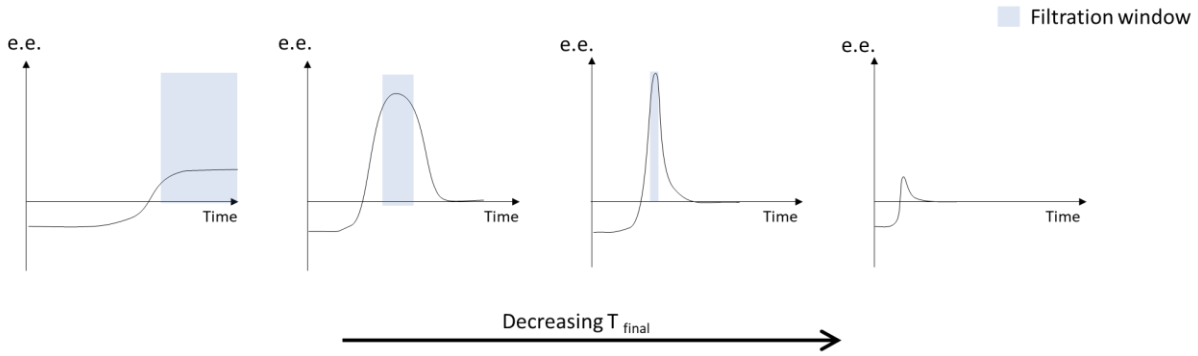

Figure 3.19: Theoretical influence of the final temperature on the preferential crystallization

In the first depicted case of Figure 3.19, the final temperature is not low enough. As a consequence, the entrainment effect is limited, but the filtration window is large. The second and third representations illustrate two possibilities of usable final temperatures. In the third case, the final temperature is lower and the entrainment effect is higher but the filtration window has shrunk so that scale up might be jeopardized. In the last case, the final temperature is definitely too low and the counter enantiomer nucleated early in the process. The first part of the curves correspond to the preferential crystallization of the enantiomer initially in excess whose concentration decreases in solution. The change in the sign of optical rotation α of the mother liquor indicates that the counter enantiomer starts to be more supersaturated (i.e., passing the 50-50 composition) but its nucleation does not occur immediately. This is the filtration window in which the best results can be obtained (best mass and e.e. of the crop, represented in blue in Figure 3.19). The last part of the curves correspond to the return to equilibrium for the system due to the nucleation and crystallization of the counter enantiomer.

Accordingly, liquid samplings were performed during three cooling runs with different cooling ramps and final temperatures to determine the optimal final temperature and cooling program. The optical rotations of the mother liquors vs. time obtained during the preferential crystallization test runs for different cooling rate are presented in Figure 3.20. It can be seen in Figure 3.20 that the cooling ramp of 0.35 °C/min gave the best results. The temperature of the filtration window for this cooling ramp f is situated between 18.7 °C and 18 °C.

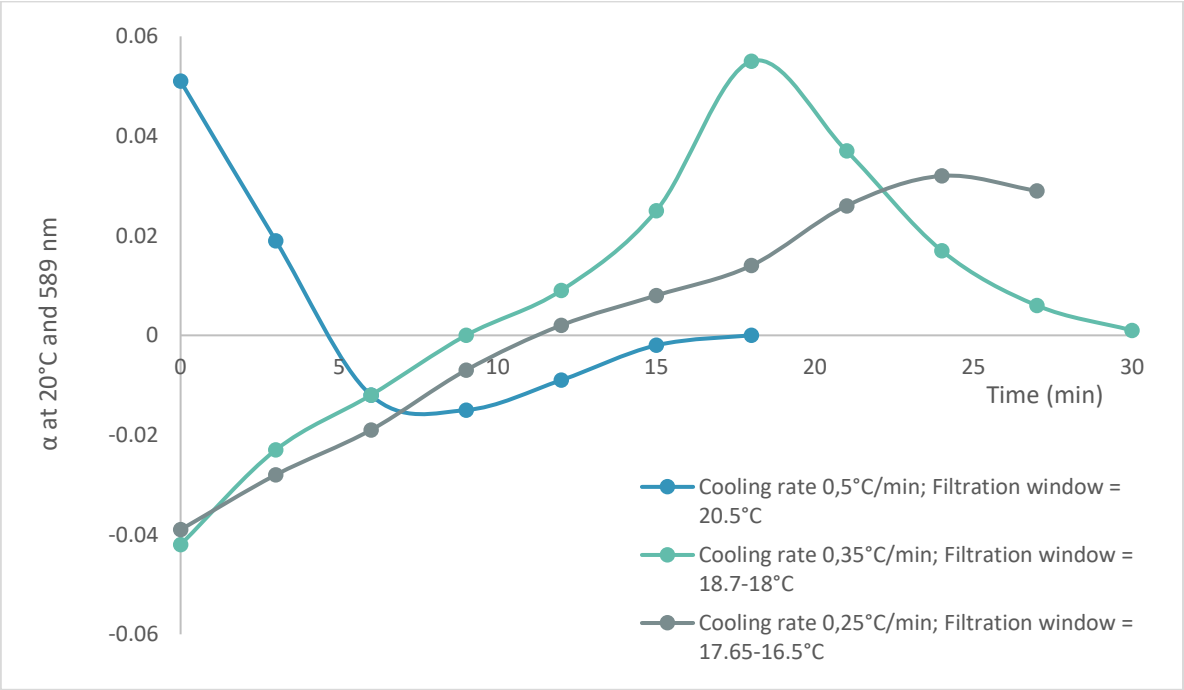

Figure 3.20: Monitoring of different cooling ramps for optimal PC ($T_{initial}$ = 25.1 °C)

3.5.3 Results

Once suitable conditions were established, a cycle of preferential crystallization was conducted in AS3PC mode (see part 1.3.3.2 for more information). The parameters are:

- Dry Solvent = THF
- dT/dt = 0.35 °C/min
- $T_{initial}$ = 25.1 °C
- A ground single crystal as seeds for the first run (7.2 mg)

The enantiomeric excess was determined by polarimetry.

The results of the PC cycle are presented in Table 3.4. Two consecutive and successful runs have been performed. In the first run, even though there is an entrainment effect, the e.e. of the crops is not satisfactory but it increases in the second run. It seems that the seeds were not pure enough in the first run. In the second run, the mass of crops is higher than in the first run as it is usually the case.

Table 3.4: Results of two consecutive runs of 'classical' AS3PC for the sulfoxide

	PARAMETERS		**SOLUTION**	**SOLID**		
	Temperature (°C)	Time (min)	α	Mass (mg)	Chirality	e.e. (%)
INITIAL STATE	• 8 ml of doubly saturated solution at 25°C • 7.8 mg of a grinded single crystal					
Run 1	23.25	5	0.004			
	21.5	10	0.012			
	19.75	15	0.036			
	18	20	0.059	35	**S (-)**	78.1
Compensation	• 33 mg of racemic sulfoxide • 4h at 25°C					
Run 2	23.25	5	0.002			
	21.5	10	-0.009			
	19.75	15	-0.037			
	17.5	21.5	-0.062	47	**R (+)**	91.1

3.6 Transfer of chirality from supramolecular chirality to intrinsic chirality

3.6.1 Deracemization of the sulfone

A suitable solvent for deracemization must fit similar requirements as for PC (see part 3.5.2.1), i.e. inducing no chemical reaction, nor forming an undesired solvate, nor dissolving too little of the solute as this diminishes the productivity of the process.[165] On the contrary, if the solubility is high, a major part of the solute remains in solution and is not recovered as enantiopure. Solubilities in various solvents were measured. Despite exhibiting similarities with the sulfoxide, the sulfone is more soluble (Table 3.5).

Table 3.5: Solubilities of the sulfone in organic solvents at 20 °C

Solvent	Solubility w/w%
Acetone	6.78
Acetonitrile	6.51
THF	11.30

The solubility of the sulfone in acetone was suitable for Viedma ripening; therefore, four Viedma ripening experiments were conducted simultaneously as represented by Figure 3.21, according to the parameters presented in Table 3.6.

Table 3.6: Viedma ripening parameters for the sulfone

Parameters	
Sulfone	150 mg
Solvent	Acetone (2 ml)
Glass beads	200 mg (Ø 1,5 mm)
Stirring rate	750 rpm
Time	4 days

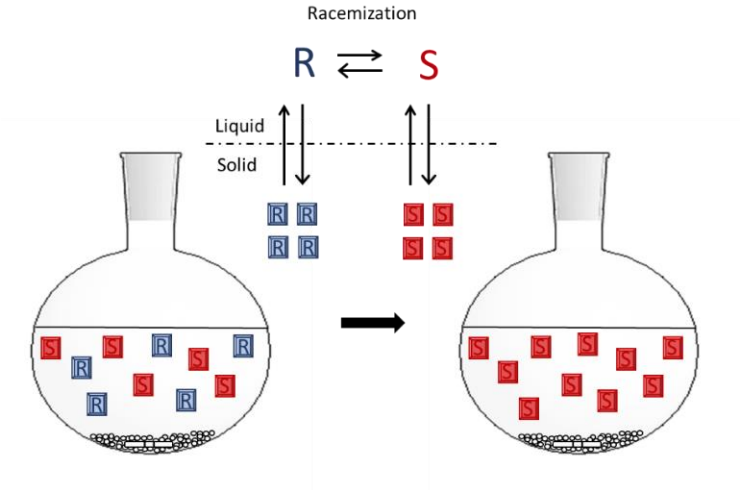

Figure 3.21: Viedma ripening of the sulfone

After 4 days, the crystals were collected by filtration; however, the optical purity could not be measured by conventional methods, because they are carried out in the liquid state and sulfone chirality is only supramolecular. Other methods exist, for instance, the recognition of the handedness of the crystals can be observed under the polarized light of a microscope.[166] However, due to the small size of the present crystals and their inadequate morphology, this method could not be employed. Another technique, not available in the lab at the time of the experiment, would be solid state Circular Dichroism (both vibrational or electronic) which is a spectroscopy method capable of providing detailed information regarding the molecular conformation (e.g. chirality, special conformation, etc).[167,168]

As the related sulfoxide and sulfone form a complete solid solution and in regard to the phase diagrams proposed in part 3.4 dedicated to heterogeneous equilibria, it was assumed that the use of the collected crystals of sulfone as seeds in the PC of the sulfoxide will induce the stereospecific crystallization of only one of the enantiomers if the sulfone crystals were, indeed, deracemized. This last option was chosen to verify the enantiopurity of the crystals of sulfone after deracemization.

3.6.2 Chirality transfer and discussion

An experiment of AS3PC -in accordance with some modification- was designed to establish the possibility of a chirality transfer between the sulfone exhibiting supramolecular chirality and the intrinsic chiral sulfoxide. Its schematic representation is given by the Figure 3.22.

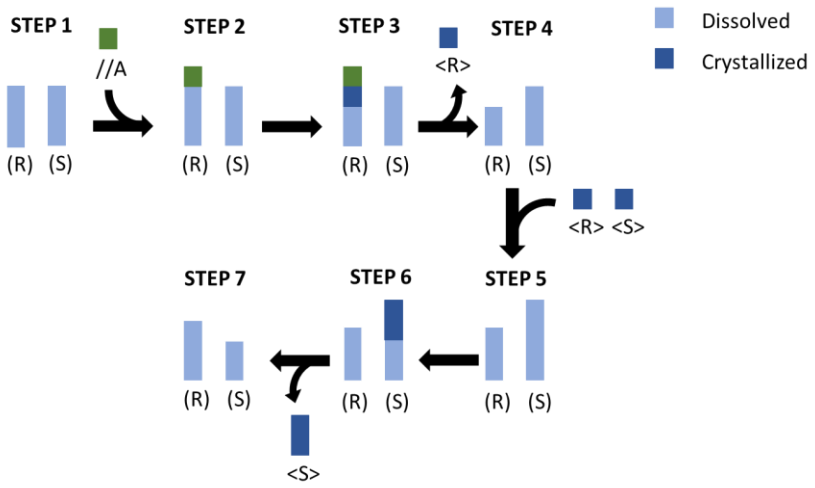

Figure 3.22: Transfer of chirality during the preferential crystallization of the sulfoxide

The exact same PC procedure (see part 3.5.1) was applied with two exceptions. The inoculated seeds came from the deracemization experiment of the sulfone and not from a single crystal of the sulfoxide. Also, step (iii) in the procedure (i.e. increasing the temperature after the seeding to dissolve part of the solid to obtain highly pure seeds) was skipped because the seeds dissolved already due to the fact that the mother liquor is not supersaturated in sulfone. The cooling step (corresponding to step (iv)) was initiated just before the inoculation of the seeds. The results of two AS3PC experiments seeded with two different solid samples of sulfone are presented in Table 3.7. Several runs were conducted each time and the e.e. was determined by chiral High Performance Liquid Chromatography (HPLC). This method was the most relevant because the presence of the sulfone would have distorted the precise mass weighted for the optical rotation measures, also chiral HPLC provides more accurate e.e.. The chiral HPLC conditions suggested by Kelly et al. have been used according to some modifications.[169]

Table 3.7: Preferential crystallization of the sulfoxide induced by sulfone seeds

	PARAMETERS		**SOLID**		
	Temperature (°C)	Time (min)	Mass (mg)	Chirality	e.e. (%)
FIRST EXPERIMENT Initial State	• 8 ml of doubly saturated solution at 25°C • 10 mg of deracemized crystals of sulfone (sample 1)				
Run 1	18	20	22	**S**	90.8
Compensation	• 20 mg of racemic sulfoxide • 4h at 25°C				
Run 2	17.8	20.5	36	**R**	90.9

SECOND EXPERIMENT Initial State	• 8 ml of doubly saturated solution at 25°C • 7 mg of deracemized crystals of sulfone (sample 3)				
Run 1	18	20	13	**R**	98.3
Compensation	• 10 mg of racemic sulfoxide • 4h at 25°C				
Run 2	18	20	25	**S**	98.3
Compensation	• 22 mg of racemic sulfoxide • 4h at 25°C				
Run 3	18	20	47	**R**	91.1

In the first experiment, the seeds induced the crystallization of the S enantiomer with a good e.e. of 90.8% meaning the crystals of sulfone were certainly right-handed, the second run produced the R-sulfoxide with a e.e. of 90.9%. A second PC experiment was conducted with another sample of solid sulfone as seeds. This sample was probably enantiomerically purer than the first one because it promoted the crystallization of the R-sulfoxide with a higher e.e. of 98.3%. A second and a third run gave respectively the S enantiomer with a e.e. of 98.3% and the R enantiomer with a e.e. of 91.1%. The reason behind the lower e.e. of the last run was not investigated further but the nucleation and crystallization of the S enantiomer explain the higher mass obtained.

The success of the entrainment effect implies that the seeds of sulfone were enantiopure and thus, the complete deracemization has been achieved. The chirality of the seeds induces the control of the chirality of the sulfoxide; a transfer occurs between the supramolecular chirality of the sulfone towards the intrinsic chirality of the sulfoxide. This is not a template effect because the sulfoxide does not only crystallizes on the sulfone but it enters the crystal lattice of the sulfone if they are chiral compatible. It is in accordance with the phase diagrams proposed in part 3.4.3. This work demonstrates the concept of a continuum between supramolecular and intrinsic chirality.

Chirality transfers have already been observed in various areas of chemistry like in the field of coordination complexes,[170] in gels,[171] in monolayers[172] and in liquid crystals[173] but, to the best of our knowledge, it is the first reported case of a chirality transfer used for resolution purposes. Without doubt, chirality transfer between related materials will find an application to bypass asymmetric synthesis to obtain enantiopure seeds when implementing the preferential crystallization of a new system.

3.7 Conclusion and prospects

Both the sulfoxide and the sulfone presented here meet the crystallographic requirements for crystallization-based resolution due to their total chiral discrimination in the solid state. Despite having no chiral center, the sulfone crystallizes in a Sohncke space group inducing a supramolecular chirality; by contrast, the asymmetry of the sulfur atom in the sulfoxide corresponds to an intrinsic chiral center.

The sulfoxide has been resolved by preferential crystallization and the sulfone, having no chirality in the liquid state, was deracemized by Viedma ripening. Suitable parameters for preferential crystallization and deracemization have been established.

The related sulfoxide and sulfone form a complete solid solution, i.e. left-handed crystals and right-handed crystals of sulfone with respectively S and R sulfoxide can specifically substitute each other in the same crystal lattice. It is worth to note that the supramolecular chirality is always compatible with the handedness of the crystal lattice of the intrinsic chiral molecule, even though the reverse is not necessary true. Therefore, it was assumed that one should be able to stereoselectively grow with the other under specific conditions. More precisely, a given sulfoxide enantiomer should be able to preferentially crystallize with enantiopure seeds of sulfone. A preferential crystallization experiment has been conducted on the sulfoxide with seed crystals of sulfone previously deracemized by means of Viedma ripening. The sulfone seeds did transfer their chirality to promote the stereoselective crystallization of the sulfoxide. It implies that the seeds were enantiopure and this work therefore demonstrates the concept of a continuum between supramolecular chirality to intrinsic chirality. New kind of ‘phase diagrams’ taking onto account the handedness of the solid phase of non-intrinsically chiral molecule are able to illustrate this relationship. Extensions of them could serve to represent the case where the intrinsic chiral component could be deracemized. The prochiral sulfone plays in this case a useful role in the selective crystallization of the chiral sulfoxide. Such chirality transfer could find an application in bypassing asymmetric synthesis to obtain enantiopure seeds when implementing preferential crystallization in new systems.

The prospects of this work are listed below.

First, it would be of interest to optimize the preferential crystallization parameters of the sulfoxide to improve the yield and scale-up the process. In view of a possible scale up to an industrial process, 2-methyltetrahydrofuran could replace the tetrahydrofuran as a solvent, to limit the toxicity.[174] Secondly, it would be compelling to run the reverse experiment, i.e. inducing a chiral break of symmetry of the sulfone by means of enantiopure seeds of sulfoxide. This experiment could be run as a Second Order Asymmetric Transformation as there is no chirality in the solution state. The enantiopurity of the sulfone would have to be checked by a solid-state technique like the Vibrational Circular Dichroism.

General conclusion

This work is dedicated to the understanding of crystallization-based resolution methods. Synthesis and solid-state characterization of two model compounds have been conducted.

BINOL-OBn, a compound exhibiting axial chirality, is not commercially available and had to be synthesized and then characterized by complementary methods. Despite having been reported as a conglomerate forming system, this compound presents a stable racemic compound up to its melting point. This heterochiral phase appears to be more stable than the conglomerate irrespective of the temperature. The binary phase diagram between this pair of enantiomers has been revised. Furthermore, the crystal structures of the racemic compound and of the pure enantiomer have been compared in an attempt to understand the late emergence of the new heterochiral phase. It was found that, in the structure of the racemic compound, hydrogen bonds are present, whereas in the structure of the pure enantiomer only π–π and van der Waals interactions are observed, which explains the higher stability of the racemic compound over that of the conglomerate. An explanation of the delayed crystallization of the heterochiral phase resides in the complexity of its crystalline structure. With three molecules in the asymmetric unit, with three different conformations (one of them possessing a relatively high energy), the probability for this form to spontaneously nucleate was low. One should be aware of the threat of the appearance of a more stable racemic compound, especially when working with conglomerates whose structure mainly depends on Van der Waals interactions, whereas H-bond donors and acceptors are available in the molecule, in particular when combined with molecular flexibility.

The second part of this work was devoted to a chiral aryl sulfoxide and its corresponding prochiral sulfone. The two components meet the crystallographic requirements for a crystallization-based resolution owing to their total chiral discrimination in the solid state. Suitable parameters for Preferential Crystallization of the sulfoxide have been established; and the sulfone, having no chirality in the liquid state, was deracemized by Viedma ripening. However, no conventional method was available to assert the result of the deracemization. A new stereoselective crystallization of the sulfoxide had to be implemented to verify the enantiopurity of the crystals of sulfone. This process is based on the complete solid solution linking the sulfoxide to its corresponding sulfone and rationalized by phase diagrams. Accordingly, the last part of this work was devoted to the implementation of a chirality transfer from supramolecular chirality to intrinsic chirality to induce stereoselective crystallization. The success of the stereoselective crystallization of the sulfoxide triggered by deracemized seeds of sulfone proves the concept of a continuum in chirality between a prochiral molecule and a related chiral compound. The chirality transfer depicted in this study will probably find more applications in bypassing asymmetric synthesis to obtain enantiopure seeds when implementing preferential crystallization in new systems.

References

(1) Collet, A.; Crassous, J.; Dutasta, J.-P.; Guy, L. Molécules Chirales : Stéréochimie et Propriétés, EDP SCIENCES.; Savoirs Actuels; 2006.

(2) Cahn, R. S.; Ingold, C.; Prelog, V. Specification of Molecular Chirality. Angew. Chem. Int. Ed. Engl. 1966, 5 (4), 385–415. https://doi.org/10.1002/anie.196603851.

(3) L, J. Lord Kelvin on Optical and Molecular Dynamics. Nature 1904, 70 (1801), iii–v. https://doi.org/10.1038/070iiia0.

(4) Hauy, R. J. Traité de Minéralogie. 1801.

(5) Pasteur, L. Mémoire Sur La Relation Qui Peut Exister Entre La Forme Cristalline et La Composition Chimique et Sur La Cause de La Polarisation Rotatoire. C. R. Acad. Sci. Paris 1848, 26, 535–539.

(6) Pasteur, L. Recherches Sur Les Relations Qui Peuvent Exister Entre La Forme Cristalline, La Composition Chimique et Le Sens de La Polarisation Rotatoire. C. R. Acad. Sci. Paris 1849, 28, 477–478.

(7) Gernez, D. C. R. Acad. Sci. Paris 1866, 63, 843.

(8) van't Hoff, J. H. Bul.l Soc. Chim. Fr. 1875, 23, 295.

(9) Le Bel, J. A. Bul.l Soc. Chim. Fr. 1874, 22, 337.

(10) Challener, C. A. Chiral Drugs; Routledge: London, 2019. https://doi.org/10.4324/9781315209906.

(11) Blackmond, D. G. The Origin of Biological Homochirality. Cold Spring Harb. Perspect. Biol. 2010, 2 (5), a002147. https://doi.org/10.1101/cshperspect.a002147.

(12) McBride, J. M.; Tully, J. C. Did Life Grind to a Start? Nature 2008, 452 (7184), 161–162. https://doi.org/10.1038/452161a.

(13) Ribó, J. M.; Hochberg, D.; Crusats, J.; El-Hachemi, Z.; Moyano, A. Spontaneous Mirror Symmetry Breaking and Origin of Biological Homochirality. J. R. Soc. Interface 2017, 14 (137), 20170699. https://doi.org/10.1098/rsif.2017.0699.

(14) Brooks, W. H.; Guida, W. C.; Daniel, K. G. The Significance of Chirality in Drug Design and Development. Curr. Top. Med. Chem. 2011, 11 (7), 760–770.

(15) Katzung, B. G. Introduction: The Nature of Drugs & Drug Development & Regulation. In Basic & Clinical Pharmacology; Katzung, B. G., Ed.; McGraw-Hill Education: New York, NY, 2017.

(16) Rentsch, K. M. The Importance of Stereoselective Determination of Drugs in the Clinical Laboratory. J. Biochem. Biophys. Methods 2002, 54 (1), 1–9. https://doi.org/10.1016/s0165-022x(02)00124-0.

(17) Nguyen, L. A.; He, H.; Pham-Huy, C. Chiral Drugs: An Overview. Int. J. Biomed. Sci. IJBS 2006, 2 (2), 85–100.

(18) Agranat, I.; Caner, H.; Caldwell, J. Putting Chirality to Work: The Strategy of Chiral Switches. Nat. Rev. Drug Discov. 2002, 1 (10), 753–768. https://doi.org/10.1038/nrd915.

(19) Sheldon, R. A. Chirotechnology: Industrial Synthesis of Optically Active Compounds, Marcel Dekker.; CRC Press: New York, 1993.

(20) Evans, A. M. Pharmacodynamics and Pharmacokinetics of the Profens: Enantioselectivity, Clinical Implications, and Special Reference to S(+)-Ibuprofen. J. Clin. Pharmacol. 1996, 36 (12 Suppl), 7S-15S.

(21) Penicillamine. In Meyler's Side Effects of Drugs (Sixteenth Edition); Aronson, J. K., Ed.; Elsevier: Oxford, 2016; pp 559–590. https://doi.org/10.1016/B978-0-444-53717-1.01236-1.

(22) Introduction: Organocatalysis – From Biomimetic Concepts to Powerful Methods for Asymmetric Synthesis. In Asymmetric Organocatalysis; John Wiley & Sons, Ltd, 2005; pp 1–8. https://doi.org/10.1002/3527604677.ch1.

(23) Diederich, F.; Stang, P. J.; Wiley InterScience (Online service). Metal-Catalyzed Cross-Coupling Reactions; Wiley-VCH: New York, 1998.

(24) Soai, K.; Shibata, T.; Sato, I. Enantioselective Automultiplication of Chiral Molecules by Asymmetric Autocatalysis. Acc. Chem. Res. 2000, 33 (6), 382–390. https://doi.org/10.1021/ar9900820.

(25) Hall, M. Enzymatic Strategies for Asymmetric Synthesis. RSC Chem. Biol. 2021, 2 (4), 958–989. https://doi.org/10.1039/D1CB00080B.

(26) Sie Yon, L.; Gonawan, F. N.; Kamaruddin, A. H.; Uzir, M. H. Enzymatic Deracemization of (R,S)-Ibuprofen Ester via Lipase-Catalyzed Membrane Reactor. Ind. Eng. Chem. Res. 2013, 52 (27), 9441–9453. https://doi.org/10.1021/ie400795j.

(27) Wang, G.; Lu, R.; He, C.; Liu, L. Kinetic Resolution of Indolines by Asymmetric Hydroxylamine Formation. Nat. Commun. 2021, 12 (1), 2512. https://doi.org/10.1038/s41467-021-22658-3.

(28) Marchand, P.; Lefèbvre, L.; Querniard, F.; Cardinaël, P.; Perez, G.; Counioux, J.-J.; Coquerel, G. Diastereomeric Resolution Rationalized by Phase Diagrams under the Actual Conditions of the Experimental Process. Tetrahedron Asymmetry 2004, 15 (16), 2455–2465. https://doi.org/10.1016/j.tetasy.2004.06.044.
(29) Andersson, S.; Allenmark, S. G. Preparative Chiral Chromatographic Resolution of Enantiomers in Drug Discovery. J. Biochem. Biophys. Methods 2002, 54 (1), 11–23. https://doi.org/10.1016/S0165-022X(02)00126-4.
(30) Coquerel, G. Preferential Crystallization. In Novel Optical Resolution Technologies; Topics in current chemistry; Springer, 2007; pp 1–53.
(31) Tamura, R.; Takahashi, H.; Coquerel, G. Chapter 20: Twenty-Five Years' History, Mechanism, and Generality of Preferential Enrichment as a Complexity Phenomenon. In Advances in Organic Crystal Chemistry, Comprehensive Reviews 2020; Springer; pp 405–432.
(32) Nakano, K.; Kitamura, M. Dynamic Kinetic Resolution (DKR). In Separation of Enantiomers; John Wiley & Sons, Ltd, 2014; pp 161–216. https://doi.org/10.1002/9783527650880.ch5.
(33) Viedma, C. Chiral Symmetry Breaking During Crystallization: Complete Chiral Purity Induced by Nonlinear Autocatalysis and Recycling. Phys. Rev. Lett. 2005, 94 (6), 065504. https://doi.org/10.1103/PhysRevLett.94.065504.
(34) Intaraboonrod, K.; Lerdwiriyanupap, T.; Hoquante, M.; Coquerel, G.; Flood, A. E. Temperature Cycle Induced Deracemization. Mendeleev Commun. 2020, 30 (4), 395–405. https://doi.org/10.1016/j.mencom.2020.07.002.
(35) Oketani, R.; Hoquante, M.; Brandel, C.; Cardinael, P.; Coquerel, G. Resolution of an Atropisomeric Naphthamide by Second-Order Asymmetric Transformation: A Highly Productive Technique. Org. Process Res. Dev. 2019, 23 (6), 1197–1203. https://doi.org/10.1021/acs.oprd.9b00133.
(36) Mislow, K.; Siegel, J. Stereoisomerism and Local Chirality. J. Am. Chem. Soc. 1984, 106 (11), 3319–3328. https://doi.org/10.1021/ja00323a043.
(37) McNaught, A. D.; Wilkinson, A. Compendium of Chemical Terminology - IUPAC Recommendations (IUPAC Chemical Data), 2nd ed.; Blackwell Scientific Publications: Oxford, 1997.
(38) Suárez, M.; Branda, N.; Lehn, J.-M.; Decian, A.; Fischer, J. Supramolecular Chirality: Chiral Hydrogen-Bonded Supermolecules from Achiral Molecular Components. Helv. Chim. Acta 2004, 81 (1), 1–13. https://doi.org/10.1002/hlca.19980810102.
(39) Jähnigen, S.; Scherrer, A.; Vuilleumier, R.; Sebastiani, D. Chiral Crystal Packing Induces Enhancement of Vibrational Circular Dichroism. Angew. Chem. Int. Ed. 2018, 57 (40), 13344–13348. https://doi.org/10.1002/anie.201805671.
(40) Schindler, M. Deracemization of Sodium Chlorate with or without the Influence of Sodium Dithionate. PhD Thesis, University of Rouen, 2020.
(41) Tschoegl, N. W. Inroduciton to Equilibrium Thermodynamics. In Fundamentals of Equilibrium and Steady-State Thermodynamics; Tschoegl, N. W., Ed.; Elsevier Science: Amsterdam, 2000; p 1. https://doi.org/10.1016/B978-0-444-50426-5.50045-8.
(42) Scott, R. L. Modification of the Phase Rule for Optical Enantiomers and Other Symmetric Systems. J. Chem. Soc. Faraday Trans. 2 Mol. Chem. Phys. 1977, 73 (3), 356–360. https://doi.org/10.1039/F29777300356.
(43) Ashcroft, N. W.; W, A.; Mermin, N. D. Solid State Physics; Holt, Rinehart and Winston, 1976.
(44) Nishinaga, T. Handbook of Crystal Growth: Fundamentals; Elsevier, 2014.
(45) Hahn, Th. The 230 Space Groups. In International Tables for Crystallography Volume A: Space-group symmetry; Hahn, Th., Ed.; International Tables for Crystallography; Springer Netherlands: Dordrecht, 2002; pp 112–717. https://doi.org/10.1107/97809553602060000513.
(46) Flack, H. D. Chiral and Achiral Crystal Structures. Helv. Chim. Acta 2003, 86 (4), 905–921. https://doi.org/10.1002/hlca.200390109.
(47) Hahn, T.; Klapper, H.; Müller, U.; Aroyo, M. I. Point Groups and Crystal Classes. In International Tables for Crystallography; American Cancer Society, 2016; pp 720–776. https://doi.org/10.1107/97809553602060000930.
(48) Coquerel, G. Review on the Heterogeneous Equilibria between Condensed Phases in Binary Systems of Enantiomers. Enantiomer 2000, 5 (5), 481–498.
(49) Jacques, J.; Collet, A.; Wilen, S. H. Enantiomers, Racemates and Resolutions; John Wiley & Sons Inc: New York, 1981.
(50) Gendron, F.-X.; Mahieux, J.; Sanselme, M.; Coquerel, G. Resolution of Baclofenium Hydrogenomaleate By Using Preferential Crystallization. A First Case of Complete Solid Solution at High Temperature and a Large

Miscibility Gap in the Solid State. Cryst. Growth Des. 2019, 19 (8), 4793–4801. https://doi.org/10.1021/acs.cgd.9b00665.

(51) Gendron, F.-X. Contribution to Chiral Discrimination in the Solid State and Access to Pure Enantiomer via Crystallization, Normandie Université, 2018.

(52) Mbodji, A.; Gbabode, G.; Sanselme, M.; Cartigny, Y.; Couvrat, N.; Leeman, M.; Dupray, V.; Kellogg, R. M.; Coquerel, G. Evidence of Conglomerate with Partial Solid Solutions in Ethylammonium Chlocyphos. Cryst. Growth Des. 2020, 20 (4), 2562–2569. https://doi.org/10.1021/acs.cgd.9b01699.

(53) Zlokazov, M. V.; Pivnitsky, K. K. Lamellar Conglomerates. Mendeleev Commun. 2020, 30 (1), 1–6. https://doi.org/10.1016/j.mencom.2020.01.001.

(54) Ndzié, E.; Cardinael, P.; Schoofs, A.-R.; Coquerel, G. An Efficient Access to the Enantiomers of α-Methyl-4-Carboxyphenylglycine via a Hydantoin Route Using a Practical Variant of Preferential Crysallization AS3PC (Auto Seeded Programmed Polythermic Preferential Crystallization)11. Tetrahedron Asymmetry 1997, 8 (17), 2913–2920. https://doi.org/10.1016/S0957-4166(97)00349-2.

(55) Noorduin, W. L.; Meekes, H.; Bode, A. A. C.; van Enckevort, W. J. P.; Kaptein, B.; Kellogg, R. M.; Vlieg, E. Explanation for the Emergence of a Single Chiral Solid State during Attrition-Enhanced Ostwald Ripening: Survival of the Fittest. Cryst. Growth Des. 2008, 8 (5), 1675–1681. https://doi.org/10.1021/cg701211a.

(56) Druot, S.; Petit, N.; Petit, S.; Coquerel, G.; Chanh, N. Experimental Data and Modelling of the Interactions in Solid State and in Solution between (R) and (S) N -Acetyl-α- Methylbenzylamine. Influence on Resolution by Preferential Crystallization. Mol. Cryst. Liq. Cryst. Sci. Technol. Sect. Mol. Cryst. Liq. Cryst. 1996, 275 (1), 271–291. https://doi.org/10.1080/10587259608034081.

(57) Harfouche, L. C.; Brandel, C.; Cartigny, Y.; Ter Horst, J. H.; Coquerel, G.; Petit, S. Enabling Direct Preferential Crystallization in a Stable Racemic Compound System. Mol. Pharm. 2019. https://doi.org/10.1021/acs.molpharmaceut.9b00805.

(58) Belletti, G.; Tortora, C.; Mellema, I. D.; Tinnemans, P.; Meekes, H.; Rutjes, F. P. J. T.; Tsogoeva, S. B.; Vlieg, E. Photoracemization-Based Viedma Ripening of a BINOL Derivative. Chem. – Eur. J. 2020, 26 (4), 839–844. https://doi.org/10.1002/chem.201904382.

(59) Wacharine-Antar, S.; Levilain, G.; Dupray, V.; Coquerel, G. Resolution of (±)-Imeglimin-2,4-Dichlorophenylacetate Methanol Solvate by Preferential Crystallization. Org. Process Res. Dev. 2010, 14 (6), 1358–1363. https://doi.org/10.1021/op100173r.

(60) Coquerel, G. Solubility of Chiral Species as Function of the Enantiomeric Excess. J. Pharm. Pharmacol. 2015, 67 (6), 869–878. https://doi.org/10.1111/jphp.12395.

(61) Noorduin, W. L.; Vlieg, E.; Kellogg, R. M.; Kaptein, B. From Ostwald Ripening to Single Chirality. Angew. Chem. Int. Ed. 2009, 48 (51), 9600–9606. https://doi.org/10.1002/anie.200905215.

(62) Galland, A.; Dupray, V.; Berton, B.; Morin-Grognet, S.; Sanselme, M.; Atmani, H.; Coquerel, G. Spotting Conglomerates by Second Harmonic Generation. Cryst. Growth Des. 2009, 9 (6), 2713–2718. https://doi.org/10.1021/cg801356m.

(63) Simon, F.; Clevers, S.; Dupray, V.; Coquerel, G. Relevance of the Second Harmonic Generation to Characterize Crystalline Samples. Chem. Eng. Technol. 2015, 38 (6), 971–983. https://doi.org/10.1002/ceat.201400756.

(64) Kurtz, S. K.; Perry, T. T. A Powder Technique for the Evaluation of Nonlinear Optical Materials. J. Appl. Phys. 1968, 39 (8), 3798–3813. https://doi.org/10.1063/1.1656857.

(65) Clevers, S.; Coquerel, G. Kryptoracemic Compound Hunting and Frequency in the Cambridge Structural Database. Cryst Eng Comm 2020. https://doi.org/10.1039/D0CE00303D.

(66) Fábián, L.; Brock, C. P. A List of Organic Kryptoracemates. Acta Crystallogr. B 2010, 66 (1), 94–103. https://doi.org/10.1107/S0108768109053610.

(67) Chion, B.; Lajzerowicz, J.; Bordeaux, D.; Collet, A.; Jacques, J. Structural Aspects of Solid Solutions of Enantiomers: The 3-Hydroxymethyl- and 3-Carboxy-2,2,5,5-Tetramethylpyrrolidinyl 1-Oxyl Systems as Examples. J. Phys. Chem. 1978, 82 (25), 2682–2688. https://doi.org/10.1021/j100514a010.

(68) Dufour, F.; Gervais, C.; Petit, M.-N.; Perez, G.; Coquerel, G. Investigations on the Reciprocal Ternary System (±)-2-Phenylpropionic Acid–(±)-α-Methylbenzylamine. Impact of an Unstable Racemic Compound on the Simultaneous Resolution of Chiral Acids and Bases by Preferential Crystallisation. J. Chem. Soc. Perkin Trans. 2 2001, No. 10, 2022–2036. https://doi.org/10.1039/B100706H.

(69) Kashchiev, D.; Rosmalen, G. M. van. Review: Nucleation in Solutions Revisited. Cryst. Res. Technol. 2003, 38 (7–8), 555–574. https://doi.org/10.1002/crat.200310070.

(70) McCabe, W.; Smith, J.; Harriott, P. Unit Operations of Chemical Engineering, 7th edition.; McGraw-Hill Education: Boston, 2004.

(71) Kondepudi, D. K.; Sabanayagam, C. Secondary Nucleation That Leads to Chiral Symmetry Breaking in Stirred Crystallization. Chem. Phys. Lett. 1994, 217 (4), 364–368. https://doi.org/10.1016/0009-2614(93)E1392-T.
(72) Ostwald, W. Studien Über Die Bildung Und Umwandlung Fester Körper. Z. Für Phys. Chem 1897, 22U (1), 289–330.
(73) Uwaha, M. 8 - Growth Kinetics: Basics of Crystal Growth Mechanisms. In Handbook of Crystal Growth (Second Edition); Nishinaga, T., Ed.; Elsevier: Boston, 2015; pp 359–399. https://doi.org/10.1016/B978-0-444-56369-9.00008-3.
(74) Bennema, P. Spiral Growth and Surface Roughening: Developments since Burton, Cabrera and Frank. J. Cryst. Growth 1984, 69 (1), 182–197. https://doi.org/10.1016/0022-0248(84)90027-7.
(75) Kashchiev, D. Two-Dimensional Nucleation in Crystal Growth: Thermodynamically Consistent Description of the Nucleation Work. J. Cryst. Growth 2004, 267 (3), 685–702. https://doi.org/10.1016/j.jcrysgro.2004.03.070.
(76) Jetten, L. A. M. J.; Human, H. J.; Bennema, P.; Van Der Eerden, J. P. On the Observation of the Roughening Transition of Organic Crystals, Growing from Solution. J. Cryst. Growth 1984, 68 (2), 503–516. https://doi.org/10.1016/0022-0248(84)90457-3.
(77) Chemical Symmetry Breaking; Tamura, R., Ed.; MDPI AG: S.l., 2021.
(78) Coquerel, G.; Hoquante, M. Spontaneous and Controlled Macroscopic Chiral Symmetry Breaking by Means of Crystallization. Symmetry 2020, 12 (11), 1796. https://doi.org/10.3390/sym12111796.
(79) Tamura, R.; Fujimoto, D.; Lepp, Z.; Misaki, K.; Miura, H.; Takahashi, H.; Ushio, T.; Nakai, T.; Hirotsu, K. Mechanism of Preferential Enrichment, an Unusual Enantiomeric Resolution Phenomenon Caused by Polymorphic Transition during Crystallization of Mixed Crystals Composed of Two Enantiomers. J. Am. Chem. Soc. 2002, 124 (44), 13139–13153. https://doi.org/10.1021/ja020454r.
(80) Gonnade, R. G.; Iwama, S.; Mori, Y.; Takahashi, H.; Tsue, H.; Tamura, R. Observation of Efficient Preferential Enrichment Phenomenon for a Cocrystal of (Dl)-Phenylalanine and Fumaric Acid under Nonequilibrium Crystallization Conditions. Cryst. Growth Des. 2011, 11 (2), 607–615. https://doi.org/10.1021/cg1015274.
(81) De Saint Jores, C. Towards a Deeper Understanding of Preferential Enrichment. A Case Study : DL Arginine Fumarate in Ethanol-Water 50-50 Mixture. PhD Thesis, University of Rouen, 2019.
(82) Coquerel, G. Chiral Discrimination in the Solid State: Applications to Resolution and Deracemization. In Advances in Organic Crystal Chemistry: Comprehensive Reviews 2015; Tamura, R., Miyata, M., Eds.; Springer Japan: Tokyo, 2015; pp 393–420. https://doi.org/10.1007/978-4-431-55555-1_20.
(83) Oketani, R.; Marin, F.; Tinnemans, P.; Hoquante, M.; Laurent, A.; Brandel, C.; Cardinael, P.; Meekes, H.; Vlieg, E.; Geerts, Y.; Coquerel, G. Deracemization in a Complex Quaternary System with a Second-Order Asymmetric Transformation by Using Phase Diagram Studies. Chem. – Eur. J. 2019, 25, 1–10. https://doi.org/10.1002/chem.201903338.
(84) Rougeot, C.; Guillen, F.; Plaquevent, J.-C.; Coquerel, G. Ultrasound-Enhanced Deracemization: Toward the Existence of Agonist Effects in the Interpretation of Spontaneous Symmetry Breaking. Cryst. Growth Des. 2015, 15 (5), 2151–2155. https://doi.org/10.1021/cg501765g.
(85) Iggland, M.; Fernández-Ronco, M. P.; Senn, R.; Kluge, J.; Mazzotti, M. Complete Solid State Deracemization by High Pressure Homogenization. Chem. Eng. Sci. 2014, 111, 106–111. https://doi.org/10.1016/j.ces.2014.02.034.
(86) Cameli, F.; Xiouras, C.; D. Stefanidis, G. Intensified Deracemization via Rapid Microwave-Assisted Temperature Cycling. CrystEngComm 2018, 20 (21), 2897–2901. https://doi.org/10.1039/C8CE00575C.
(87) Steendam, R. R. E.; Dickhout, J.; van Enckevort, W. J. P.; Meekes, H.; Raap, J.; Rutjes, F. P. J. T.; Vlieg, E. Linear Deracemization Kinetics during Viedma Ripening: Autocatalysis Overruled by Chiral Additives. Cryst. Growth Des. 2015, 15 (4), 1975–1982. https://doi.org/10.1021/acs.cgd.5b00127.
(88) Sakamoto, M. Asymmetric Synthesis Involving Dynamic Enantioselective Crystallization. In Advances in Organic Crystal Chemistry: Comprehensive Reviews 2020; Sakamoto, M., Uekusa, H., Eds.; Springer: Singapore, 2020; pp 433–456. https://doi.org/10.1007/978-981-15-5085-0_21.
(89) Steendam, R. R. E.; Brouwer, M. C. T.; Huijs, E. M. E.; Kulka, M. W.; Meekes, H.; van Enckevort, W. J. P.; Raap, J.; Rutjes, F. P. J. T.; Vlieg, E. Enantiopure Isoindolinones through Viedma Ripening. Chem. – Eur. J. 2014, 20 (42), 13527–13530. https://doi.org/10.1002/chem.201404320.
(90) Viedma, C.; Cintas, P. Homochirality beyond Grinding: Deracemizing Chiral Crystals by Temperature Gradient under Boiling. Chem. Commun. 2011, 47 (48), 12786–12788. https://doi.org/10.1039/C1CC14857E.
(91) Suwannasang, K.; Flood, A. E.; Rougeot, C.; Coquerel, G. Using Programmed Heating–Cooling Cycles with Racemization in Solution for Complete Symmetry Breaking of a Conglomerate Forming System. Cryst. Growth Des. 2013, 13 (8), 3498–3504. https://doi.org/10.1021/cg400436r.

(92) Suwannasang, K.; Flood, A. E.; Coquerel, G. A Novel Design Approach To Scale Up the Temperature Cycle Enhanced Deracemization Process: Coupled Mixed-Suspension Vessels. Cryst. Growth Des. 2016, 16 (11), 6461–6467. https://doi.org/10.1021/acs.cgd.6b01139.
(93) Schindler, M.; Brandel, C.; Kim, W.-S.; Coquerel, G. Temperature Cycling Induced Deracemization of NaClO3 under the Influence of Na2S2O6. Cryst. Growth Des. 2020, 20 (1), 414–421. https://doi.org/10.1021/acs.cgd.9b01337.
(94) Suwannasang, K.; Flood, A. E.; Rougeot, C.; Coquerel, G. Use of Programmed Damped Temperature Cycles for the Deracemization of a Racemic Suspension of a Conglomerate Forming System. Org. Process Res. Dev. 2017, 21 (4), 623–630. https://doi.org/10.1021/acs.oprd.7b00028.
(95) Maggioni, G. M.; Fernández-Ronco, M. P.; Meijden, M. W. van der; Kellogg, R. M.; Mazzotti, M. Solid State Deracemisation of Two Imine-Derivatives of Phenylglycine Derivatives via High-Pressure Homogenisation and Temperature Cycles. CrystEngComm 2018, 20 (27), 3828–3838. https://doi.org/10.1039/C8CE00356D.
(96) Xiouras, C.; Fytopoulos, A. A.; Ter Horst, J. H.; Boudouvis, A. G.; Van Gerven, T.; Stefanidis, G. D. Particle Breakage Kinetics and Mechanisms in Attrition-Enhanced Deracemization. Cryst. Growth Des. 2018, 18 (5), 3051–3061. https://doi.org/10.1021/acs.cgd.8b00201.
(97) Uchin, R.; Suwannasang, K.; Flood, A. E. Model of Temperature Cycle-Induced Deracemization via Differences in Crystal Growth Rate Dispersion. Chem. Eng. Technol. 2017, 40 (7), 1252–1260. https://doi.org/10.1002/ceat.201600746.
(98) Bodák, B.; Maggioni, G. M.; Mazzotti, M. Population-Based Mathematical Model of Solid-State Deracemization via Temperature Cycles. Cryst. Growth Des. 2018, 18 (11), 7122–7131. https://doi.org/10.1021/acs.cgd.8b01292.
(99) Uwaha, M. A Model for Complete Chiral Crystallization. J. Phys. Soc. Jpn. 2004, 73 (10), 2601–2603. https://doi.org/10.1143/JPSJ.73.2601.
(100) Katsuno, H.; Uwaha, M. Monte Carlo Simulation of a Cluster Model for the Chirality Conversion of Crystals with Grinding. J. Cryst. Growth 2009, 311 (17), 4265–4269. https://doi.org/10.1016/j.jcrysgro.2009.07.005.
(101) Katsuno, H.; Uwaha, M. Mechanism of Chirality Conversion by Periodic Change of Temperature: Role of Chiral Clusters. Phys. Rev. E 2016, 93 (1), 013002. https://doi.org/10.1103/PhysRevE.93.013002.
(102) Kaptein, B.; Noorduin, W. L.; Meekes, H.; van Enckevort, W. J. P.; Kellogg, R. M.; Vlieg, E. Attrition-Enhanced Deracemization of an Amino Acid Derivative That Forms an Epitaxial Racemic Conglomerate. Angew. Chem. Int. Ed. 2008, 47 (38), 7226–7229. https://doi.org/10.1002/anie.200802468.
(103) Kondepudi, D. K.; Bullock, K. L.; Digits, J. A.; Hall, J. K.; Miller, J. M. Kinetics of Chiral Symmetry Breaking in Crystallization. J. Am. Chem. Soc. 1993, 115 (22), 10211–10216. https://doi.org/10.1021/ja00075a041.
(104) Ni, X.; Shepherd, R.; Whitehead, J.; Liu, T. Chiral Symmetry Breaking Due to Impeller Size in Cooling Crystallization of Sodium Chlorate. CrystEngComm 2018, 20 (43), 6894–6899. https://doi.org/10.1039/C8CE01318G.
(105) Kondepudi, D. K.; Kaufman, R. J.; Singh, N. Chiral Symmetry Breaking in Sodium Chlorate Crystallizaton. Science 1990, 250 (4983), 975–976. https://doi.org/10.1126/science.250.4983.975.
(106) Kondepudi, D. K.; Laudadio, J.; Asakura, K. Chiral Symmetry Breaking in Stirred Crystallization of 1,1‘-Binaphthyl Melt. J. Am. Chem. Soc. 1999, 121 (7), 1448–1451. https://doi.org/10.1021/ja983418u.
(107) Noorduin, W. L.; Izumi, T.; Millemaggi, A.; Leeman, M.; Meekes, H.; Van Enckevort, W. J. P.; Kellogg, R. M.; Kaptein, B.; Vlieg, E.; Blackmond, D. G. Emergence of a Single Solid Chiral State from a Nearly Racemic Amino Acid Derivative. J. Am. Chem. Soc. 2008, 130 (4), 1158–1159. https://doi.org/10.1021/ja7106349.
(108) Steendam, R. R. E.; Harmsen, B.; Meekes, H.; van Enckevort, W. J. P.; Kaptein, B.; Kellogg, R. M.; Raap, J.; Rutjes, F. P. J. T.; Vlieg, E. Controlling the Effect of Chiral Impurities on Viedma Ripening. Cryst. Growth Des. 2013, 13 (11), 4776–4780. https://doi.org/10.1021/cg400927m.
(109) Belletti, G.; Meekes, H.; Rutjes, F. P. J. T.; Vlieg, E. Role of Additives during Deracemization Using Temperature Cycling. Cryst. Growth Des. 2018, 18 (11), 6617–6620. https://doi.org/10.1021/acs.cgd.8b00856.
(110) Hawbaker, N. A.; Blackmond, D. G. Energy Threshold for Chiral Symmetry Breaking in Molecular Self-Replication. Nat. Chem. 2019, 11 (10), 957–962. https://doi.org/10.1038/s41557-019-0321-y.
(111) Hein, J. E.; Huynh Cao, B.; Viedma, C.; Kellogg, R. M.; Blackmond, D. G. Pasteur’s Tweezers Revisited: On the Mechanism of Attrition-Enhanced Deracemization and Resolution of Chiral Conglomerate Solids. J. Am. Chem. Soc. 2012, 134 (30), 12629–12636. https://doi.org/10.1021/ja303566g.
(112) Addadi, L.; Van Mil, J.; Lahav, M. Useful Impurities for Optical Resolutions. 2. Generality and Mechanism of the Rule of Reversal. J. Am. Chem. Soc. 1981, 103 (5), 1249–1251. https://doi.org/10.1021/ja00395a059.

(113) Niinomi, H.; Sugiyama, T.; Tagawa, M.; Murayama, K.; Harada, S.; Ujihara, T. Enantioselective Amplification on Circularly Polarized Laser-Induced Chiral Nucleation from a NaClO3 Solution Containing Ag Nanoparticles. CrystEngComm 2016, 18 (39), 7441–7448. https://doi.org/10.1039/C6CE01464J.
(114) Hein, J. E.; Cao, B. H.; van der Meijden, M. W.; Leeman, M.; Kellogg, R. M. Resolution of Omeprazole Using Coupled Preferential Crystallization: Efficient Separation of a Nonracemizable Conglomerate Salt under Near-Equilibrium Conditions. Org. Process Res. Dev. 2013, 17 (6), 946–950. https://doi.org/10.1021/op400081c.
(115) The Top 300 of 2021 https://clincalc.com/DrugStats/Top300Drugs.aspx (accessed 2021 -07 -27).
(116) Levilain, G.; Eicke, M. J.; Seidel-Morgenstern, A. Efficient Resolution of Enantiomers by Coupling Preferential Crystallization and Dissolution. Part 1: Experimental Proof of Principle. Cryst. Growth Des. 2012, 12 (11), 5396–5401. https://doi.org/10.1021/cg3009943.
(117) Coquerel, G.; Petit, M.-N.; Bouaziz, R. Method of Resolution of Two Enantiomers by Crystallization. WO1995008522A1, March 30, 1995.
(118) Coquerel, G.; Levilain, G. Procédé De Résolution D'énantiomères Par Cristallisation Par Évaporation Préférentielle. WO2011073300A1, June 23, 2011.
(119) Boyle, W. J.; Sifniades, S.; Van Peppen, J. F. Asymmetric Transformation of .Alpha.-Amino-.Epsilon.-Caprolactam, a Lysine Precursor. J. Org. Chem. 1979, 44 (26), 4841–4847. https://doi.org/10.1021/jo00394a021.
(120) Black, S. N.; Williams, L. J.; Davey, R. J.; Moffatt, F.; Jones, R. V. H.; McEwan, D. M.; Sadler, D. E. The Preparation of Enantiomers of Paclobutrazol: A Crystal Chemistry Approach. Tetrahedron 1989, 45 (9), 2677–2682. https://doi.org/10.1016/S0040-4020(01)80097-1.
(121) Spix, L.; Meekes, H.; Blaauw, R. H.; van Enckevort, W. J. P.; Vlieg, E. Complete Deracemization of Proteinogenic Glutamic Acid Using Viedma Ripening on a Metastable Conglomerate. Cryst. Growth Des. 2012, 12 (11), 5796–5799. https://doi.org/10.1021/cg301343a.
(122) Hoquante, M.; Sanselme, M.; Rietveld, I. B.; Coquerel, G. Disappearing Conglomerates, Assessment of the Threat. Cryst. Growth Des. 2019, 19 (12), 7396–7401. https://doi.org/10.1021/acs.cgd.9b01316.
(123) Zhang, M.; Schuster, G. B. Photoracemization of Optically Active 1,1'-Binaphthyl Derivatives: Light-Initiated Conversion of Cholesteric to Compensated Nematic Liquid Crystals. J. Phys. Chem. 1992, 96 (7), 3063–3067. https://doi.org/10.1021/j100186a053.
(124) Flegel, M.; Lukeman, M.; Wan, P. Photochemistry of 1,1'-Bi-2-Naphthol (BINOL) — ESIPT Is Responsible for Photoracemization and Photocyclization. Can. J. Chem. 2008, 86 (2), 161–169. https://doi.org/10.1139/v07-143.
(125) Solntsev, K. M.; Bartolo, E.-A.; Pan, G.; Muller, G.; Bommireddy, S.; Huppert, D.; Tolbert, L. M. Excited-State Proton Transfer in Chiral Environments: Photoracemization of BINOLs. Isr. J. Chem. 2009, 49 (2), 227–233. https://doi.org/10.1560/IJC.49.2.227.
(126) Maria, T. M. R.; Marins, F. A.; Costa, J. B. S.; Silva, M. R.; Carrilho, R. M. B.; Monteiro, C. J. P.; Pereira, M. M.; Eusébio, M. E. S. Solid State Investigation of BINOL and BINOL Derivatives: A Contribution to Enantioselective Symmetry Breaking by Crystallization. Thermochim. Acta 2017, 648, 32–43. https://doi.org/10.1016/j.tca.2016.12.008.
(127) Takahashi, M.; Ogasawara, K. An Expedient Route to Some Monoalkyl Ethers of Enantiomerically Pure Bi-β-Naphthol. Tetrahedron Asymmetry 1997, 8 (18), 3125–3130. https://doi.org/10.1016/S0957-4166(97)00398-4.
(128) Carrilho, R. M. B.; Abreu, A. R.; Petöcz, G.; Bayón, J. C.; Moreno, M. J. S. M.; Kollár, L.; Pereira, M. M. New Binaphthyl-Based C3-Symmetric Chiral Hemilabile Monophosphite Ligands: Synthesis and Characterization of Their Platinum Complexes. Chem. Lett. 2009, 38 (8), 844–845. https://doi.org/10.1246/cl.2009.844.
(129) But, T. Y. S.; Toy, P. H. The Mitsunobu Reaction: Origin, Mechanism, Improvements, and Applications. Chem. – Asian J. 2007, 2 (11), 1340–1355. https://doi.org/10.1002/asia.200700182.
(130) Prigogine, I.; Defay, R. Chemical Thermodynamics; Longmans, 1967.
(131) Dunitz, J. D.; Bernstein, J. Disappearing Polymorphs. Acc. Chem. Res. 1995, 28 (4), 193–200. https://doi.org/10.1021/ar00052a005.
(132) Bučar, D.-K.; Lancaster, R. W.; Bernstein, J. Disappearing Polymorphs Revisited. Angew. Chem. Int. Ed Engl. 2015, 54 (24), 6972–6993. https://doi.org/10.1002/anie.201410356.
(133) Cruz-Cabeza, A. J.; Bernstein, J. Conformational Polymorphism. Chem. Rev. 2014, 114 (4), 2170–2191. https://doi.org/10.1021/cr400249d.
(134) W. C. McCrone. Polymorphism. In Physics and Chemistry of the Organic Solid State; 1965; Vol. 2, pp 725–767.

(135) Henck, J.-O.; Bernstein, J.; Ellern, A.; Boese, R. Disappearing and Reappearing Polymorphs. The Benzocaine:Picric Acid System. J. Am. Chem. Soc. 2001, 123 (9), 1834–1841. https://doi.org/10.1021/ja002113o.
(136) Brandel, C.; Amharar, Y.; Rollinger, J. M.; Griesser, U. J.; Cartigny, Y.; Petit, S.; Coquerel, G. Impact of Molecular Flexibility on Double Polymorphism, Solid Solutions and Chiral Discrimination during Crystallization of Diprophylline Enantiomers. Mol. Pharm. 2013, 10 (10), 3850–3861. https://doi.org/10.1021/mp400308u.
(137) Davey, R. J.; Sadiq, G.; Back, K.; Wilkinson, L.; Seaton, C. C. The Isolation of a Metastable Conglomerate Using a Combined Computational and Controlled Crystallization Approach. Chem. Commun. 2012, 48 (14), 1976–1978. https://doi.org/10.1039/C1CC16173C.
(138) Hammond, G. S.; Gotthardt, H.; Coyne, L. M.; Axelrod, M.; Rayner, D. R.; Mislow, K. Energy Transfer in the Racemization of Aryl Sulfoxides1,2. J. Am. Chem. Soc. 1965, 87 (21), 4959–4960. https://doi.org/10.1021/ja00949a053.
(139) Aurisicchio, C.; Baciocchi, E.; Gerini, M. F.; Lanzalunga, O. Thermal and Photochemical Racemization of Chiral Aromatic Sulfoxides via the Intermediacy of Sulfoxide Radical Cations. Org. Lett. 2007, 9 (10), 1939–1942. https://doi.org/10.1021/ol070500y.
(140) Fernández, I.; Khiar, N. Recent Developments in the Synthesis and Utilization of Chiral Sulfoxides. Chem. Rev. 2003, 103 (9), 3651–3706. https://doi.org/10.1021/cr990372u.
(141) Bentley, R. Role of Sulfur Chirality in the Chemical Processes of Biology. Chem. Soc. Rev. 2005, 34 (7), 609–624. https://doi.org/10.1039/B418284G.
(142) Solladié, G. Asymmetric Synthesis Using Nucleophilic Reagents Containing a Chiral Sulfoxide Group. Synthesis 1981, 1981 (3), 185–196. https://doi.org/10.1055/s-1981-29378.
(143) Wojaczyńska, E.; Wojaczyński, J. Enantioselective Synthesis of Sulfoxides: 2000−2009. Chem. Rev. 2010, 110 (7), 4303–4356. https://doi.org/10.1021/cr900147h.
(144) O'Mahony, G. E.; Ford, A.; Maguire, A. R. Asymmetric Oxidation of Sulfides. J. Sulfur Chem. 2013, 34 (3), 301–341. https://doi.org/10.1080/17415993.2012.725247.
(145) Han, J.; Soloshonok, V. A.; Klika, K. D.; Drabowicz, J.; Wzorek, A. Chiral Sulfoxides: Advances in Asymmetric Synthesis and Problems with the Accurate Determination of the Stereochemical Outcome. Chem. Soc. Rev. 2018, 47 (4), 1307–1350. https://doi.org/10.1039/C6CS00703A.
(146) Scott, L. J.; Dunn, C. J.; Mallarkey, G.; Sharpe, M. Esomeprazole. Drugs 2002, 62 (10), 1503–1538. https://doi.org/10.2165/00003495-200262100-00006.
(147) Garnock-Jones, K. P.; Dhillon, S.; Scott, L. J. Armodafinil. CNS Drugs 2009, 23 (9), 793–803. https://doi.org/10.2165/11203290-000000000-00000.
(148) Belin, V.; Hodge, T.; Picaut, P.; Jordan, R.; Algate, C.; Gosselin, S.; Nohynek, G.; Cavero, I. The Myocardial Lesions Produced by the Potassium Channel Opener Aprikalim in Monkeys and Rats Are Prevented by Blockade of Cardiac β-Adrenoceptors. Toxicol. Sci. 1996, 31 (2), 259–267. https://doi.org/10.1093/toxsci/31.2.259.
(149) Freedman, H. H.; Fox, A. E.; Shavel, J.; Morrison, G. C. Oxisuran: A Differential Inhibitor of Cell-Mediated Hypersensitivity. Proc. Soc. Exp. Biol. Med. Soc. Exp. Biol. Med. N. Y. N 1972, 139 (3), 909–912. https://doi.org/10.3181/00379727-139-36264.
(150) Gupta, G. K.; Kumar, V. Chemical Drug Design; Walter de Gruyter GmbH & Co KG, 2016.
(151) Wermester, N.; Lambert, O.; Coquerel, G. Preferential Crystallization (AS3PC Mode) of Modafinic Acid: An Example of Productivity Enhancement by Addition of a Non-Chiral Base. CrystEngComm 2008, 10 (6), 724–733. https://doi.org/10.1039/B715975G.
(152) Fuller, A. L.; Aitken, R. A.; Ryan, B. M.; Slawin, A. M. Z.; Woollins, J. D. The X-Ray Structures of Sulfoxides. J. Chem. Crystallogr. 2009, 39 (6), 407–415. https://doi.org/10.1007/s10870-008-9493-9.
(153) Thomas, R.; Shoemaker, C. B.; Eriks, K. The Molecular and Crystal Structure of Dimethyl Sulfoxide, (H3C)2SO. Acta Crystallogr. 1966, 21 (1), 12–20. https://doi.org/10.1107/S0365110X66002263.
(154) Vandermeeren, L.; Leyssens, T.; Peeters, D. Theoretical Study of the Properties of Sulfone and Sulfoxide Functional Groups. J. Mol. Struct. THEOCHEM 2007, 804 (1), 1–8. https://doi.org/10.1016/j.theochem.2006.10.006.
(155) Azizi, N.; Khajeh Amiri, A.; Bolourtchian, M.; Saidi, M. R. A Green and Highly Efficient Alkylation of Thiols in Water. J. Iran. Chem. Soc. 2009, 6 (4), 749–753. https://doi.org/10.1007/BF03246165.
(156) Azizi, M.; Maleki, A.; Hakimpoor, F.; Ghalavand, R.; Garavand, A. A Mild, Efficient and Highly Selective Oxidation of Sulfides to Sulfoxides Catalyzed by Lewis Acid–Urea–Hydrogen Peroxide Complex at Room Temperature. Catal. Lett. 2017, 147 (8), 2173–2177. https://doi.org/10.1007/s10562-017-2126-1.

(157) Jeon, H. B.; Kim, K. T.; Kim, S. H. Selective Oxidation of Sulfides to Sulfoxides with Cyanuric Chloride and Urea–Hydrogen Peroxide Adduct. Tetrahedron Lett. 2014, 55 (29), 3905–3908. https://doi.org/10.1016/j.tetlet.2014.05.080.
(158) Kaczorowska, K.; Kolarska, Z.; Mitka, K.; Kowalski, P. Oxidation of Sulfides to Sulfoxides. Part 2: Oxidation by Hydrogen Peroxide. Tetrahedron 2005, 61 (35), 8315–8327. https://doi.org/10.1016/j.tet.2005.05.044.
(159) Lakouraj, M. M.; Abdi, H.; Hasantabar, V. Cyanuric Chloride Promoted Oxidation of Sulfides to Sulfoxides or Sulfones in the Presence of Hydrogen Peroxide. J. Sulfur Chem. 2011, 32 (5), 435–441. https://doi.org/10.1080/17415993.2011.613938.
(160) Li, B.; Liu, A.-H.; He, L.-N.; Yang, Z.-Z.; Gao, J.; Chen, K.-H. Iron-Catalyzed Selective Oxidation of Sulfides to Sulfoxides with the Polyethylene Glycol/O 2 System. Green Chem. 2012, 14 (1), 130–135. https://doi.org/10.1039/C1GC15821J.
(161) Li, Y.-S.; Su, W.-K. 4-Methyl-phen-yl Benz-yl Sulfone. Acta Crystallogr. Sect. E Struct. Rep. Online 2005, 61 (8), o2450–o2451. https://doi.org/10.1107/S1600536805021434.
(162) Naso, F.; Cardellicchio, C.; Capozzi, M. A. M.; Capitelli, F.; Bertolasi, V. Self-Assemblies of Chiral p-Haloaryl Sulfoxides through C–H···O Short Contacts and Halogen Involving Interactions. New J. Chem. 2006, 30 (12), 1782–1789. https://doi.org/10.1039/B607545B.
(163) Gonella, S.; Mahieux, J.; Sanselme, M.; Coquerel, G. Spotting a Conglomerate Is Just Halfway to Achieving a Preparative Resolution by Preferential Crystallization. Org. Process Res. Dev. 2012, 16 (2), 286–293. https://doi.org/10.1021/op200092f.
(164) Coquerel, G.; Tauvel, G.; Petit, M.-N. Procede de dedoublement de sels de l'omeprazole. WO2009027614A2, March 5, 2009.
(165) Oketani, R.; Hoquante, M.; Brandel, C.; Cardinael, P.; Coquerel, G. Practical Role of Racemization Rates in Deracemization Kinetics and Process Productivities. Cryst. Growth Des. 2018, 18 (11), 6417–6420. https://doi.org/10.1021/acs.cgd.8b01263.
(166) Ahn, J.; Kim, D. H.; Coquerel, G.; Kim, W.-S. Chiral Symmetry Breaking and Deracemization of Sodium Chlorate in Turbulent Flow. Cryst. Growth Des. 2018, 18 (1), 297–306. https://doi.org/10.1021/acs.cgd.7b01247.
(167) McLaughlin, D. T.; Nguyen, T. P. T.; Mengnjo, L.; Bian, C.; Leung, Y. H.; Goodfellow, E.; Ramrup, P.; Woo, S.; Cuccia, L. A. Viedma Ripening of Conglomerate Crystals of Achiral Molecules Monitored Using Solid-State Circular Dichroism. Cryst. Growth Des. 2014, 14 (3), 1067–1076. https://doi.org/10.1021/cg401577m.
(168) Quesada-Moreno, M. M.; Virgili, A.; Monteagudo, E.; Claramunt, R. M.; Avilés-Moreno, J. R.; López-González, J. J.; Alkorta, I.; Elguero, J. A Vibrational Circular Dichroism (VCD) Methodology for the Measurement of Enantiomeric Excess in Chiral Compounds in the Solid Phase and for the Complementary Use of NMR and VCD Techniques in Solution: The Camphor Case. The Analyst 2018, 143 (6), 1406–1416. https://doi.org/10.1039/c7an01855j.
(169) Kelly, P.; Lawrence, S. E.; Maguire, A. R. Asymmetric Synthesis of Aryl Benzyl Sulfoxides by Vanadium-Catalysed Oxidation: A Combination of Enantioselective Sulfide Oxidation and Kinetic Resolution in Sulfoxide Oxidation. Eur. J. Org. Chem. 2006, 2006 (19), 4500–4509. https://doi.org/10.1002/ejoc.200600320.
(170) Crassous, J. Chiral Transfer in Coordination Complexes: Towards Molecular Materials. Chem. Soc. Rev. 2009, 38 (3), 830–845. https://doi.org/10.1039/B806203J.
(171) Duan, P.; Cao, H.; Zhang, L.; Liu, M. Gelation Induced Supramolecular Chirality: Chirality Transfer, Amplification and Application. Soft Matter 2014, 10 (30), 5428–5448. https://doi.org/10.1039/C4SM00507D.
(172) Fasel, R.; Parschau, M.; Ernst, K.-H. Chirality Transfer from Single Molecules into Self-Assembled Monolayers. Angew. Chem. Int. Ed. 2003, 42 (42), 5178–5181. https://doi.org/10.1002/anie.200352232.
(173) Lemieux, R. P. Chirality Transfer in Ferroelectric Liquid Crystals. Acc. Chem. Res. 2001, 34 (11), 845–853. https://doi.org/10.1021/ar9901164.
(174) Antonucci, V.; Coleman, J.; Ferry, J. B.; Johnson, N.; Mathe, M.; Scott, J. P.; Xu, J. Toxicological Assessment of 2-Methyltetrahydrofuran and Cyclopentyl Methyl Ether in Support of Their Use in Pharmaceutical Chemical Process Development. Org. Process Res. Dev. 2011, 15 (4), 939–941. https://doi.org/10.1021/op100303c.

Appendices

A. Experimental part

Many different techniques were used during this PhD. The order of presentation of the techniques is intended to guide the reader through the two studies presented previously. After the compounds were synthetized, it had to be confirmed that the desired molecule was produced. To do so, a TLC procedure was implemented to monitor the reaction advancement; at the end of the synthesis, the crude product was either recrystallized or subjected to column chromatography. It was then characterized by NMR. If the interpretation of the NMR spectrum was consistent with the desired molecule, the next step was to characterize the solid state by running DSC and PXRD analyses, sometimes infrared measurements were also used. Moreover, a visual investigation of the crystals under a microscope can also be very valuable. Analysis techniques related to the chiral resolution and the determination of suitable crystallization parameters for PC are presented in the part of the appendix part related to chapter 3.

Chromatography

Thin Layer Chromatography and column Chromatography are based on the same principle. Both are techniques used to separate the components of an impure mixture. A stationary phase retains the components depending on their affinity as a mobile phase carries them through it resulting in a separation. In this work, three different variations of chromatography were used, Thin Layer Chormatography (TLC), silica gel column chromatography and chiral High-Performance Liquid Chromatography. The employed stationary phases were made of silica gel whether it was for thin layer chromatography or preparative column chromatography. Silicagel 60, F254, 0.2 mm TLC plates from Merck were used for TLC and were revealed under UV. Silicagel 60, 230-400 mesh, particle size 40-60 µm was used for flash column chromatography.

Nuclear Magnetic Resonance

NMR is an analytical technique used to determine the structure of organic compounds. It can be realized on either solids or liquids but the probe in the equipment differs. In this study only liquid ^{1}H NMR was used. The analysis is based on the properties of specific atomic nuclei to absorb and re-emit electromagnetic radiation when they are in a magnetic field (^{1}H, ^{13}C, ^{19}F). When the spin returns to its base level after absorbing energy in the magnetic field, the excess energy is emitted at a given frequency. The resonance frequency of an observed nucleus is dependent on the effective magnetic field around the nucleus, electron shielding altering this field. Thus, the resonance frequency is highly dependent on the chemical environment, it is measured in Hertz but represented as a chemical shift in ppm on the NMR spectrum to eliminate the strength of the magnet dependence of the value. When the nucleus is closely

related to other nuclei reacting to the magnetic field, its effective magnetic field is also altered. The spin-spin coupling effect generates a signal split. The size of the splitting is the coupling constant and the number of splitting indicates the number of chemically bonded nuclei in the neighborhood of the nucleus. The intensity of the peaks corresponds to the number of nuclei emitting at this precise frequency. The NMR spectra were recorded on a Bruker spectrospin 300 MHz Instrument and were calibrated with the solvent ($CDCl_3$: 7.27 ppm and DMSO-d6: 2.50 ppm for ^1H NMR). The deuterated solvent's purity was 99.9%. The data was treated with the software ACD/NMR Processor.

Microscopy

Optical microscopy pictures were obtained on a Nikon Eclipse LV100 optical microscope equipped with a pair of cross polarizers.

Differential Scanning Calorimetry

DSC is an analytical technique used to determine the temperature of phase transitions and their corresponding enthalpy, for instance, the fusion, crystallization, glass transitions and solid-solid transitions can be characterized. The measurement is based on the difference in the quantity of heat needed to increase the temperature of a sample compared to a reference. In an oven, the two crucibles are heated or cooled at a controlled rate. When the sample undergoes a phase transition, it either releases or produces heat, whether it is an exothermic or an endothermic event, respectively. Therefore, the heat required to maintain the sample crucible at the same temperature as the reference is not the same. The result of a DSC experiment is a thermogram of the compensated heat between the two crucibles versus temperature or time. DSC experiments were performed using a Netzsch DSC 214 Polyma apparatus on powdered samples in pierced aluminum crucibles under a controlled atmosphere of nitrogen. The Netzsch Thermal Analyses Proteus Software was used to treat the data.

X-Ray diffraction

X-ray diffraction techniques are used to obtain information about the crystal structure and to identify crystalline phases of the materials. These techniques are based on observations of the diffracted X-Ray beam hitting a sample as a function of incident angle and wavelength. The condition for diffraction is defined by Bragg's law (Eq. 6):

$$n\lambda = 2d\sin\theta \qquad \text{Eq. } 6$$

n is an integer

λ is the characteristic wavelength of the X-rays hitting the sample

d is the distance between plans of high electronic density

θ is the angle of the X-ray beam

When this equation is fulfilled, the interferences are in phase and diffraction arises on the plane of the periodic structure for an angle θ. It is a very suitable method to study crystals because they are periodically arranged with high electronic density crystal planes (characterized by their Miller indexes).

Powder X-Ray Diffraction (PXRD)

In a powdered sample, numerous small crystallites exist with many different orientations so that there will always be planes fulfilling bragg's condition for diffraction. PXRD experiments provide a set of diffraction intensities as a function of the angles at which they are observed. The diffraction pattern is the fingerprint of a single given structural packing. Identification can be conducted by comparing diffractograms. This is why, X-ray powder diffractograms are widely used to identify polymorphs. PXRD analyses were performed using a D8-Discover diffractometer (Bruker, Germany) equipped with a goniometer of geometry (θ/θ). The incident X-ray beam consisted of the Cu Kα radiation (λ=1.5418 Å). The X-ray diffraction patterns were collected with a Lynx Eye® linear detector (Bruker, Germany). The X-ray diffraction patterns were recorded by steps of 0.04° over the angular 2θ range 3-30° with a counting time of 0.5 second per step with a sample rotation of 20 rpm to reduce preferential orientation only for experiments corresponding to the third chapter (the sulfoxide and the sulfone crystallize with a needle morphology). The position of characteristic powder diffraction peaks are expressed in degrees 2-theta. The EVA software (Bruker) was used for the treatment of the data.

Single Crystal X-Ray Diffraction (SC-XRD)

SC-XRD provides more detailed information than PXRD. A single crystal is rotated in the apparatus in order to record intensity and angles of diffraction for every plane of the crystal. It allows to study the crystal lattice precisely by providing a 3D image of the electron density in the crystal which facilitates determining the unit cell parameters, and the bond-lengths and angles of the molecules. After the refinement of the crystal structure (cell parameters, space group…), the electronic densities can be interpreted to resolve the chemical structure and find the 3-dimensional position of every atom in the structure. The crystal structures were determined from single crystal diffraction on a SMART APEX diffractometer (with Mo Kα1 radiation: λ=0.71073Å). The cell parameters and the orientation matrix of the crystal were preliminary determined by using the SMART Software. Data integration and global cell refinement were performed with the SAINT Software. The structures were solved by direct

methods (SHEL-XS3). Anisotropic displacement parameters were refined for all non-hydrogen atoms using SHEL-XL available with the WinGX package.

Infrared Spectroscopy

Infrared spectroscopy is the measurement of the interaction of infrared radiation with matter by absorption, emission, or reflection. It is based on the fact that molecules absorb frequencies that are characteristic of their structure. The frequency of the absorbed radiation matches the vibrational frequency of the molecule. Each functional group in the molecule will present vibrations (e.g. stretching, scissoring, twisting, …) resulting in various absorption frequencies with diverse intensities. It is possible to plot these to produce an absorption or emission spectrum which will represent the chemical conformation and functional groups of the sample. The method can be conducted on solid, liquid, or gaseous forms. It is possible to detect polymorphism via infrared spectroscopy if there are changes in the molecular conformations or hydrogen bonding in the different forms. Infrared spectra were acquired using an ATR-FTIR spectrometer (Alpha FT-IR spectrometer, Bruker). The powdered samples were slightly ground before being deposited on the ATR. For each spectrum, a total of 64 scans were recorded at room temperature between 4000 and 400 cm^{-1}. The Opus software from Bruker was used for the data treatment.

Materials Studio

The software Materials Studio from Dassault Systemes is a modeling and simulation suite that was selected for the visualization of the molecules in order to measure the bond distances, the torsion angles and the energy of the conformation in the crystal packings. For the conformational energy measurements, the molecules were considered in vacuum.

Materials

Chemical starting materials and reagents were acquired from Alfa Aesar, Sigma Aldrich or VWR™. All the solvents were acquired from Fisher Scientific™ or VWR™ and were HPLC grade.

B. A disappearing conglomerate: BINOL-OBn

Synthesis of (R)-2'-benzyloxy-1-1'-binaphtalene-2-ol (CAS: 133942-18-4)

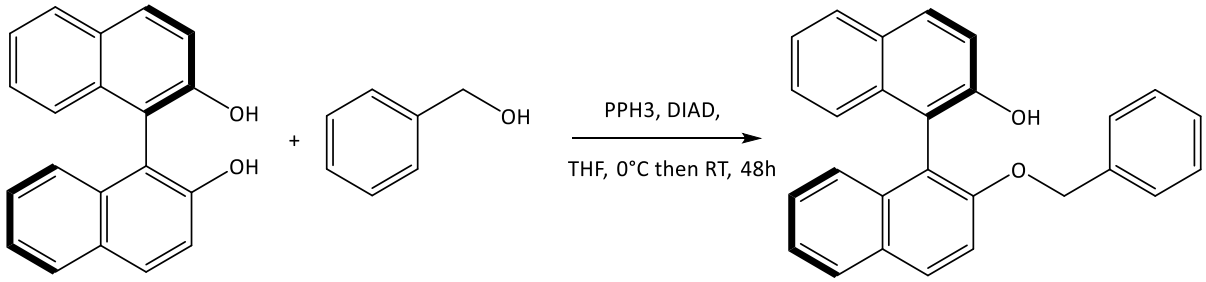

Figure B.1: Synthesis of (R)-2'-benzyloxy-1-1'-binaphtalene-2-ol

(R)-BINOL (5.0 g, 17 mmol) was dried azeotropically with toluene. It was dissolved in 100 ml of distilled THF and triphenylphosphine (PPh_3) (4.5 g, 17 mmol) and benzyl alcohol (2.1 ml, 20 mmol) were added to the stirred solution. Diisopropyl azodicarboxylate (DIAD) (3.35 ml, 17 mmol diluted in THF 5 ml) was slowly added dropwise at 0 °C. Then the mixture was stirred at room temperature for 48h. The reaction's progress was followed by TLC (CH_2Cl_2/n-hexane 2:1). At near completion, the reaction was quenched by addition of a few drops of distilled water, the solvent was evaporated under reduced pressure and the crude mixture was dissolved in dichloromethane (50 ml). The organic layer was washed with water and brine (3×50 ml). The organic layer was then dried over anhydrous $MgSO_4$. After solvent removal under reduced pressure, the product BINOL-OBn was isolated by column chromatography on silica gel, using a gradient mixture of CH_2Cl_2/n-hexane as eluent, and further purified by crystallization from CH_2Cl_2/n-hexane. (Colorless crystals, 5.696 g, 89% yield) (Note: DIAD is toxic, so the appropriate safety procedures must be taken for its manipulation).

^{1}H NMR (300 MHz, chloroform-*d*) δ=8.01–7.88 (m, 4 H, Ar-H), 7.49–7.30 (m, 5 H, Ar-H), 7.19–7.06 (m, 8 H, Ar-H), 5.16–5.06 (m, 2 H, CH2), 4.93 (s, 1 H, OH) ppm.

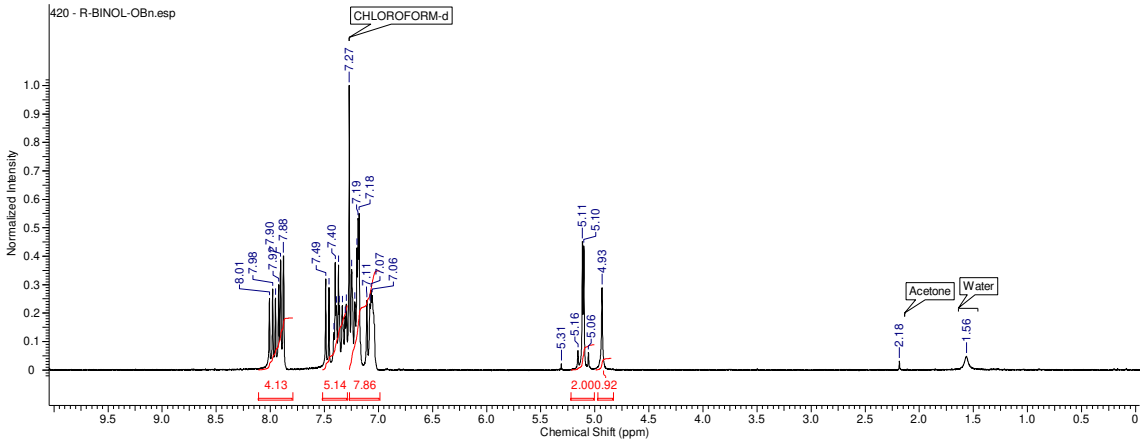

Figure B.2: ^{1}H NMR spectrum of (R)-BINOL-OBn in $CDCl_3$, 300 MHz

Synthesis of (rac)-2'-benzyloxy-1-1'-binaphtalene-2-ol (CAS: 181767-12-4)

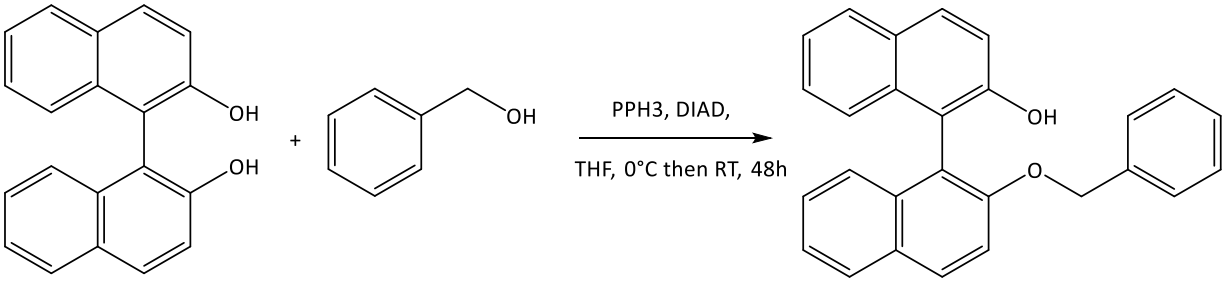

Figure B.3: Synthesis of (rac)-2'-benzyloxy-1-1'-binaphtalene-2-ol

The same procedure was applied to the racemic starting material to give (rac)-2'-benzyloxy-1-1'-binaphtalene-2-ol as white crystals (4.9917 g, 78% yield).

^{1}H NMR (300 MHz, chloroform-*d*) δ=8.01–7.87 (m, 4 H, Ar-H), 7.49–7.32 (m, 5 H, Ar-H), 7.18–7.07 (m, 8 H, Ar-H), 5.16–5.06 (m, 2 H, CH2), 4.93 (s, 1 H, OH) ppm.

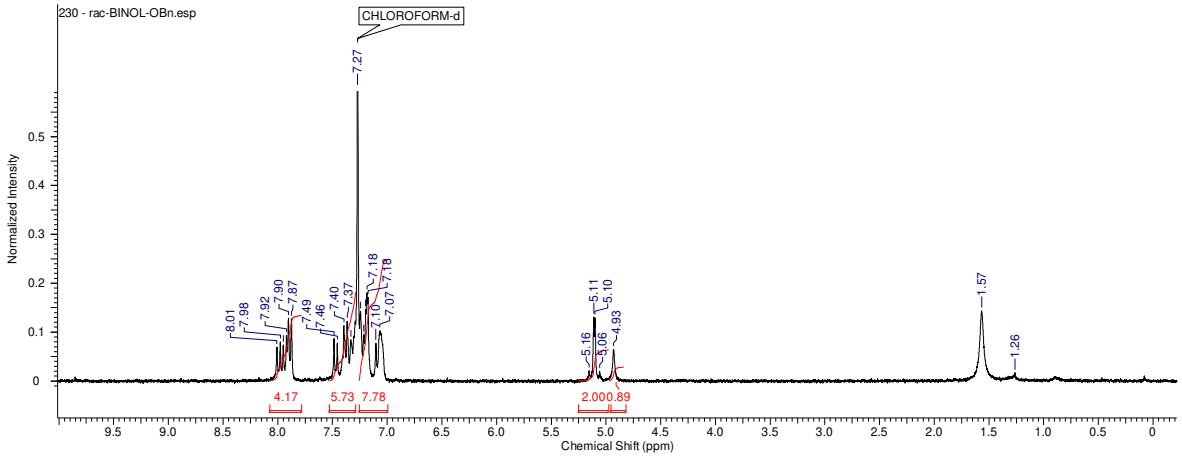

Figure B.4: ^{1}H NMR spectrum of (rac)-BINOL-OBn in $CDCl_3$, 300 MHz

Synthesis of (S)-2'-benzyloxy-1-1'-binaphtalene-2-ol (CAS: 89867-54-9)

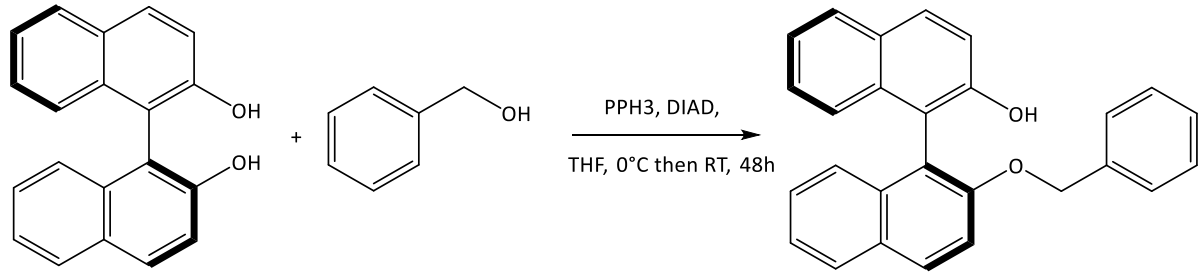

Figure B.5: Synthesis of (rac)-2'-benzyloxy-1-1'-binaphtalene-2-ol

The same procedure was applied to the S-enantiomer starting material to give (S)-2'-benzyloxy-1-1'-binaphtalene-2-ol as white crystals (2.8012 g, 80% yield).

^{1}H NMR (300 MHz, chloroform-*d*) δ=8.02–7.89 (m, 4 H, Ar-H), 7.50–7.07 (m, 13 H, Ar-H), 5.17–5.07 (m, 2 H, CH2), 4.94 (s, 1 H, OH) ppm.

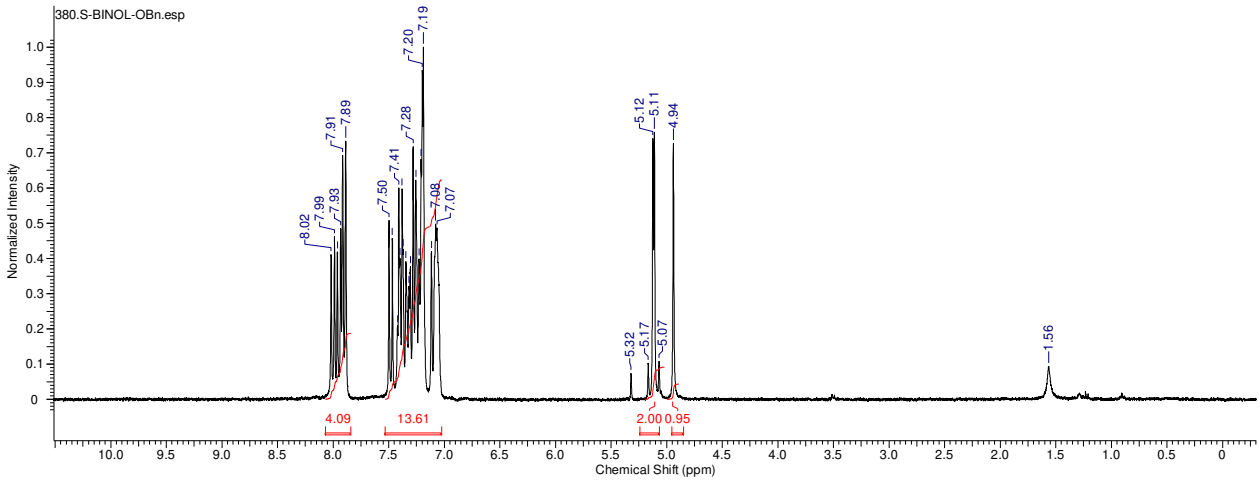

Figure B.6: ^{1}H NMR spectrum of (S)-BINOL-OBn in $CDCl_3$, 300 MHz

Thermal analysis:

All the samples at different enantiomeric compositions were prepared by grinding either between the pure R enantiomer and the racemic compound or between the pure enantiomers together. Similarly, an artificial conglomerate was prepared by mixing rigorously weighted 200 mg of (R)-BINOL-OBn crystals and 200 mg of (S)-BINOL-OBn crystals and the physical mixture was gently grinded.

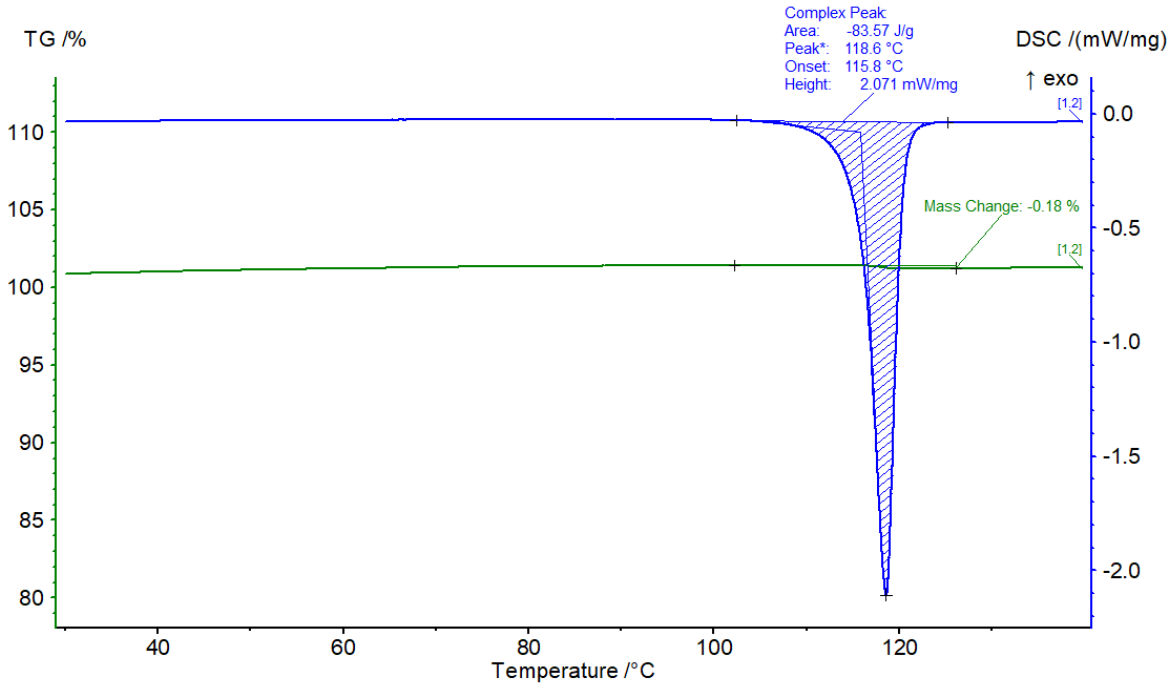

Figure B.7: TG-DSC Thermogram (heating rate 5 k/min) of (rac)-BINOL-OBn

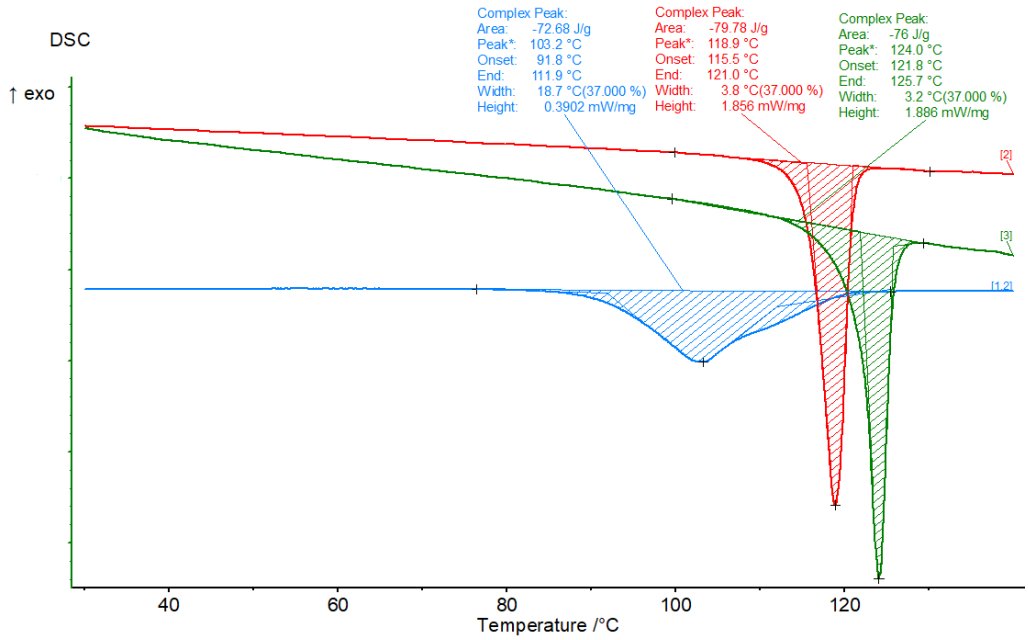

Figure B.8: DSC curves obtained for (rac)-BINOL-OBn, (R)-BINOL-OBn and the artificial conglomerate at a heating rate of 5k /min

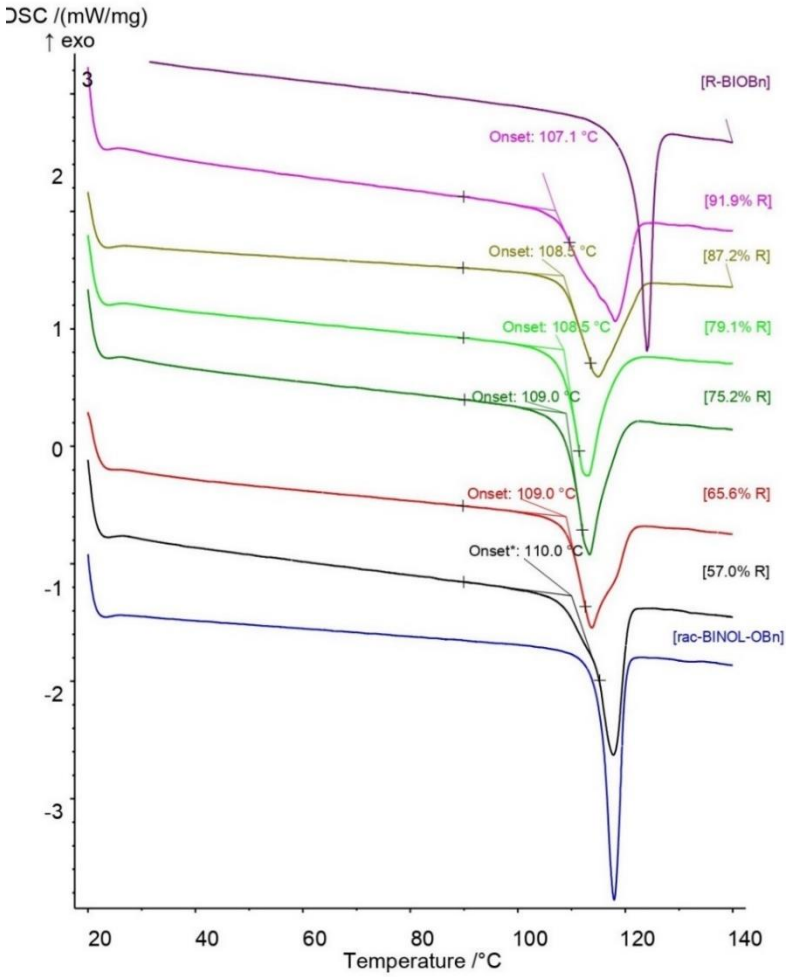

Figure B.9: DSC curves obtained for enantiomeric mixtures from (R)-BINOL-OBn to (rac)-BINOL-OBn at a heating rate of 5 k/min

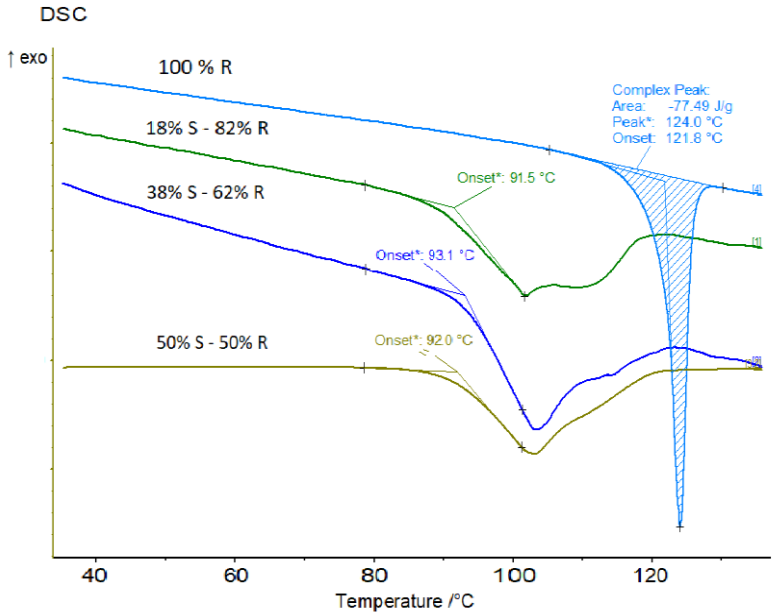

Figure B.10: DSC curves obtained for enantiomeric mixtures from (R)-BINOL-OBn to (rac)-BINOL-OBn obtained by grinding pure enantiomers at a heating rate of 5 k/min

Cross-seeding experiment between artificial conglomerate and racemic 2'-benzyloxy-1-1'-binaphtalene-2-ol:

A saturated solution of racemic BINOL-OBn was prepared in 5 ml diethyl ether at – 10°C. 200 mg of powder of artificial conglomerate and 200 mg of powder of racemic compound were added. A sample was taken after 6 hours showing the coexistence of the two phases. After 48 hours the suspension was exclusively composed of the racemic compound.

C. From supramolecular chirality to intrinsic chirality: transfer of chirality between a sulfoxide and its corresponding prochiral sulfone

Characterization of the compounds

Synthesis of sulfide (CAS: 5023-60-9)

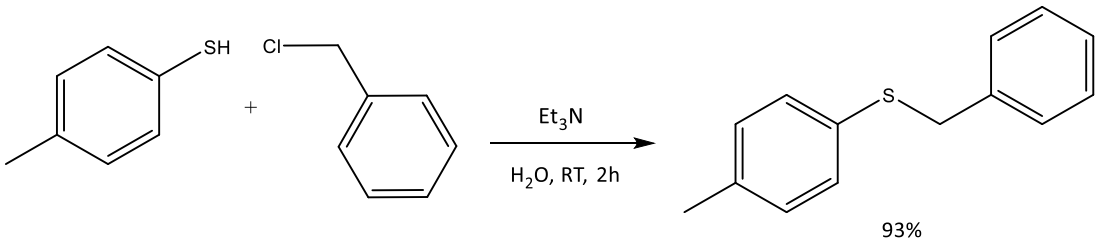

Figure C.11: Synthesis of benzyl(p-tolyl)sulfide

The procedure reported in the main text gave the sulfide as a viscous oil (12.984 g, 56.37 mmol).

^{1}H NMR (300 MHz): δ = 7.39–7.20 (m, 7 H, Ar-H), 7.02–7.06 (m, 2 H, Ar-H), 4.07 (s, 2 H, SCH2), 2.31 (s, 3 H, Ar-CH3) ppm.

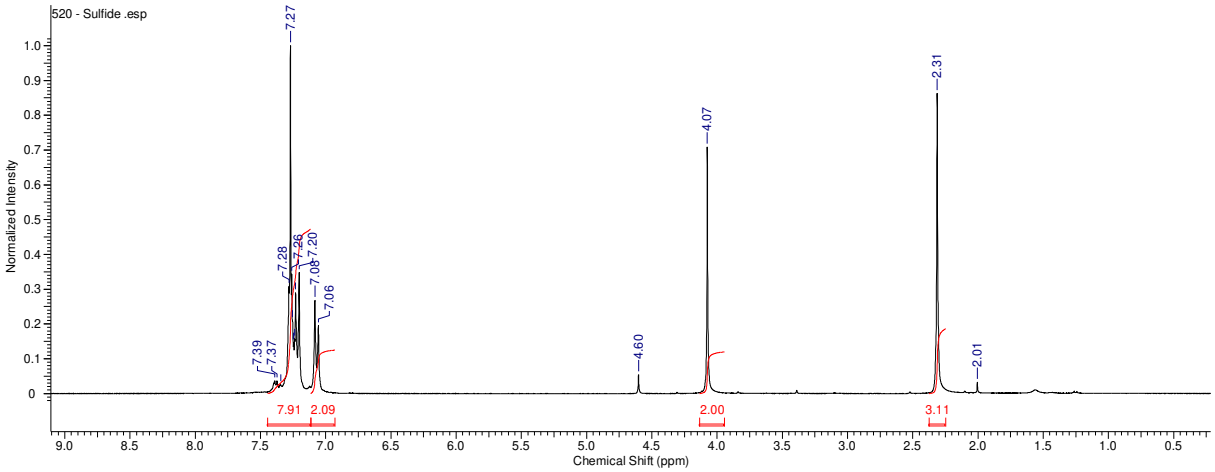

Figure C.12: ^{1}H NMR spectrum of benzyl(p-tolyl)sulfide in $CDCl_3$, 300 MHz (the aromatic integration is off due to the solvent peak)

Synthesis of (rac)-Sulfoxide (CAS: 10381-70-1)

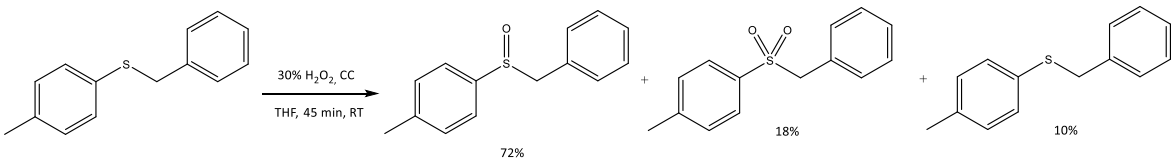

Figure C.13: Synthesis of benzyl(p-tolyl)sulfoxide and its by-products

The procedure reported in the main text afforded the sulfoxide as well as by products. Further purification was achieved by column chromatography and the pure sulfoxide was obtained as white needles (1.658 g, 7.2 mmol, 72 %).

^{1}H NMR (300 MHz): δ = 7.24–7.18 (m, 7 H, Ar-H), 6.97–6.98 (m, 2 H, Ar-H), 4.13–3.94 (dd, J = 12.5 Hz, 2 H, SCH2), 2.36 (s, 3 H, Ar-CH3) ppm

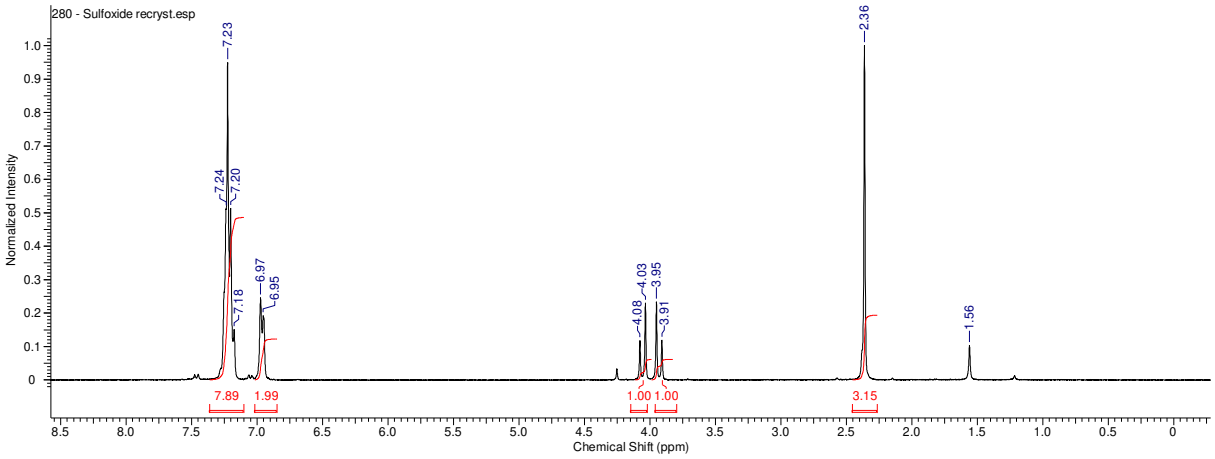

Figure C.14: ^{1}H NMR spectrum of benzyl(p-tolyl)sulfoxide in $CDCl_3$, 300MHz (the aromatic integration is off due to the solvent peak)

The R-sulfoxide CAS is 4820-07-9 and this enantiomer induces a (+) rotation of the polarized light at 589 nm. The S-enantiomer CAS is 4820-08-0 and it induces a (-) rotation at 589 nm.

The sulfone (CAS: 5395-20-0) was obtained from the purification of the sulfoxide as a white powder (432 mg, 1.76 mmol, 18%).

^{1}H NMR (300 MHz): δ = 7.50–7.52 (d, 2 H, Ar-H), 7.32–7.26 (m, 6 H, Ar-H), 7.11–7.09 (m, 2 H, Ar-H), 4.30(s, 2 H, SCH2), 2.43 (s, 3 H, Ar-CH3) ppm.

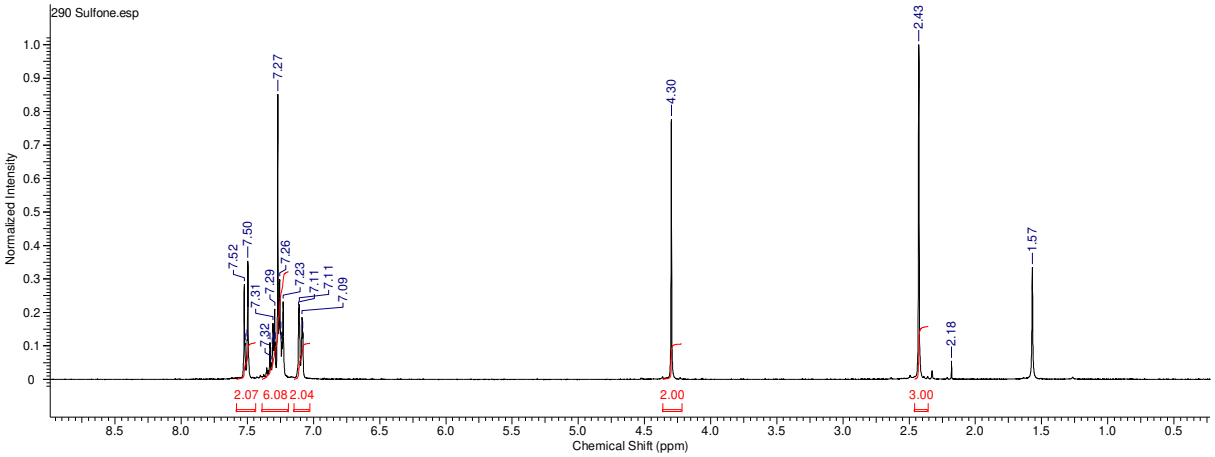

Figure C.15: ^{1}H NMR spectrum of benzyl(p-tolyl)sulfone in $CDCl_3$, 300 MHz (the aromatic integration is off due to the solvent peak)

Characterization of the solid phases

Powder X-ray diffraction

The PXRD pattern of the enantiopure sulfoxide is similar to the pattern of the racemic mixture. It confirms the conglomerate nature of the system.

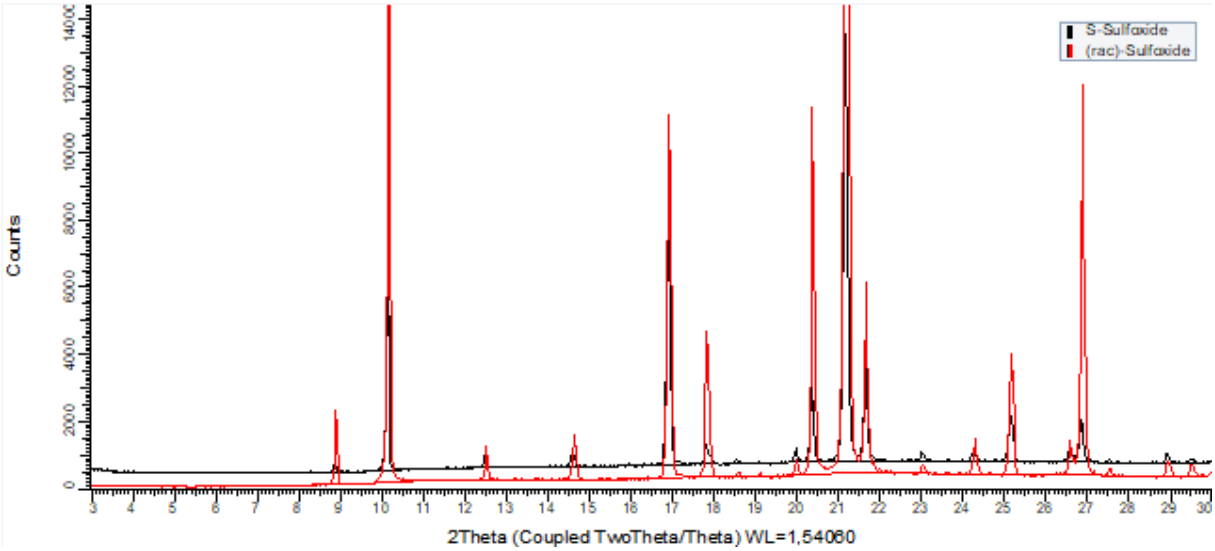

Figure C.16: PXRD patterns of racemic and S-Sulfoxide (coming from a single crystal with $\alpha_{single\ crystal}$ = -136°)

All the samples at different compositions were prepared by solvent evaporation of definite mixtures between racemic sulfoxide and racemic sulfone. The mixtures were analyzed by PXRD.

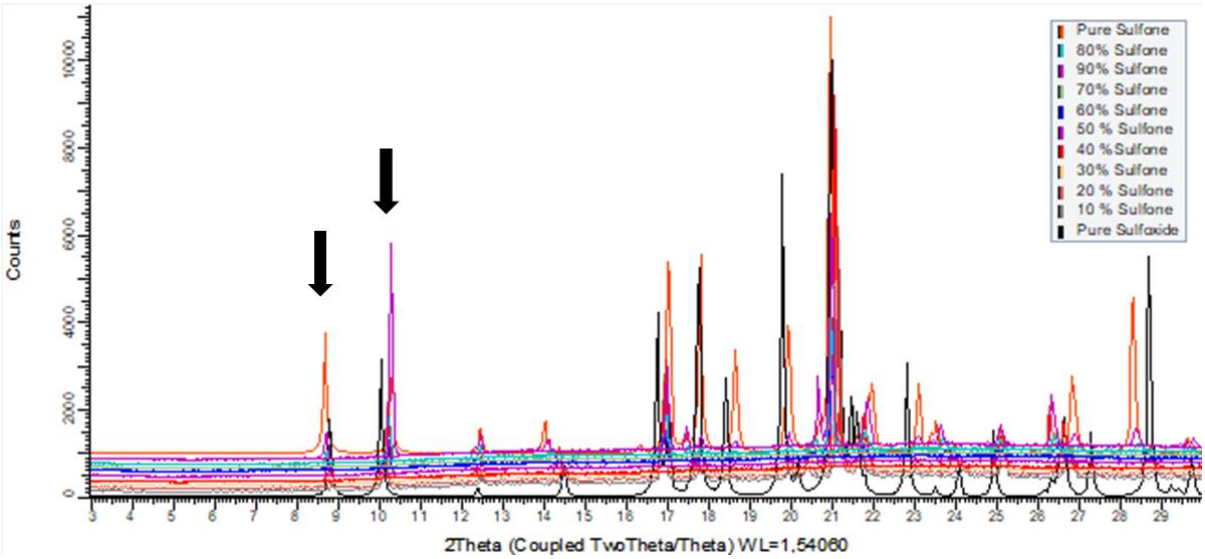

Figure C.17: PXRD of binary mixtures of (rac)-sulfoxide and (rac)-sulfone obtained by solvent evaporation crystallization (the arrows mark the peak of interest)

The PXRD pattern upon heating of a mixture of R-sulfoxide and R-sulfone (37-63 mol%) (Figure C.18) is compared to the pattern of S-sulfoxide and R-Sulfone (41-59 mol%) (Figure C.19). R-sulfone comes from the sample 3 of deracemization (the one that induced the preferential crystallization of R-sulfoxide). In the PXRD pattern of the homochiral mixture no change can be perceived, except an artifact at high temperature. In the PXRD pattern of the heterochiral mixture, there are slight changes in the pattern. At room temperature, there is one more peak at 23.5°. It could be explained by the chiral incompatibility. At 126°C, a change occurs and this peak disappear and a new peak at 25.8° appears. This could be explained by the interconversion of the sulfone at high temperature to be chiral compatible and enter the lattice of the S-sulfoxide.

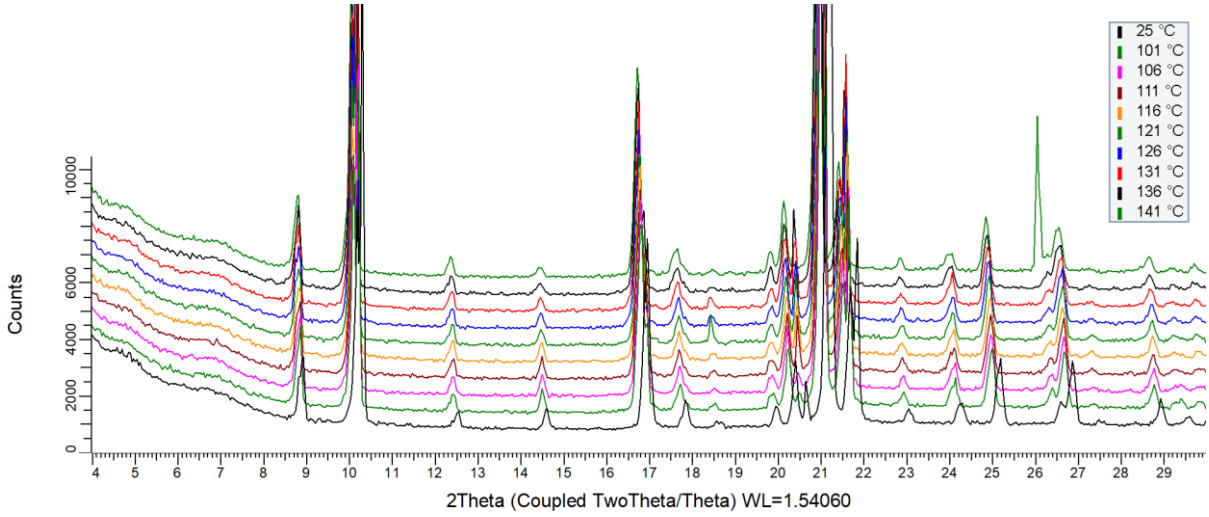

Figure C.18: PXRD pattern of a mixture of R-sulfoxide and R-sulfone (37-63 mol%) from 25 °C to 141 °C

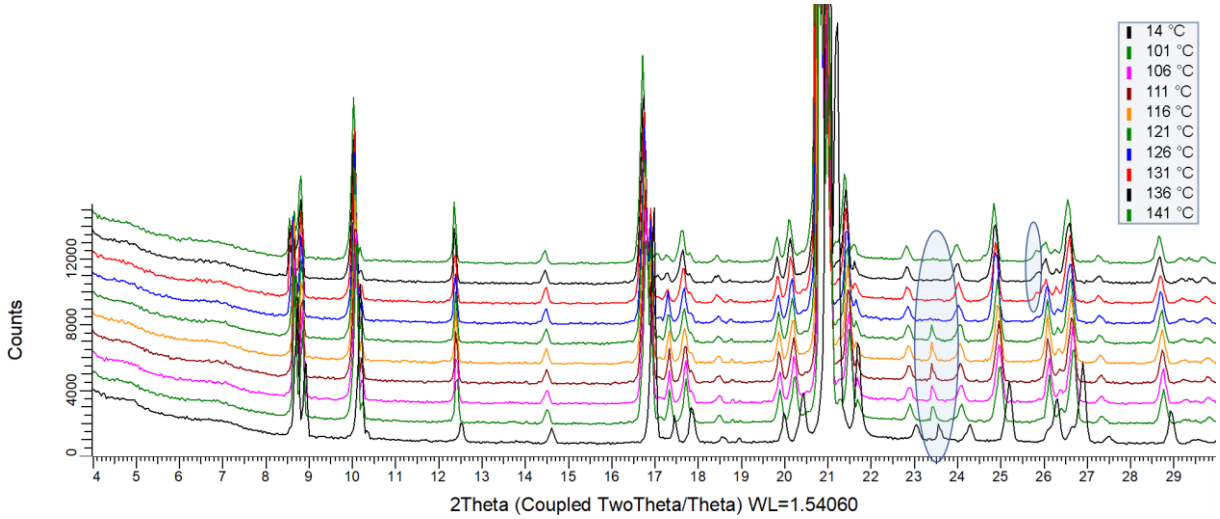

Figure C.19: PXRD pattern of a mixture of S-sulfoxide and R-sulfone (41-59 mol%) from 25 °C to 141 °C

Thermal analysis of the enantiomers of sulfoxide and of the racemic mixture:

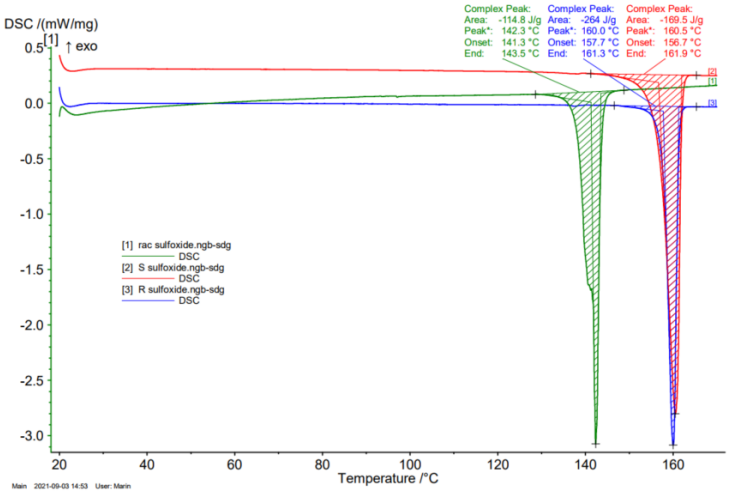

Figure C.20: DSC curves obtained for (rac)-Sulfoxide in green, S-sulfoxide in red and R-sulfoxide in blue (heating rate of 5 k/min)

Thermal analysis of binary mixtures of rac-sulfoxide and sulfone:

All the samples at different compositions were prepared by solvent evaporation of mixtures between racemic sulfoxide and racemic sulfone. The DSC experiments were run at a high heating rate of 10 k/min because of the degradation concomitant to the fusion. At lower cooling rates, the degradation was more important, the peaks were blurred and NMR analyses of the solid collected after melting showed that too much degradation occurred to extract information. However, the liquidus and solidus point must be taken very cautiously and an attempt to plot the corresponding binary section is presented in Figure C.22.

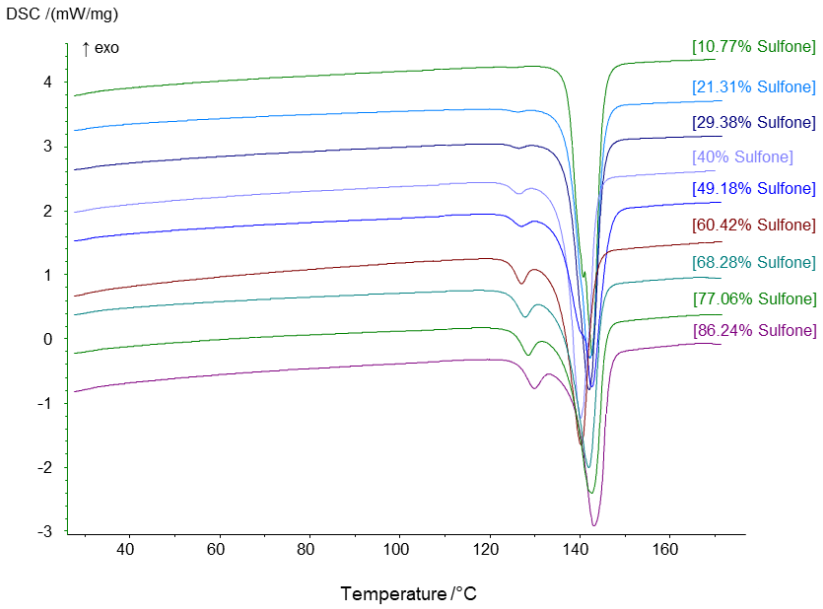

Figure C.21: DSC curves obtained for binary mixtures of (rac)-sulfoxide and (rac)-sulfone obtained by solvent evaporation crystallization at a heating rate of 10 k/min

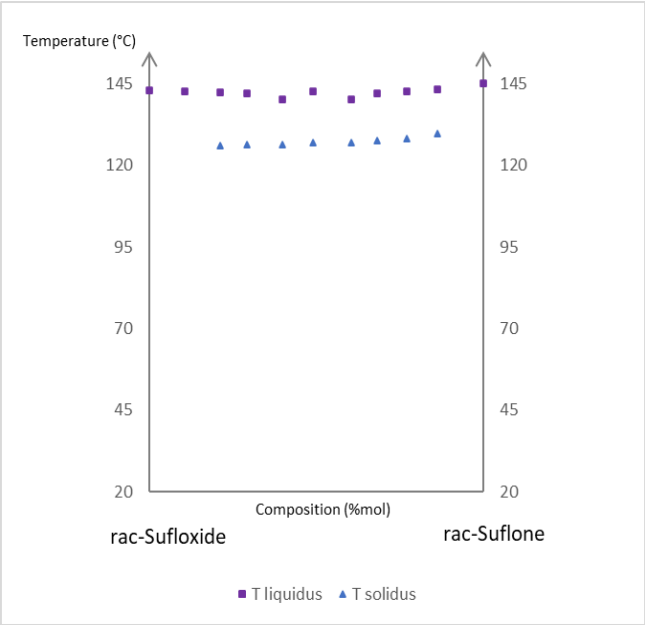

Figure C.22: Binary section between the racemic sulfoxide and the racemic sulfone

Preferential crystallization parameters determination:

Suitable crystallization parameters for the resolutions were determined by solubility measurements (dry extract method) and nucleation experiments (Crystal 16 or by eye).

Solubility

The dry extract method was employed to estimate the solubilities. For each solubility measurement, five suspensions were stirred at 20°C. After 24 hours of stirring, it was assumed that the suspensions had reached equilibrium and they were filtered on a 20µm PTFE syringe filter. The solids were analyzed by PXRD to identify the crystalline phase and to confirm the absence of a new, unknown phase. The five filtrates were split into two batches each (10 samples in total) and weighed. Afterwards, they were dried under a nitrogen flux for 24 hours. Once totally dried, the 10 solids were weighed and a mass solubility was obtained by the following equation (Eq. 7):

$$\text{Solubility w/w \%} = \frac{m_{dried\ solid}}{m_{filtrate}} * 100 \qquad Eq.7$$

Nucleation experiments

The Crystal16 parallel crystallizer was used for the determination of the Ostwald limit via turbidity measurements. It is a benchtop crystallization system comporting 16 agitated and thermostated reactors of 1 ml. The solubility curve is obtained by heating the sample with a

heating rate of 0.3 K/min and the nucleation curve is obtained upon cooling with a cooling ramp of 0.1 K/min. The CrystalClear software was used for data processing.

Determination of the enantiomeric excess:

The synthetized compounds were submitted to different resolution techniques and their optical purity was examined by polarimetry and by chiral HPLC.

Polarimetry

Polarimetry is a technique used to characterize the optical rotation of optically active compounds. Chiral entities are optically active, they change the angular direction of polarized light (the vibrations of the electromagnetic waves of this beam of light are restrained to one plane). The polarimeter measures the angle of rotation of the plane of polarized light after it passes through a solution with the chiral compounds under study. The sign of the rotation depends on the enantiomer <+> or <->. The specific optical rotation is meaningful only at a given temperature and wavelength of the light beam used. Biot's law (Eq. 8) links the deviation angle measured by the polarimeter to the specific optical rotatory power of a sample.

$$[\alpha]_T^\lambda = \frac{\alpha}{l \,.\, C} \qquad Eq.8$$

α is the measured rotation in degree

l is the length of the cell: 1 dm

C is the concentration of the solution in g/ml at a given temperature T

The optical rotations were measured at 20 °C with an incident wavelength of λ = 589 nm on an Anton Paar 5100 polarimeter.

During the experiments designed to determine the filtration window, the optical rotation of the mother liquor was measured by taking 25 µL samples of mother liquor and diluting it with THF to 1 ml.

To measure the optical purity of the solid collected after the AS3PC of the sulfoxide, the crystals were dried at 40 °C under vacuum for 24h. A precise mass was weighed (ca. 5 mg) and dissolved in 1 ml THF. The specific optical rotations are calculated according to equation 7. The enantiomeric excess is calculated according to the following equation (Eq. 9).

$$\text{Optical Purity} = \frac{\alpha_{mixture}}{\alpha_{pure}} \qquad Eq.9$$

α_{pure} was obtained by dissolving a 4 mg single crystal in 1 ml THF, the measured optical rotation was 0.556° so $\alpha_{single\ crystal}$ = 139° ml.g^{-1}.dm^{-1} in THF at 20 °C and λ = 589 nm. This single crystal was subjected to an HPLC analysis (Figure C.23, see conditions bellow) to

precisely know its enantiomeric excess (98.16 %) and the specific optical rotation of the enantiopure sulfoxide in these conditions is deduced $|\alpha_{pure}|$ = 142°.

Chiral High Performance Liquid Chromatography (HPLC)

In the mode of Preferential Crystallization involving a chirality transfer, seeds of sulfone are introduced during experiments. The mother liquor is not saturated in sulfone so the seeds start to dissolve immediately, however, they do transfer their chirality and allow stereoselective crystallization of one of the enantiomers of the sulfoxide. It is not known whether they completely dissolve, they may remain in the crystals as little embedded crystallites, so it is not clear how much sulfone remains in the solid by the end of a PC run. The determination of the e.e. by polarimetry requires an accurate knowledge of the mass of the solid, however, in this case, the solid consists of sulfoxide and a small, unknown part of sulfone, thus polarimetry cannot be applied. Therefore, chiral separations were carried out on a Chiralcel OD-H column from Daicel connected to a u-HPLC UltiMate® 3000 from Dionex. The apparatus was controlled by the ChromQuest® software. The retention time for R-sulfoxide = 28 min, tr (S-sulfoxide) = 33 min (flow rate = 1.0 ml.min^{-1}; solvent = n-heptane/2-propanol 95:5; temperature = 25 °C, detector wavelengh λ=254 nm). Enantiomeric excess was calculated according to the equation 1:

$$\text{Enantiomeric excess (e.e.)}(\%) = \frac{[\text{R}] - [\text{S}]}{[\text{R}] + [\text{S}]} \times 100 \qquad \text{Eq. 1}$$

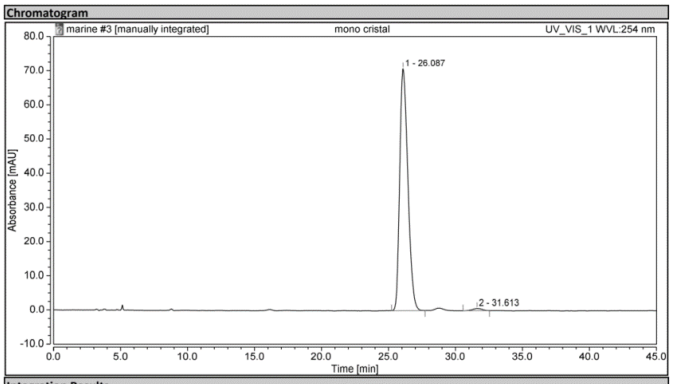

Figure C.23: Chromatogram of the monocrystal used to determine the α_{pure}

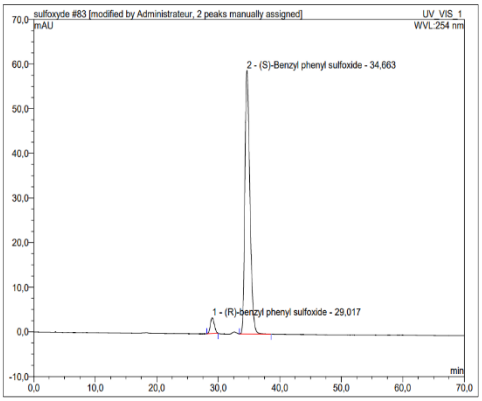

No.	Ret.Time min	Area mAU*min	Rel.Area %	Height mAU	Resolution (EP)	Asymmetry (EP)	Plates (EP)
1	29,02	2,682	4,61	3,567	4,22	1,12	9257
2	34,66	55,547	95,39	59,067	n.a.	1,33	8842

Figure C.24: Chromatogram of the solid obtained after experiment 1 run 1 of the Preferential Crystallization with chirality transfer

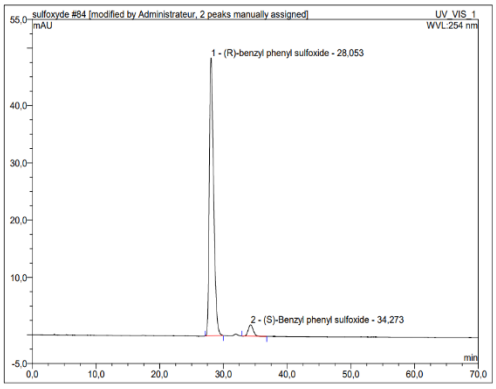

No.	Ret.Time min	Area mAU*min	Rel.Area %	Height mAU	Resolution (EP)	Asymmetry (EP)	Plates (EP)
1	28,05	38,088	95,44	48,510	4,67	1,42	8337
2	34,27	1,820	4,56	2,004	n.a.	1,11	9060
Total:			100,000	50,514	4,67	2,531	

Figure C.25: Chromatogram of the solid obtained after experiment 1 run 2 of the PC with chirality transfer

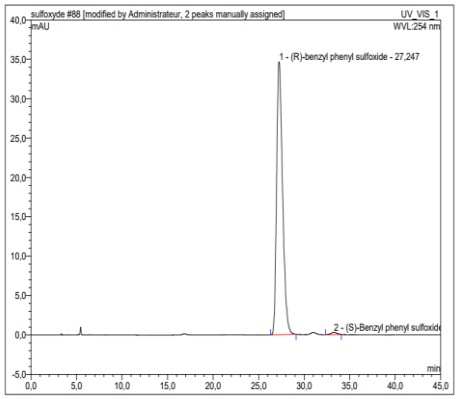

No.	Ret.Time min	Area mAU*min	Rel.Area %	Height mAU	Resolution (EP)	Asymmetry (EP)	Plates (EP)
1	27,25	26,348	99,14	34,663	4,75	1,36	8370
2	33,28	0,228	0,86	0,277	n.a.	0,96	9656
Total:			100,000	34,940	4,75	2,322	

Figure C.26: Chromatogram of the solid obtained after experiment 2 run 1 of the PC with chirality transfer

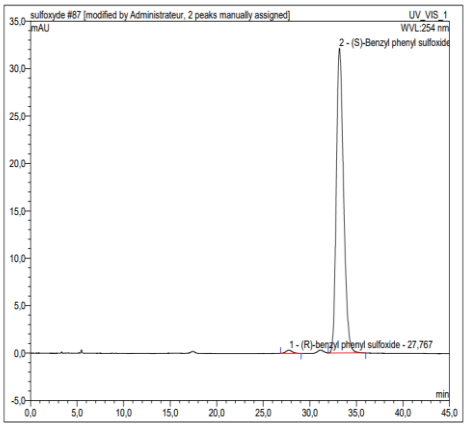

No.	Ret.Time min	Area mAU*min	Rel.Area %	Height mAU	Resolution (EP)	Asymmetry (EP)	Plates (EP)
1	27,77	0,255	0,87	0,338	4,16	1,09	8680
2	33,18	29,023	99,13	32,136	n.a.	1,25	8751
Total:			100,000	32,475	4,16	2,347	

Figure C.27: Chromatogram of the solid obtained after experiment 2 run 2 of the PC with chirality transfer

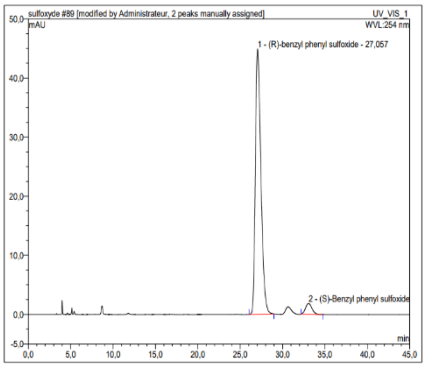

No.	Ret.Time min	Area mAU*min	Rel.Area %	Height mAU	Resolution (EP)	Asymmetry (EP)	Plates (EP)
1	27,06	34,204	95,56	44,919	4,67	1,39	8241
2	33,08	1,588	4,44	1,825	n.a.	1,11	9003
Total:			100,000	46,743	4,67	2,502	

Figure C.28: Chromatogram of the solid obtained after experiment 2 run 3 of the PC with chirality transfer

D. Scientific Production

1. Publications

- "Spontaneous and Controlled Macroscopic Chiral Symmetry Breaking by Means of Crystallization", Coquerel, G.; Hoquante, M., **Symmetry (2020),** Impact Factor: 2.71 (2020), Open access journal. This review is part of the special issue Chemical Symmetry Breaking and was also printed as a book.

symmetry

MDPI

Review

Spontaneous and Controlled Macroscopic Chiral Symmetry Breaking by Means of Crystallization

Gérard Coquerel * and Marine Hoquante

SMS EA3233, Place Emile Blondel, University of Rouen Normandy, CEDEX, F-76821 Mont-Saint-Aignan, France; marine.hoquante@univ-rouen.fr

* Correspondence: gerard.coquerel@univ-rouen.fr

Received: 21 September 2020; Accepted: 26 October 2020; Published: 30 October 2020

Abstract: In this paper, macroscopic chiral symmetry breaking refers to as the process in which a mixture of enantiomers departs from 50–50 symmetry to favor one chirality, resulting in either a scalemic mixture or a pure enantiomer. In this domain, crystallization offers various possibilities, from the classical Viedma ripening or Temperature Cycle-Induced Deracemization to the famous Kondepudi experiment and then to so-called Preferential Enrichment. These processes, together with some variants, will be depicted in terms of thermodynamic pathways, departure from equilibrium and operating conditions. Influential parameters on the final state will be reviewed as well as the impact of kinetics of the R ⇔ S equilibrium in solution on chiral symmetry breaking. How one can control the outcome of symmetry breaking is examined. Several open questions are detailed and different interpretations are discussed.

Keywords: chirality; deracemization; preferential enrichment; thermodynamics; phase diagrams; kinetics

- “Temperature Cycle Induced Deracemization”, Intaraboonrod, K.; Lerdwiriyanupap, T.; Hoquante, M.; Coquerel, G.; Flood, A. E., **Mendeleev Communications (2020),** Impact Factor: 1.75 (2020).

Available online at www.sciencedirect.com
ScienceDirect
Focus Article, *Mendeleev Commun.*, 2020, **30**, 395–405
Mendeleev Communications

Temperature cycle induced deracemization

Kritsada Intaraboonrod,[a] Tharit Lerdwiriyanupap,[b] Marine Hoquante,[c] Gerard Coquerel[c] and Adrian E. Flood*[a]

[a] *Department of Chemical and Biomolecular Engineering, School of Energy Science and Engineering, Vidyasirimedhi Institute of Science and Technology, Payupnai, Wang Chan, Rayong 21210, Thailand. E-mail: adrian.flood@vistec.ac.th*
[b] *Department of Materials Science and Engineering, School of Molecular Science and Engineering, Vidyasirimedhi Institute of Science and Technology, Payupnai, Wang Chan, Rayong 21210, Thailand*
[c] *Normandie University, SMS, EA 3233 University of Rouen, Crystal Genesis Unit, 76821 Mont Saint-Aignan Cedex, France*

DOI: 10.1016/j.mencom.2020.07.002

The problem of separation and purification of the enantiomers of chiral species is a significant issue in the production of modern chemicals of pharmaceutical, agricultural and food industries. Efficient methods enabling a complete conversion of a racemic mixture into the desired enantiomer would be of great benefit to industry. Temperature cycle induced deracemization (TCID), a process allowing an initially racemic crystal phase of a suspension to be converted into an enantiopure state, combines solution phase racemization of the solute molecules and a series of temperature cycles inducing dissolution and crystal growth. The process first described as a more convenient and scalable alternative to Viedma ripening, has now been successfully tested on a wide range of chiral components that are conglomerate forming and racemizable. This review discusses the origins of TCID, potential mechanisms responsible for the deracemization, and also some related processes.

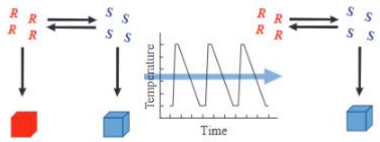

- “Disappearing Conglomerates, Assessment of the Threat”, Hoquante, M.; Sanselme, M.; Rietveld, I. B.; Coquerel, G., **Crystal Growth and design (2019),** Impact Factor: 4.089 (2019).

CRYSTAL GROWTH & DESIGN
Article
Cite This: *Cryst. Growth Des.* 2019, 19, 7396–7401
pubs.acs.org/crystal

Disappearing Conglomerates, Assessment of the Threat

Published as part of a Crystal Growth and Design virtual special issue Remembering the Contributions and Life of Prof. Joel Bernstein

Marine Hoquante,[†] Morgane Sanselme,[†] Ivo B. Rietveld,[†,‡] and Gérard Coquerel*[,†]

[†]Normandie Université, Laboratoire SMS-EA3233, Université de Rouen Normandie, F76821, Mont Saint Aignan, France
[‡]Université Paris Descartes, Faculté de Pharmacie, 4, av. de l'observatoire, 75006, Paris, France

Supporting Information

ABSTRACT: A racemic compound has been identified for the system: (+) − (−) BINOL-OBn despite having been reported as a conglomerate. This heterochiral phase appears to be more stable than the conglomerate irrespective of the temperature. Its melting point exceeds by 20 °C that of the racemic eutectic. In conjunction with the revised phase diagram, the crystal structures of the racemic compound and of the pure enantiomer have been compared. In the structure of the racemic compound ($Z' = 3$), hydrogen bonds can be found, whereas in the structure of the pure enantiomer ($Z' = 1$) only $\pi-\pi$ and van der Waals interactions are observed. The likelihood that a more stable racemic compound appears when processing a conglomerate (e.g., in preferential crystallization) is discussed.

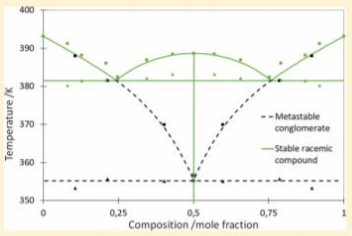

2. Communications in conferences

Poster presentation:

- Disapearing conglomerates, Hoquante, M.; Sanselme, M.; Rietveld, I. B.; Coquerel, G., BACG 50th annual conference, **9-11th July 2019**, UK

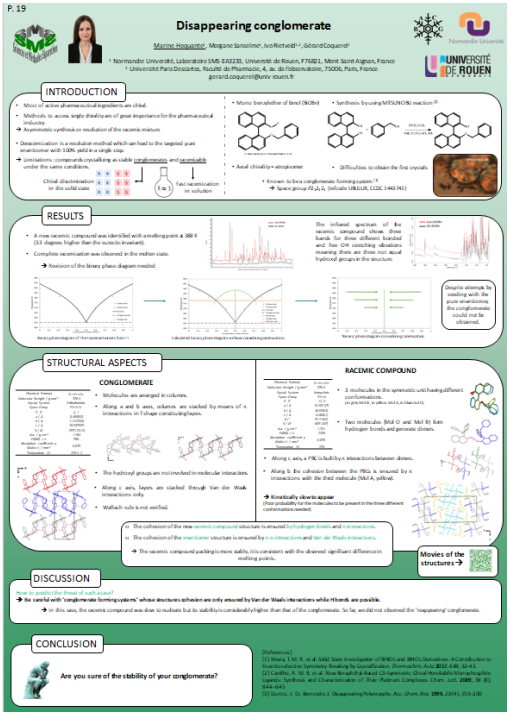

Oral communication:

- Theory and practice on the continuum between supramolecular chirality and intrinsic chirality, Hoquante, M.; Rietveld, I. B.; Coquerel, G., ChiRaFun, **19-21 April 2021**, online

Abstract

Obtaining enantiopure chemicals is a major challenge in the chemical industry, in particular for the agrochemical and pharmaceutical industries. In this thesis, crystallization of chiral systems have been studied and two approaches are presented to cover various types of chirality and their features. In chapter two, we propose a reassessed phase diagram of an atropisomer that, despite having been reported as a conglomerate forming system, presents a stable racemic compound. The emergence of the heterochiral phase is rationalized by structural considerations. Moreover, the effect of the appearance of a more stable racemic compound when using a conglomerate for resolution purposes is discussed. In chapter three, we show that a chiral sulfoxide, forming a conglomerate system, and the corresponding non-chiral sulfone exhibit an isostructural crystal packing. Consistently, the existence of complete solid solutions between the prochiral sulfone and the enantiomers of sulfoxide have been demonstrated. The sulfone was deracemized by Viedma ripening and the sulfoxide was resolved by "classical" AS3PC mode of preferential crystallization. Moreover, a variation of the AS3PC mode, in which control over the chirality is induced by seeding with enantiopure crystals of a related compound, is proposed. Experiments demonstrate its feasibility and illustrate the possibility of a continuum between supramolecular and intrinsic chirality.

Résumé

L'obtention de molécules optiquement pure est un enjeu majeur pour l'industrie chimique, en particulier pour les industries agrochimique et pharmaceutique. Dans cette thèse, la cristallisation de systèmes chiraux a été étudiée et deux approches sont proposées afin de couvrir plusieurs types de chiralité. Le chapitre deux porte sur un atropisomère qui, bien qu'il ait été présenté comme un conglomérat dans la littérature, forme un composé racémique stable. Conformément à cette observation, nous avons proposé la révision du diagramme de phase des énantiomères. L'apparition de la nouvelle phase hétérochirale est rationalisée par des considérations structurales. Nous avons également examiné la possibilité de l'émergence d'un composé racémique plus stable lorsqu'un système formant un conglomérat est utilisé dans le cadre d'une résolution par cristallisation. Le chapitre trois décrit l'étude d'un sulfoxyde chiral et de la sulfone prochirale correspondante qui cristallisent dans le même groupe d'espace avec des paramètres cristallins similaires. L'existence de solutions solides totales entre ces deux composés a été démontrée. Ces composés cristallisant dans des systèmes formant des conglomérats, la résolution chirale par cristallisation est facilitée. La sulfone a été déracémisée par murissement de Viedma et le sulfoxyde a été résolu par un mode de cristallisation préférentielle « classique » : l'AS3PC. En outre, nous proposons une variation de ce mode dans laquelle le contrôle de la chiralité est induit par des germes d'un composé apparenté. Ces expériences semblent indiquer la présence d'un continuum entre la chiralité supramoléculaire et la chiralité intrinsèque.